The University of Sydney

A Personalised ear-EEG Device

by
Leping Yu

Principal Supervisor
Prof. Omid Kavehei

A thesis submitted in fulfillment of the requirements
for the degree of Master of Philosophy

Faculty of Engineering
School of Biomedical Engineering

2025

Statement of Originality

This thesis is submitted to The University of Sydney in fulfilment of the requirements of the Master of Philosophy. I hereby declare that the work presented in this thesis report has not been submitted, either in full or in part, for a degree at this or any other institution, and this is the result of my independent work. This thesis contains no material previously used by other users except where due references are included.

Leping Yu 08 Aug 2024

Abstract

This Master of Philosophy thesis explores the potential of using 3D printing technology to create a personalised ear-EEG device capable of measuring EEG signals within the human brain from the ear. The device features a tripolar electrode and can be customised to fit any ear shape, ensuring a comfortable fit for all patients. Another proposed solution is also made with low cost components.

To validate the performance of the ear-EEG device, various tests were conducted, including Auditory Steady-State Response (ASSR), alpha modulation, Passive Oddball (MMN), Active Oddball (P300), and Directional Hearing (N100). The results from these tests were analysed using different methods, demonstrating that the ear-EEG device performs comparably to traditional scalp-EEG in response to auditory stimuli. The findings also suggest that the device holds promise for applications in brain-computer interfaces (BCI) and seizure detection in the future development.

The future technologies and possible applications for the ear-EEG has been explored.

Acknowledgements

I would like to express my deep gratitude to Nano-Dimension, especially the DragonFly System support staff: Omer Tangi, Hodaya Hovesh, Amir Shelef, Murielle Sayada Lugassy, and Tomer Dahan, for their cooperation, close interaction, and invaluable assistance throughout the development of this work.

I also deeply appreciate my fellow students in the research group, especially Luis Fernando Herbozo Contreras and Zhaojing Huang. Their diverse knowledge backgrounds and support from various aspects have been instrumental in the progress of this project.

I extend my heartfelt thanks to my parents for their unwavering support and encouragement throughout my master's degree journey.

Finally, I am profoundly grateful to my supervisor for their continuous support and for providing me with the necessary resources to complete this work successfully.

Impact Statement

The company that I worked with in this project, Nano Dimension, is an Israeli company with an office in Sydney at the time I started my project. Unfortunately, our collaboration was severely and significantly interrupted by the terrible events of October 7th, 2023. This impact was to the extent that their Sydney office had to be closed, and I could not continue with the manufacturing of the device until after the initial submission of my thesis. I did communicate this with the University of Sydney at the time of submission, but it seems it was not considered, so I am adding this Impact Statement to clarify the depth and breadth of the impact on my work. Fortunately, I have been able to work with their US Office after my initial thesis submission and continued to finalise device manufacturing with them as they came back to work towards the end of last year (2024). Despite the unforeseen events and delays, I remained committed to the production of a quality Master's thesis. I thank again my primary supervisor, collaborators, and my family for helping me and supporting me through these challenges.

Declaration of Generative AI

During the preparation of this work, I used OpenAI's ChatGPT with full adherence to The University of Sydney's generative AI use policy in order to find useful online resources and to refine the academic language of my own original work. I understand that I am fully responsible for this publication's content, its scientific factual accuracy, and its presentation.

Contents

List of Tables

List of Figures

Chapter 1

Introduction

This research aims to develop a wirelessly portable electroencephalogram (EEG) device capable of recording EEG signals from within the patient's ear. EEG is a foundational tool in both neuroscience and clinical practice, used to measure the brain's electrical activity. Its applications span from Brain Computer Interfaces (BCIs) [3] to seizure detection and prediction.

1.1 Research Motivations

The investigation of brain activities employs diverse methodologies, including EEG and functional Magnetic Resonance Imaging (fMRI) [4]. EEG, a neurophysiological technique capturing electrical potentials within the human brain, is predominantly conducted via scalp electrodes due to its accuracy and capability to record multiple channels [5]. However, setup complexity, discomfort, and conspicuousness limit its utility for prolonged monitoring or BCI applications [6]. Traditional EEG systems typically rely on scalp electrodes for multi-channel EEG signal acquisition. Nevertheless, these systems face various challenges, including visibility issues, complex setup procedures, discomfort during long-lasting wear, and the overly complex nature of numerous wires [3]. Consequently, such systems prove unfeasible for extended monitoring periods or usage beyond laboratory or hospital settings [7]. To address these limitations, "ear-EEG" technology has emerged as an alternative solution.

Ear-EEG, which appeared in 2011, involves the placement of electrodes within the ear canal to capture EEG signals, offering several advantages over conventional scalp-based EEG setups [8]. First, ear-EEG setups are simpler in practice, as they require fewer electrodes, do not rely on strict placement according to the 10-20 system, and involve minimal preparation compared to conventional scalp-based EEG. Secondly, the ergonomic design of ear-EEG devices enhances wearer comfort, enabling prolonged usage without significant discomfort. Lastly, the discreet profile of ear-EEG renders it less conspicuous compared to traditional scalp-based systems, thereby promoting user acceptance and facilitating long-term monitoring endeavours.

Fig. 1.1 presents the electrode concept, which was manufactured using 3D printing.

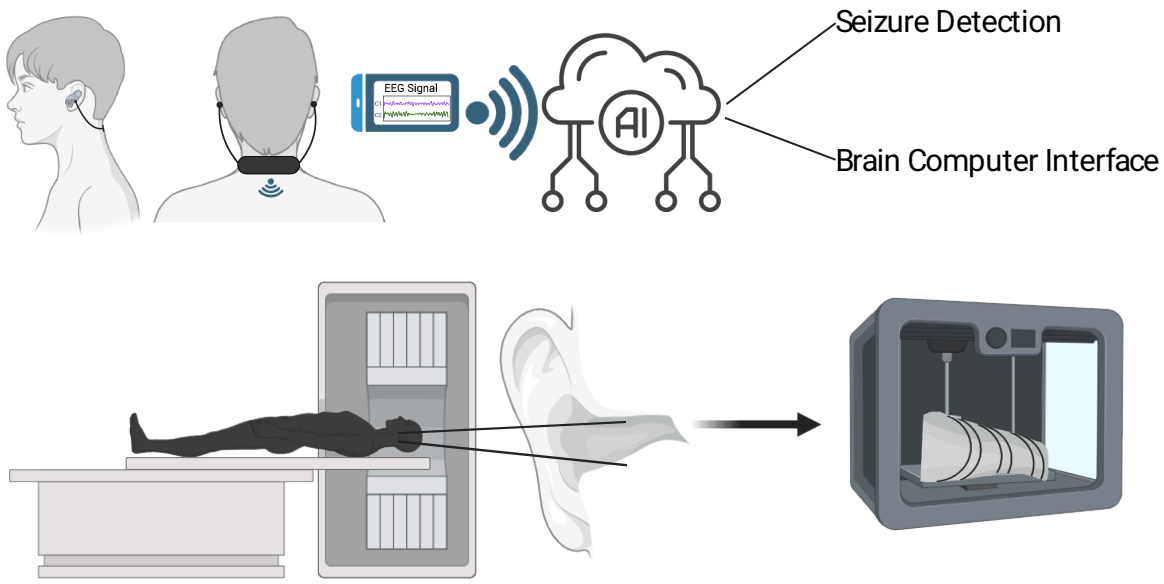

Figure 1.1: A three-dimensional (3D) model of the patient's ear canal can be obtained through a Computed Tomography (CT) scan. Subsequently, a personalised electrode will be fabricated based on the scanning results. This approach ensures that the electrode conforms to the unique curvature of the individual's ear canal, facilitating optimal contact and signal acquisition. The data can then be transmitted to the cloud through a smartphone for a brain-computer interface or seizure detection. The data acquisition component is positioned in the ear to capitalise on lower noise levels. Meanwhile, the system control and data transmission components are situated on the back of the neck for efficient management and communication.

While traditional scalp-EEG remains the clinical gold standard, its limitations in wearability, privacy, and long-term usability hinder real-world deployment. Thus, a growing body of research has explored alternatives such as ear-EEG. This research takes a step further by proposing a fabrication method using 3D printing, allowing the creation of custom-fitted in-ear devices. These devices aim to deliver high signal quality, user comfort, and long-term monitoring capacity suitable for seizure detection and BCI applications. A critical aspect of EEG-based seizure monitoring is the choice of montage, which refers to the configuration of electrodes and their referencing scheme. This setup significantly influences the quality of the recorded signals, spatial resolution, and susceptibility to artifacts.

1.2 Problem Statement

Despite the ear EEG has different advantages compared to other EEG technologies like scalp EEG or ambulatory EEG, ear-EEG faces several technical challenges right now. A primary barrier lies in the anatomical variability of the human ear canal, which makes standardised

electrode designs unsuitable for all users. Poor fit may lead to unreliable signal acquisition and reduced comfort. To overcome this, 3D printing has been explored to fabricate custom earpieces that conform precisely to the patient's anatomy.

However, current 3D-printed ear-EEG devices typically require multiple post-processing steps, such as embedding separate electrodes and soldering components, which make the whole procedure complex. Moreover, connecting the electrodes to the analog front end (AFE) often involves long, exposed wiring, increasing susceptibility to noise and reducing signal integrity. Therefore, this research aims to demonstrate the feasibility of simultaneously printing both the electrodes and circuit layout in a single integrated step using conductive materials. This approach reduces interconnect length, improves shielding, and enhances signal quality, all while allowing future adaptation to flexible materials for real-time clinical use.

1.3 Research Questions

This thesis investigates whether 3D printing can be leveraged to fabricate a compact, in-ear-EEG system with embedded electrodes as a *proof of concept*. Specifically, it explores:

- Can 3D printing enable custom-fit electrode designs that conform to the ear canal for optimal comfort and electrode–skin contact?
- Is it feasible to fabricate the EEG electrode housing in a way that allows direct integration with the analog front end, minimising wiring distance and improving signal quality?
- How does the ear-EEG signal quality compare to traditional scalp-EEG for capturing auditory evoked responses and other brain activity?

This research emphasises additive manufacturing as a tool for producing individualised EEG solutions. The long-term goal is to simplify the fabrication of user-friendly, wearable EEG systems optimised for real-world monitoring, without requiring complex post-processing steps such as integrating electrodes or attaching circuits.

1.4 Thesis Organizations

This thesis comprises 7 chapters:

1. Literature Review: This section will discuss the current literature in the field of ear-EEG, addressing the various necessities, solutions, and applications of ear-EEG technology.

2. Method: This section will detail the construction and manufacturing processes of the ear-EEG device.

3. Experiment and Data Processing: This section will describe the design of the experiments and the procedures for recording EEG signals to verify the performance of the developed ear-EEG device. This section will also explain the methods used to process the recorded EEG signals for further analysis.

4. Results: This section will present the performance results of the electrode.

5. Conclusion and Future Development: This section will summarise the findings and discuss potential future developments in-ear-EEG technology.

The content presented in chapter 2 and 6 are adapted from the submitted publication:

- L. Yu, L. F. Herbozo Contreras, Z. Huang, Y. Yang, B. Chan, and O. Kavehei, "Hearables: Bioelectronics Technological Challenges and Opportunities," accepted for publication in Wearable Technologies, 2025.

Statement of Contributions of Joint Authorship

- Leping Yu (Candidate):: Conceptualization; Methodology; Data Curation; Visualization; Writing – Review & Editing; Approval of Final Manuscript.
- Luis Fernando Herbozo Contreras: Visualization; Writing, Review & Editing; Approval of Final Manuscript.
- Zhaojing Huang: Visualization; Writing, Review & Editing; Approval of Final Manuscript.
- Yang Yang: Writing, Review & Editing; Approval of Final Manuscript; Resources.
- Bobby Chan: Writing, Review & Editing; Approval of Final Manuscript; Resources.
- Omid Kavehei: Conceptualization; Methodology; Visualization; Writing, Review & Editing; Approval of Final Manuscript.

In addition to the statements above, in cases where I am not the corresponding author of a published item, permission to include the published material has been granted by the corresponding author.

Leping Yu Date: July 19 2025

As supervisor for the candidature upon which this thesis is based, I can confirm that the authorship attribution statements above are correct to the best of my knowledge.

Dr. Omid Kavehei Date: July 19 2025

Chapter 2

Literature Review

2.1 Electroencephalography (EEG)

EEG signals reflect the summed postsynaptic activity of large populations of neurons, primarily in the cerebral cortex. These signals are generated by synchronised excitatory and inhibitory synaptic inputs that produce detectable voltage fluctuations on the scalp. Due to the spatial and temporal summation of these signals, EEG captures the brain's dynamic electrical activity in a non-invasive manner [9].

There are typically three kinds of electrodes that can be used: dry, semi-dry, and wet electrodes for recording EEG signals. Wet electrodes require the application of a conductive gel before use, which ensures a good connection with the scalp but can be messy and time-consuming to apply. Semi-dry electrodes use a small amount of liquid or gel, reducing setup time and improving user comfort. Dry electrodes, on the other hand, do not require any gel and are, therefore, the most suitable for daily monitoring applications due to their ease of use and minimal preparation time. However, dry electrodes provide lower signal quality compared to wet electrodes [10].

A typical EEG recording system consists of several key components that work together to capture and preprocess brain signals. Electrodes are sensors that are used to capture electrical activity, commonly made from materials like silver/silver chloride (Ag/AgCl) due to their high conductivity so that the impedance between skin-electrode interface can be reduced [1]. The captured signals, typically in the range of 10 μV to 100 μV, are then amplified using differential amplifiers to ensure adequate signal strength while minimising noise [11]. Analog Front-End (AFE) circuits further refine the signals through filtering, removing unwanted frequency components to improve the signal-to-noise ratio. The Analogue-to-Digital Converter (ADC) digitises the continuous signals for further processing [12]. Once digitised, the signals are transmitted through data transmission systems, which can be wired or wireless, utilising protocols such as Bluetooth or Wi-Fi for real-time monitoring. The processing and storage

unit applies advanced signal processing techniques, including filtering, artifact removal, and feature extraction, before storing the data for further analysis. Finally, a power supply ensures stable operation, with battery-powered designs being crucial for portable and wearable EEG applications. These components collectively enable reliable EEG acquisition, making the technology suitable for clinical diagnostics, brain-computer interfaces, and long-term neurophysiological monitoring.

EEG is usually recorded using standardised electrode placements, such as the international 10-20 system [13]. This system ensures consistent electrode positioning between subjects and studies, enabling reliable spatial localisation of neural activity. It forms the basis for both clinical EEG and research applications, serving as a reference for comparing new electrode designs, such as ear-EEG, to traditional scalp-EEG. The 10-20 system uses letters and numbers to represent different regions. The letters used in the 10-20 system represent different cortical regions, where F stands for frontal, T for temporal, C for central (a non-anatomical reference used for symmetry), P for parietal, O for occipital, and Fp for frontal pole; electrodes positioned along the midline are labelled with a z, such as in Fz, Cz, Pz, and Oz, where z denotes the midline ("zero") axis [13]. The numbers in the 10-20 system indicate the lateral position of the electrodes, with odd numbers placed on the left side of the head and even numbers on the right; smaller numbers are positioned closer to the midline, while larger numbers are located more laterally [13]. The 10-20 system can be seen from Fig. 2.1.

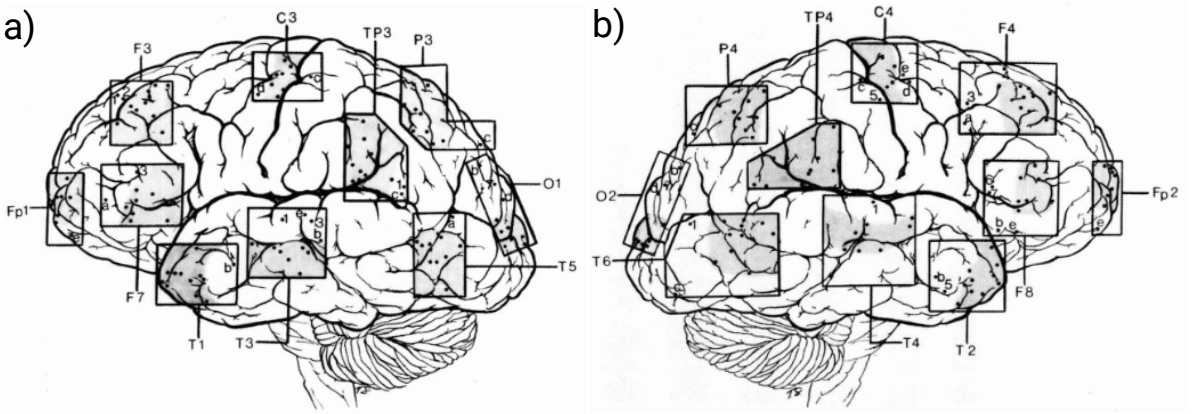

Figure 2.1: The international 10-20 system for EEG electrode placement. Electrodes are positioned according to fixed percentages of the head's surface dimensions, ensuring reproducible and standardised measurements across individuals. (a) Left lateral view of the head, (b) Right lateral view of the head. *Reprinted from [14]. Permission for non-commercial use in a research thesis is granted by the publisher, Taylor & Francis Group.*

EEG signals can be categorised into five different frequency bands: Delta, Theta, Alpha, Beta and Gamma [1]. The corresponding band and related states can be seen from table 2.1. In order to detect the abnormalities within the EEG signal, different approaches have been applied, encompassing both traditional signal processing techniques and advanced machine learning approaches. One example is the Neurophysiological Biomarker Toolbox (NBT) which is an open-source MATLAB toolbox that facilitates the computation and integration of neurophysiological biomarkers derived from EEG data [15]. Recent progress has also led to the use

of artificial intelligence (AI) to find or forecast cognitive decline by looking at brain wave patterns collected while people sleep.

Table 2.1: EEG Frequency Bands and Their Associated States [1].

Band	Frequency Range	Associated states (by examples)
Delta	0.5–4 Hz	Deep sleep and unconscious states
Theta	4–8 Hz	Drowsiness, meditation, and early stages of sleep
Alpha	8–12 Hz	Relaxed wakefulness; often observed during resting states
Beta	12–30 Hz	Active thinking, problem-solving, and focus
Gamma	>30 Hz	Higher cognitive functions such as perception and complex problem-solving

2.2 Ear-EEG

2.2.1 Needs for ear-EEG

Scalp-EEG has long been recognised for its superior signal-to-noise ratio and capability to record multiple channels simultaneously compared to other recording methods like portable EEG recording methods or other methods like functional near-infrared spectroscopy (fNIRS) [16]. However, its practical application for daily monitoring is limited by the requirement for numerous wires for each electrode and the use of wet electrodes, which are necessary to maintain signal quality but result in a complex setup procedure. To address these challenges and facilitate routine EEG monitoring, ambulatory EEG (aEEG) technology has been developed. aEEG enables continuous, prolonged recording of EEG data, making it suitable for long monitoring periods [17]. aEEG typically has a battery life of 24 to 72 hours per charge [18]. Since its inception in 1983, commercially available aEEG systems have supported 8-channel continuous EEG recording with digital time and event markers, allowing clinicians to monitor brain activity trends over extended periods and correlate them with clinical events such as seizures or medication administration [19, 20]. aEEG has demonstrated a high diagnostic yield of 72%, providing valuable information for patient management. This non-invasive method is particularly useful for characterising non-epileptic events, clarifying uncertain epilepsy diagnoses, and quantifying spikes and seizures, thereby enhancing medical management [18].

Despite these advancements, the widespread adoption of aEEG remains limited, primarily due to discomfort and social acceptability issues that hinder long-term use. One notable issue is cosmetic acceptability, as noted in Seneviratne and D'Souza [17]. While modern aEEG devices are lightweight and portable, the requirement for electrodes to be affixed to the scalp remains a cosmetic concern for some patients. This aspect of visible electrodes can contribute to feelings of discomfort and unwillingness among individuals, discouraging them from using long-term EEG monitoring. Additionally, research such as Schulze-Bonhage et al. [22] has highlighted other barriers to accepting conventional scalp-EEG for extended monitoring.

Figure 2.2: aEEG devices offer compact, portable solutions for long-term brain monitoring, enabling EEG signal acquisition outside of traditional hospital settings. However, the design of the headset does not yet provide sufficient comfort for long-term wear. Adopted from [21], licensed under CC BY 4.0.

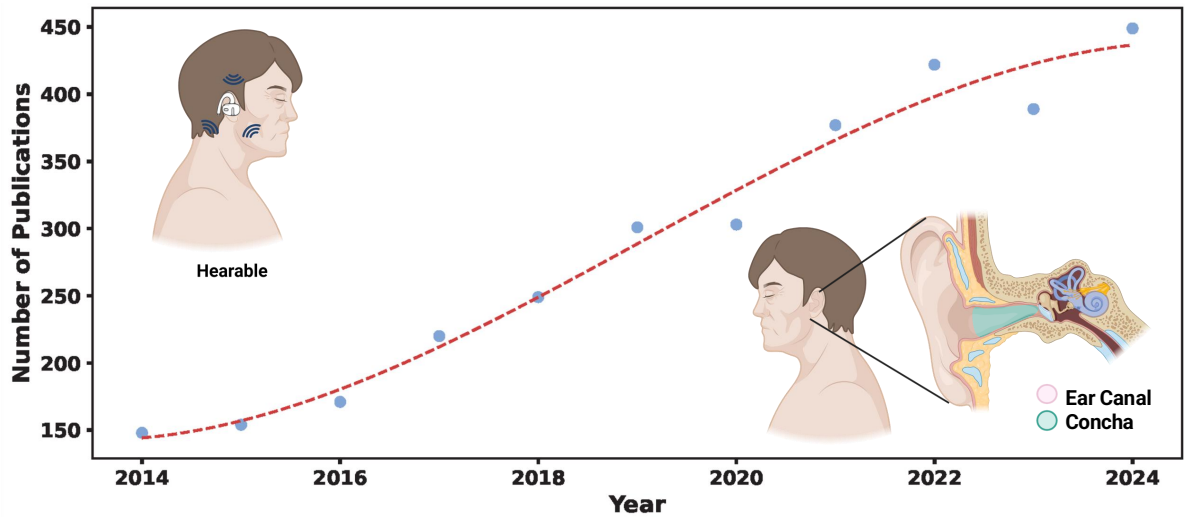

Figure 2.3: Hearables represent a promising direction for wearable technology by leveraging the unique anatomical features of the ear, such as the concha and ear canal. These regions support discreet, comfortable, and stable sensor placement, enabling long-term physiological monitoring. The increasing research interest in ear-based wearables underscores their potential for personalised, low-power, and socially integrated health solutions.

Among these are concerns related to social ackwardness due to the visible nature of scalp electrodes, which can be associated with medical conditions and lead to social discomfort. Moreover, the physical discomfort caused by multiple electrodes on the scalp, including possible irritation and inconvenience, further undermines the further applications of long-term EEG monitoring among patients. Macea et al. [23] conducted a survey examining the use of portable EEG devices. They identified key challenges in patient compliance, pointing out that individuals often hesitate to use the devices during holidays, likely due to disruptions in routine or discomfort [23]. Additionally, skin-related side effects, such as irritation caused by prolonged contact with electrodes, further contribute to reluctance to use portable EEG devices [23]. Adding to it, the device setup, including applying conductive gel into the electrode of the EEG device, is also complex and may require professionals to deal with it. These factors underscore the need for ongoing technological advancements and personalised approaches to enhance the acceptance and adoption of EEG monitoring in clinical practice. Hearables, introduced by Nick Hunn [24], were initially designed to measure biosignals within the ear canal, making them a unique wearable technology for healthcare and wellness applications. In comparison with other wearable technologies such as smartwatches and fitness trackers, hearables are uniquely suited for sensing brain signals, particularly EEG. While devices like smartwatches typically focus on cardiovascular metrics such as photoplethysmography (PPG) or electrocardiography (ECG), the ear is not an optimal site for these modalities due to anatomical and signal quality limitations. Instead, hearables are primarily designed for EEG acquisition, offering low spatial resolution brain signal monitoring in a compact and discreet form factor. This allows for comfortable, all-day wear without attracting attention or requiring special adjustments [25]. Although ECG and PPG can also be recorded by hearables, these signals are typically used as auxiliary data to support context-aware interpretation of EEG. A comprehensive comparison of hearables and other wearable technologies, including their respective sensing capabilities, advantages, and limitations, is provided in Table 2.2. Beyond their suitability for EEG sensing, hearables also take advantage of the ear canal's unique auditory of the ear canal, providing a stable and unobtrusive site for long-term monitoring with fewer motion artifacts than wrist- or chest-mounted devices [26]. In the future, hearables are expected to expand from single-modality EEG recording to multimodal systems that integrate brain signals with acoustic information, motion tracking, and complementary physiological measures, enabling more comprehensive, context-aware health and cognitive monitoring. Key directions include personalised ear-mould fabrication, ultra–low-power on-device AI, and robust clinical validation frameworks, all of which will be essential for transitioning hearables from experimental prototypes into widely adopted healthcare technologies.

Various approaches have been investigated to realise portable EEG systems, including innovative sensor placements, such as on smartwatches [27], and advancements in sensor and hardware designs. Among these, ear-EEG has emerged as a standout option due to its unique advantages. Placed within the ear canal, it offers a discreet, non-invasive, and comfortable solution while ensuring high-quality signal acquisition. The ear-EEG approach is particularly advantageous for daily use, as it combines convenience with reliable performance. Its compact and user-friendly design makes it well-suited for applications requiring long-term monitoring, such as brain-computer interfaces and seizure detection [28]. These characteristics highlight

Table 2.2: Comparison of Standard, Wearable, Invasive, and Hearable Devices for Brain Signal Sensing.

	Standard [1]	**Other wearables** [2]	**Invasive** [3]	**Hearable**
Portability	Poor	Medium	Excellent [4]	Good
Battery Life	Plugged-in	Low (hours)	Varies [5]	Enough (a day)
Wear Comfort	Very low	Low to medium	n/a [6]	High
Ease of Use and Wear	Difficult	Easy	n/a [6]	Easy
Cost	High to very high	High	Very high	Low
Long-Term Use (Months)	Very limited	Limited	Excellent	Good

[1] Standard refers to clinical-grade systems, such as traditional scalp or surface EEG in all forms of wet or dry electrodes.

[2] Other wearables refer to wearable devices other than hearables, such as research-grade EEG, mainly in dry electrodes form.

[3] Invasive refers to the invasive device, such as long-term brain implants (e.g., NeuraLink device) or endovascular electrocardiography, ECoG (e.g., Synchron's Stentrode), or short-term intracranial electroencephalography (iEEG), also known as ECoG.

[4] Mainly depends on the external companion of an implantable brain interfacing device. For example, NeuraLink's device does not have a companion that needs to be worn continuously, or Synchron's device's external companion sits on the patient's chest.

[5] Some brain (recording or sensing) interfacing implants are battery powered with recharge capability (e.g., NeuraLink's device with more than 1,000 electrodes), but many are harvesting energy from a source outside the body (e.g., radio-frequency energy harvesting solution), which means there is no internal battery.

[6] For invasive brain interfacing solutions, this mainly relates to the wearable companion device or external unit which is either magnetically or using skin adhesive is placed right above the implanted device in an easy and not complicated way.

ear-EEG's potential as a transformative tool in both clinical and consumer contexts. This placement not only enhances cosmetic acceptability but also improves the overall user experience by reducing the physical discomfort associated with traditional scalp electrodes. The ear canal's unique anatomy can provide stable electrode placement, improving signal quality and consistency over extended monitoring periods. Furthermore, the development of ear-EEG systems can leverage advancements in miniaturisation and wireless technology, enabling seamless integration with mobile devices and wearables. Compared to smartwatch EEG systems, ear-EEG offers a significant advantage due to its proximity to the brain. This closer placement allows ear-EEG devices to capture neural signals with greater fidelity, reducing the influence of other biopotentials such as ECG, which can interfere with signal quality in more distal placements like the wrist [29]. The anatomical location of the ear canal provides a natural shield against muscle and motion artifacts, further enhancing the Signal-to-Noise Ra-

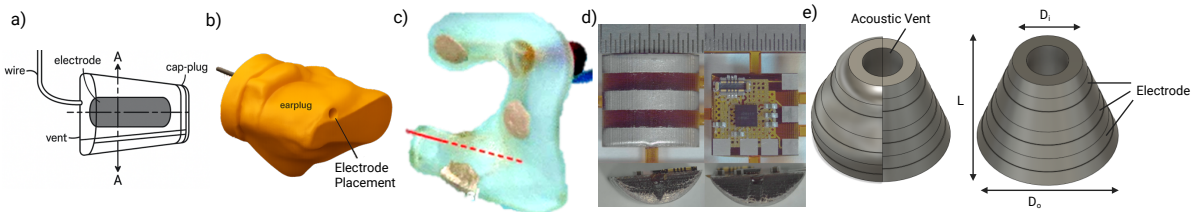

Figure 2.4: Various types of ear-EEG electrodes developed in the field. (a) Generalized electrode design based on common ear-hub [30]; (b) Earhub-style electrode produced by moulding [31]; (c) Earhub-style electrode with an integrated auricle holder [28]; (d) Single-piece design combining the ear electrode and circuit board (Our ear-EEG) [32] (e) 3D model of the integrated electrode and circuit board, featuring adjustable parameters including D_{o} (outer diameter), D_{i} (inner diameter), and L (length) as well as customizable electrode shape and curvature. This design enables on-demand manufacturing tailored to individual anatomies across different age groups and genders. Also, the rigid structure ensures a durable and reliable product suitable for everyday life.

tio (SNR) [29]. These benefits make ear-EEG particularly suitable for applications requiring precise neural data, such as BCI, cognitive state monitoring, and seizure detection. This integration can facilitate real-time data transmission and remote monitoring, making it easier for healthcare providers to continuously track patients' EEG data and intervene promptly when necessary.

2.2.2 Ear-EEG Electrode

Ear-EEG technology records EEG signals from within the ear canal, offering a more practical and discreet alternative to conventional scalp-EEG, which requires extensive setup, equipment, and is unsuitable for daily wearability [31]. However, the anatomical variability of the human ear presents challenges to using standardised ear-EEG electrodes, often leading to inconsistent performance. To address this, electrodes must either be flexible enough to adapt to individual ear shapes or be manufactured into customised forms. For ear-EEG electrodes, several key features are essential to ensure effective signal acquisition. The electrode–skin interface impedance must be low to minimise noise, the contact surface area should balance stability with comfort, and the material must be biocompatible and durable for long-term use. Finally, conformability is crucial so the electrode fits each user's ear without causing discomfort.

To address these issues, generalised ear-EEG electrodes have been developed and designed to fit everyone. Such electrodes are typically constructed from flexible materials, enabling them to compress and expand to conform to the unique shape of an individual's ear canal. This adaptability ensures a secure fit, enhancing signal quality and user comfort during prolonged use. This approach is favoured due to its straightforward manufacturing process, which simplifies production while offering a "one-size-fits-all" solution. For instance, Goverdovsky et al. [33] designed an ear-EEG electrode using a foam substrate that can adapt to the shape of the

ear canal. This design features two electrodes and two microphones for applying stimulation. The choice of material effectively mitigates motion artefacts arising from both minor and substantial mechanical deformations of the ear canal walls [33]. This electrode design also incorporates the use of two microphones to capture acoustic signals traversing through dense head tissues and use these signals to cancel the motion artefacts in the EEG signal [33]. Similarly, Juez et al. [34] utilised conductive silver fabric, foam earplugs, heat-shrinkable tubing, and copper wire to construct a generalised electrode as a regular earhub shape with an analog front end of an OpenBCI Cyton board sampled at 250 Hz. To address the issue of long manufacture time and short lifespan for personalised ear-EEG electrodes, Liang et al. [35] developed a method using impressions which are negative mould into which material is injected, to create a generalized ear-EEG device based on average ear measurements at three key anatomical landmarks: the aperture, isthmus, and canal length. Ge et al. [36] developed an EEG electrode with hydrogels to achieve the feature of both low impedance and high longevity. However, the recording effort of the generalised ear-EEG might vary significantly due to the use of elastic materials. The fact that these electrodes rely on the plastic material's tension means the electrode's connection and the impedance between the electrode and the ear canal will vary. While plastic materials can expand and contract to accommodate a certain range of sizes, their adaptability is inherently limited. This limitation arises due to the natural variance in human anatomy, particularly in the ear canal, which differs in shape and size across individuals. As a result, a one-design-fits-all approach may not be sufficient for ensuring a secure, comfortable fit and long durability, potentially impacting both user experience and signal quality. The limited size of the ear canal presents a challenge, as all electronic components must fit within a restricted space [37]. Additionally, because the device is intended for daily wear, comfort is a critical consideration. Another challenge arises from the significant anatomical variability in ear canals across individuals, necessitating that the electrode design be adaptable for a customised fit for each patient. Currently, various studies are exploring these issues, focusing on miniaturising components, enhancing comfort through ergonomic designs, and developing personalised solutions to accommodate diverse ear canal anatomies.

Table 2.3: Comparison between different ear-EEG electrodes.

Ref	Modality	Electrode Number	Impedance (kΩ)	Sampling Rate (Hz)	Electrode Material	Dry / Wet	Signal Type	Data Telemetry	Verification	Novelty
[33]	EEG, ECG, motion artifacts	2	<10	1200	Cloth electrode with Conductive Thread	Wet	Analog	Wire	SSVEP[1], ASSR[2], VEP[3], Alpha rhythm	Detect motion artifacts
[34]	EEG	6	-	250	Conductive fabric of silver	Wet	Analog	Wire	Alpha rhythm	Electrode made by conductive fabric
[35]	EEG		35 and 45	500	AgCl	Dry	Analog	Wire	Alpha rhythm, ASSR[2], VEP[3], MMN	Expression moulding by average measuring of the ear
[38]	EEG	3	<134.27	-	Conducting Au Wires and Insulating Polyimide (PI)	Dry	analog	Wire	SSVEP[1], auditory decoding	Extendable spiral structure that can adapt to the subject's ear

Continued on next page

Table 2.3 continued from previous page

Ref	Modality	Electrode Number	Impedance (kΩ)	Sampling Rate (Hz)	Electrode Material	Dry / Wet	Signal Type	Data Telemetry	Verification	Novelty
[36]	EEG	1	<3	1000	HPMC in PVA matrix	Semi-dry		Wire	Attention of the testers	High-conductivity, low-impedance, biologically adaptable hydrogel
[39]	EEG	10	<20	500	Ag/AgCl	Gel	Digital	BLE[4]	Attention modulation of the ERP	Around ear-EEG
[40]	EEG	6	435	500	IrO_2	Dry	Analog	Wire	ASSR[2], SSVEP[1], Alpha rhythm	-
[3]	EEG, EMG	4, 2 ref	-	-	Silver	Dry	Digital	BLE[4]	EOG, Alpha rhythm, ASSR[2]	Generalized 3D printed silver dry electrode
[41]	EEG	1	-	250	Silver coated plastic	Gel	Analog	Wire	PVT	-
[42]	EEG	4	<5	512	Highly Porous Platinum	Dry	Analog	Wire	Alpha rhythm	Low impedance platinum dry electrode
[43]	EEG	6	<20	1200	Silver	Gel	Analog	Wire	ASSR[2], PTA	-
[44]	EEG	6 each ear	-	200	Silver	Gel	Analog	Wire	ASSR[2], PSG	-

Continued on next page

Table 2.3 continued from previous page

Ref	Modality	Electrode Number	Impedance (kΩ)	Sampling Rate (Hz)	Electrode Material	Dry / Wet	Signal Type	Data Telemetry	Verification	Novelty
[45]	EEG	2, 1 ref, 1 ground	-	1000	-	Dry	Digital	BCC[5]	ASSR[2]	Wireless transmission using BCC
[46]	EEG	15	-	500	IrO_2	Saltwat	Analog	Wire	ASSR[2], SSVEP[1]	Large electrode number
[47]	EEG, EOG, lactate conc.	3 EEG, 1 Ref, 1 DRL	386	500	Stretchable silver (Ag) ink	Dry	Digital	BLE[4]	Alpha modulation, ASSR[2], Eye movement, lactate sensing	Multisensor ear-EEG

[1] SSVEP: Steady-State Visual Evoked Potential.
[2] ASSR: Auditory Steady-State Response.
[3] VEP: Visual Evoked Potential.
[4] BLE: Bluetooth.
[5] BCC: Body Channel Communication.

Researchers have increasingly employed 3D printing technology to optimise EEG signal acquisition within the ear-EEG domain. By utilising the feature of the additive manufacturing method, certain shapes can be formed and therefore a good fit of the ear canal can be achieved. Notable advancements, such as those by Kaveh et al. [3], demonstrated the development of personalized wireless ear-EEG electrodes using 3D-printed moulds, which are shown in Fig. 2.5. It enables the manufacture of both personalised electrodes and generalised electrodes. Despite these advances, the process often involves additional steps, including casting and chemical treatments, to apply conductive material onto the electrode surface, therefore causing the manufacturing procedure to be complex. Jeong and Jeong [41] used 3D printing to create impressions of the ear canal with mouldable plastic beads and applied silver paste to make them conductive. Mikkelsen et al. [44] used soft silicone to build earplugs and silver buttons as electrodes with copper wires soldered onto them, employing this device for automatic sleep staging. Tabar et al. [48] employed 3D printing to create customised ear-EEG electrodes, enhancing user comfort and signal accuracy. While 3D printing enables customised and anatomically conformal designs, it often falls short in integrating functional materials such as conductive layers directly into the print. This typically requires post-processing steps like coating, casting, or manual assembly, which increase complexity and reduce scalability.

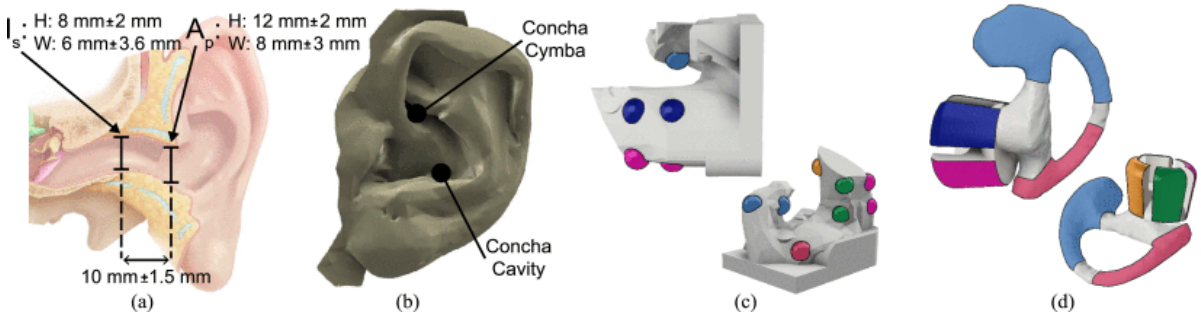

Figure 2.5: (a) Illustration of the ear canal with average anatomical measurements based on references [49] and [50]. (b) High-resolution 3D scan of an individual subject's ear. (c) Custom-fit earpiece designed for the scanned ear in (b), shown from two different angles with correlated electrode pairs highlighted in matching colours. (d) User-generic earpiece with electrodes colour-coded to correspond to the electrode groups shown in (c).

Furthermore, Wang et al. [38] developed an ear-EEG electrode with an extendable spiral structure that can expand under electrothermal actuation and conform to an individual's ear canal, exploring the possibility of using this device as a visual or auditory BCI. The figure of this device is shown in Fig. 2.6. This electrode features a dual-layer design, encompassing shape memory polymers (SMPs) containing an Electrothermal Actuation Layer (EAL) and an EEG Detection Layer (EEGDL). The EEGDL comprises Au wires and insulating polyimide (PI) [38]. A noteworthy feature of this electrode design is its capability to expand and spiral within the auditory meatus upon applying heat, enabling it to seamlessly adapt to the unique curvature of the auditory meatus during the expansion process, resulting in a customised fit tailored to the individual's anatomical features.

An alternative approach for creating personalised ear-EEG electrodes involves incorporat-

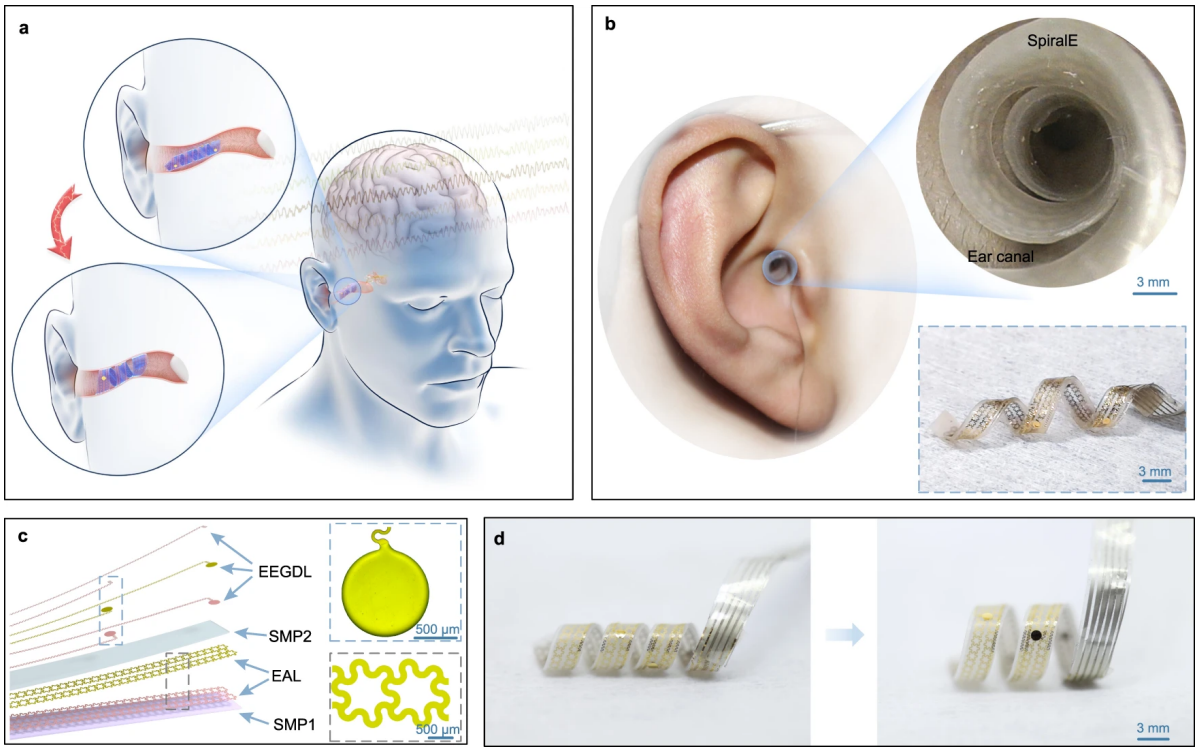

Figure 2.6: Schematic illustration (a) shows the in-ear-EEG recording mechanism of SpiralE. Photographs (b) demonstrate how SpiralE conformally adapts to the inner wall of the ear canal, with the upper-right inset showing an endoscopic image of the device in place and the lower-right inset revealing its complex 3D structure after removal. Panel (c) presents an exploded-view schematic of SpiralE's functional layers, with insets displaying the EEGDL and the EAL. In panel (d), SpiralE is shown in its temporarily fixed shape (left) and after recovery to its permanent shape with a larger radius (right). While this device can adapt to the specific curvature of a user's ear, its durability may be limited due to the need for shape adjustment with each use. Adopted from [38] Licensed under CC BY 4.0.

ing standard electrodes into custom-moulded soft earpieces. For instance, Kappel et al. [40] developed a dry ear-EEG system using an IrO_2-coated titanium substrate electrode and elastic earmold silicone. To achieve superior signal quality, Kappel and Kidmose [46] designed a high-density ear-EEG system comprising 15 electrodes per ear, yielding results comparable to or surpassing those of scalp-EEG in certain assessments including ASSR and SSVEP with a distance of 10mm in between different electrodes, with IrO_2 as the electrode material. Bech Christensen et al. [43] used 3D printing to manufacture the ear canal model and installed six silver electrodes for objective threshold estimation.

2.2.3 Front End

Additional technologies, such as around-ear-EEG systems, have been developed to investigate optimal electrode placement. Bleichner et al. [39] created an around-ear-EEG system using several layers of biocompatible polyimide, with conductive components consisting of gold-plated ends, pure copper traces, and conductive Ag/AgCl-based polymer thick film ink. The

device is shown in Fig. 2.7.

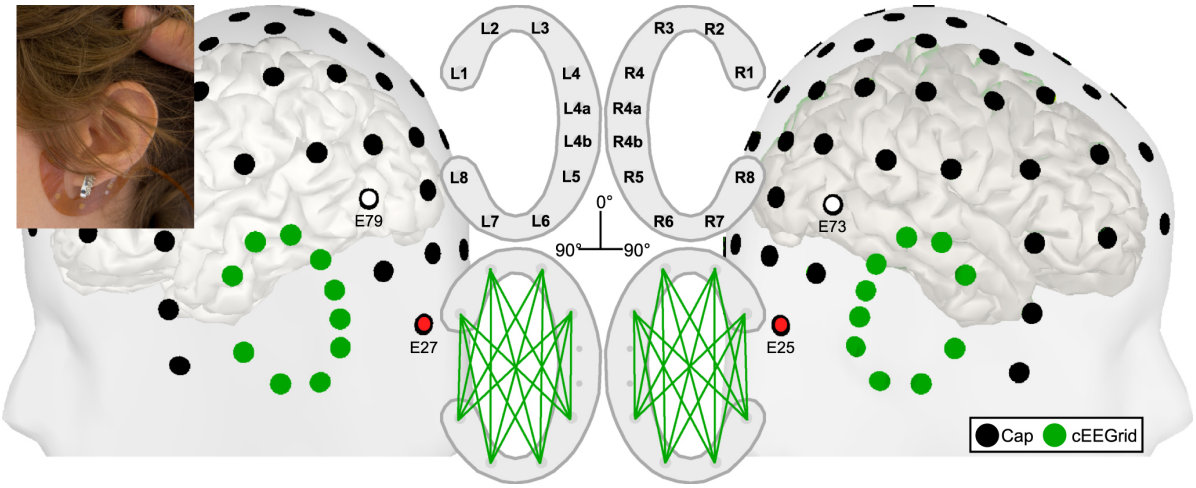

Figure 2.7: The electrode position for scalp-EEG (black), ear-EEG (green), and reference (red). Adopted from [39] Licensed under CC BY 3.0.

After gathering the data from the electrode, it is necessary to pre-process the signal and convert the signal from analog domain into digital domain and send it onto a host device for further applications. While an AFE is often necessary to convert the analogue signal into digital form to enhance the ear-EEG devices' portability, integrating the circuit board in a natural and unobtrusive manner presents another challenge [51]. Methods to reduce the device's visibility are required. Bleichner et al. [52] developed an ear-EEG system with an analogue front end integrated into the back of a hat.

There is an emerging need to integrate the analog front end directly onto the printed electrode, further to augment the functionality and discretion of ear-EEG electrodes [53]. This approach minimises the electrode's size and visibility while optimising signal reception. Integrating the analogue front end with the ear-EEG electrode makes it possible to achieve a less obtrusive and more efficient EEG recording system. This integration streamlines the manufacturing process and enhances the performance and user experience of ear-EEG technology.

Different sensors are also integrated into the ear-EEG piece to gather additional information for medical and research use. Xu et al. [47] developed an in-ear integrated array of multi-modal electrophysiological and electrochemical sensors that can sense the EEG, Electrooculography (EOG), and lactate concentration for this purpose. The figure of this device is shown in Fig. 2.8. This demonstrates the feasibility of integrating multiple sensors into a single device, enabling the collection of diverse biosignals. Such a multi-sensor approach enhances the device's capacity to provide comprehensive physiological data, facilitating advanced applications such as personalised health monitoring, real-time diagnostics, and sophisticated data analysis for medical and research purposes.

Seamlessly integrating the complete AFE and the microcontroller (MCU) into a single earpiece to facilitate the wireless transmission of digital signals to a designated device remains a substantial challenge in this field [54]. This challenge is further accentuated by the ne-

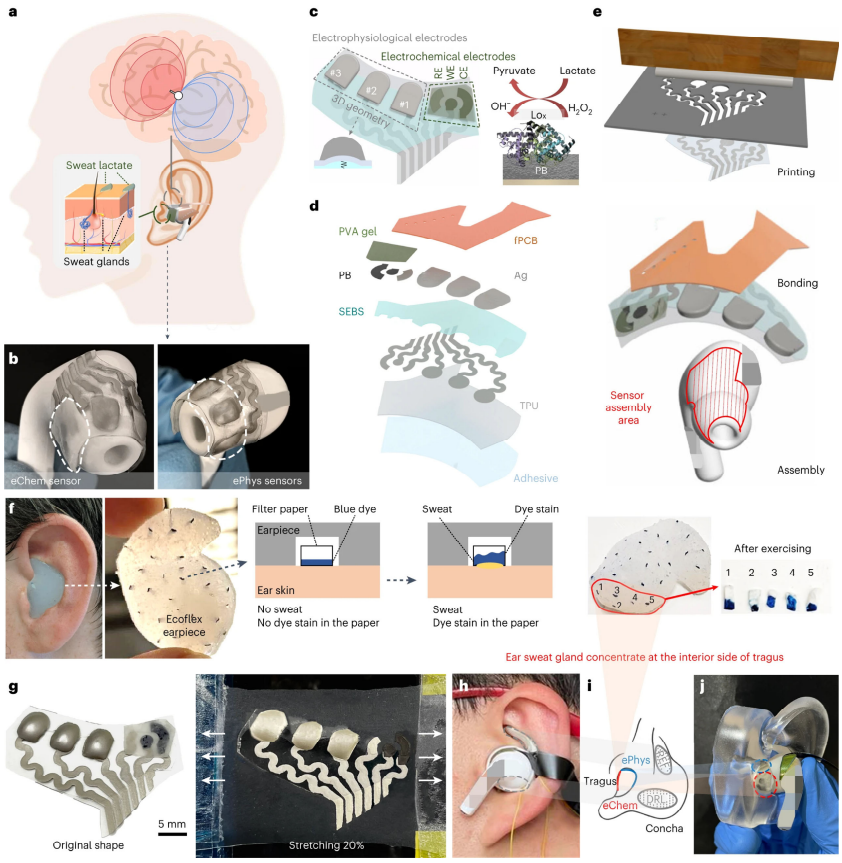

Figure 2.8: a. Schematic diagram of the in-ear sensor system, with grey and green dashed lines indicating the locations of the EEG and electrochemical (sweat-sensing) electrodes, respectively. b. Photograph of the fully assembled in-ear device featuring both electrophysiological (ePhys) and electrochemical (eChem) sensors. White dashed lines mark the positions of each sensing site. c. Sensor layout (left), highlighting the 3D cushioning beneath the ePhys electrodes and the mechanism of sweat lactate sensing. The working electrode surface is coated with LOx, which catalyses lactate into pyruvate and H_2O_2. The Prussian blue (PB) layer converts H_2O_2 into OH^-, producing a current proportional to lactate concentration. d. Cross-sectional layer structure of the device, consisting of (from bottom to top): adhesive, thermoplastic polyurethane (TPU), SEBS elastomer, Prussian blue, stretchable silver (Ag), PVA hydrogel, and a flexible printed circuit board (fPCB). e. Sensor fabrication workflow, which includes sensor printing, electronics integration, and final assembly onto earphones. f. Mapping of sweat secretion inside the ear using an Ecoflex mould with embedded filter paper indicators to visualise sweat distribution. g. Images of the sensors before and after 20% lateral stretching to demonstrate mechanical flexibility. h. Photograph of the complete device worn in the ear. Grey dashed lines mark the REF and DRL electrode locations for EEG. i. Design geometry of the ePhys, REF, DRL, and eChem electrodes. j. Skin contact points of both ePhys and eChem sensors visualised using an ear phantom model. Although the device conforms to the unique curvature of each user's ear, its durability may be compromised by the repeated deformation required during each use. Adopted from [47] Licensed under CC BY 4.0.

cessity of minimising the distance between the electrode and the analogue front end and the size of the auditory meatus [55]. One suggested approach entails the strategic distribution of electrical components around the external ear rather than direct insertion into the ear canal

[3]. However, even with this approach, the visibility of these components remains noticeable, potentially causing social discomfort. In practical scenarios, this situation might require additional accessories, such as a hat, to effectively conceal the components.

While integrating all necessary electronics into a compact ear-EEG device is technically challenging, it is becoming increasingly achievable according to recent developments in the field. One promising approach reported in the literature is the use of Application-Specific Integrated Circuits (ASICs), which enable high performance and low power consumption in a miniaturised form factor. Although the cost of producing ASICs in small quantities can be high, ongoing advancements in electronics manufacturing and component miniaturisation are steadily reducing these barriers. These trends suggest that integrating the required components directly into ear-EEG devices is becoming feasible, paving the way for more compact, wearable, and unobtrusive neural recording systems.

Ensuring that users can still capture environmental sounds is crucial for most electrodes. A hollow structure is often applied to ensure the patient can hear surrounding sounds effectively.

2.2.4 Ear-EEG Signal Processing

Processing EEG signals is vital to enhancing the signal-to-noise ratio (SNR), ensuring their reliability for applications such as on-chip learning and seizure detection. Key techniques include filtering to eliminate noise and artifacts, segmentation to focus on specific events, and feature extraction to emphasise critical signal patterns. These steps collectively enable precise analysis and informed decision-making. In portable EEG systems, various AFE designs have been proposed to improve signal quality, such as using active electrodes. However, the size constraints inherent to ear-EEG devices pose challenges for implementing complex circuit designs. To address this limitation, an integrated circuit (IC) analog front-end offers a promising solution, potentially delivering better performance within the compact form factor required for ear-EEG applications [56]. Given the small size of ear-EEG devices, there is limited space for the analogue front end and the battery. Consequently, a low-cost and compact analog front end is required to meet the needs of long-term daily EEG monitoring.

To address these constraints, various low-cost and efficient solutions have been developed. For instance, Teversham et al. [57] designed a low-cost ear EEG system using an ESP32 microcontroller as the central controller. The analogue front end of this system includes a bandpass filter, differential amplifier, and notch filter, achieving a total cost of around £20. This device demonstrated real-time decoding of Steady-State Visual Evoked Potentials (SSVEPs), highlighting its potential for cost-effective and practical EEG monitoring applications.

Utilising existing devices for additional signal processing offers a practical solution to save space and enhance portability in compact systems. For example, Hölle and Bleichner [58] introduced a setup comprising a commercial amplifier, generalised ear-EEG electrodes, and a smartphone for sound analysis in everyday environments. This device utlises the compu-

tational capabilities of a smartphone for advanced signal processing, reducing the need for complex hardware within the EEG system itself [58]. Such integration demonstrates the potential for smartphones and similar devices to handle resource-intensive tasks, enabling efficient, real-time analysis while maintaining the compactness and usability of wearable EEG solutions.

In addition to cost considerations, power efficiency is crucial for the practicality of ear-EEG systems. Lee et al. [45] developed a low-power consumption system that utilises body channel communication which is the method that utilises the human body to carry signals [59]. These advancements underscore the ongoing efforts to create cost-effective, efficient, and user-friendly ear-EEG systems suitable for diverse applications.

Specific chips tailored for ear-EEG applications focus on optimising high input impedance and low noise to effectively capture delicate bioelectrical signals, essential for wearable EEG solutions in various environments. This innovation ensures robust signal acquisition, critical for minimising interference in ear-EEG devices, making them suitable for real-world applications. In addition, Jin et al. [60] developed a low-power consumption EEG analog front-end ASIC, designed to support portable EEG devices. The low power consumption aspect is especially valuable for wearable applications where battery life is a constraint [60].

AI further enhances the capabilities of ear-EEG devices by improving signal processing and interpretation. Mai et al. [61] integrated a 1D-Convolutional Neural Network (1D-CNN) model onto an embedded system, utilising Fast Fourier Transform (FFT) and Power Spectral Density (PSD) for emotion classification. This integration demonstrates how AI can process complex EEG data in real-time, providing valuable insights into emotional states and other cognitive functions. Jayas et al. [62] introduced an algorithm designed to detect EEG signal segments contaminated by artifacts such as electrooculogram (EOG) or electromyogram (EMG) signals. This method aims to improve EEG data quality by isolating and identifying these noisy segments for better analysis and application.

Additionally, AI has been applied to specific medical applications of ear-EEG. Torres Gaona et al. [63] developed an on-device AI-based seizure detection model utilising ear-EEG data. This system was part of the SERAS-EEG study, which prospectively compared recordings from scalp-EEG and a wearable ear-EEG device. The proposed model enables real-time seizure monitoring, offering a portable, non-invasive, and continuous monitoring solution tailored for epilepsy patients. The study demonstrates that the wearable system can achieve clinically relevant detection capabilities comparable to conventional scalp-EEG systems. The emphasis on on-device computation suggests that the model is optimised for edge AI deployment, with low-latency and energy-efficient inference, making it feasible for daily, long-term use in ambulatory settings. However, further validation in different clinical scenarios is needed to assess generalisability and robustness. Sun et al. [64] developed a cross-domain feature distillation framework for ear-EEG BCI applications, where the source domain is scalp-EEG and the target domain is ear-EEG. The work was evaluated on SSVEP tasks and demonstrated improved classification performance across multiple experimental conditions, including single-

session, cross-session, and cross-subject scenarios. These results indicate that the framework enhances the practical applicability of ear-EEG in BCI systems [64]. This framework leverages AI to improve the accuracy and robustness of BCI systems, making them more reliable for long-term use.

These advancements in AFE design, power efficiency, and AI integration are pivotal in advancing ear-EEG technology. By addressing the challenges of cost, size, and signal processing, researchers are paving the way for more widespread and effective use of ear-EEG in various fields, from healthcare and neuroscience to consumer electronics and beyond. Integrating AI into ear-EEG systems can significantly enhance their functionality and usability. AI models can be embedded into the system for real-time processing and classification of EEG signals, enabling applications such as emotion detection, seizure detection, and BCIs. These AI-driven enhancements can provide more accurate and timely insights, making ear-EEG systems more effective for continuous monitoring and diverse neurophysiological applications.

Some devices can autonomously analyse signals and provide results directly to patients without requiring professional intervention. Neuromorphic chips are one example of such technology, capable of running on-chip models while maintaining low power consumption. This feature makes them particularly well-suited for wearable applications, where power availability is inherently limited [65]. Field Programmable Gate Arrays (FPGAs) can also be a power-efficient way to deploy AI models instead of standard MCUs.FPGAs let you process data in a way that uses less energy by mimicking logical gates. For example, Al-Ashmouny et al. [66] successfully implemented sleep apnoea detection models using EEG signals on an FPGA, demonstrating its potential for similar wearable applications.

2.2.5 Applications for ear-EEG

Ear-EEG, due to its portability and discreet nature, has shown potential in fields that require long-term and daily EEG monitoring. The design facilitates continuous wear, addressing challenges in capturing transient or infrequent events. However, while the feasibility of using ear-EEG has been demonstrated in multiple contexts, its performance often lags behind scalp-EEG in terms of SNR, resolution, and robustness, particularly in real-world scenarios. Thus, the effectiveness of ear-EEG across different domains remains an active area of research.

Recent advances have demonstrated that ear-EEG can support BCI applications with increasing effectiveness. Wang et al. [38] developed a conformal, flexible ear-EEG device and demonstrated its use in high-performance SSVEP-based BCI spellers, achieving competitive accuracy while improving wearability and user comfort. Similarly, Zhou et al. [67] enhanced signal quality through electrode and algorithm optimisation, enabling robust motor imagery classification using ear-EEG. These works validate the potential of ear-EEG in practical BCI applications. However, challenges remain, particularly lower classification accuracy compared to conventional scalp-EEG and increased vulnerability to motion artifacts in mobile

environments. Addressing these issues will require improved signal enhancement techniques, personalised calibration protocols, and adaptive algorithms that can handle real-world variability.

For instance, epilepsy, a common neurological disorder, affects a significant portion of the population, with annual rates ranging from approximately 40–70 per 100,000 in adults [68] to 41–187 per 100,000 in children [69]. Despite medical interventions, a substantial percentage of patients, estimated at 20-30%, continue to experience more than one seizure per month [70]. Accurate seizure detection plays a crucial role in quantifying seizure occurrences precisely, assisting clinicians in devising tailored treatment strategies [70]. Moreover, seizure prediction technologies can potentially alert individuals to approaching seizures, thereby boosting patient and family confidence and enhancing the overall quality of life [70]. In the realm of seizure detection, the integration of AI algorithms has become an efficient method for identifying and forecasting seizures [71]. However, achieving optimal AI performance necessitates substantial datasets for robust model training, underlining the importance of continuous EEG monitoring by patients and emphasising the significance of daily EEG signal tracking. Seizure detection is a major clinical application, and while Joyner et al. [25] shows that ear-EEG can support long-term remote recording, actual detection of seizure events using ear-EEG remains underexplored. Signal fidelity and the spatial limitation of ear-placed electrodes are two key concerns. Our current work takes a preliminary step in validating seizure-related waveform acquisition but further research is needed to benchmark sensitivity and specificity compared to gold-standard scalp-EEG.

In the domain of sleep staging, systems such as those by Tabar et al. [72] and Borup et al. [73] have shown encouraging results. However, accuracy is still lower than that of full polysomnography, especially for distinguishing N1 and REM stages. Additionally, ear-EEG signal quality can vary across individuals, raising concerns about generalisability. Therefore, personalised modelling and improved device calibration remain open areas of development.

In applications like fatigue detection or pilot monitoring [74, 75], ear-EEG offers a less obtrusive solution. However, these applications often rely on subtle EEG features, which may be harder to resolve reliably from the limited spatial sampling of ear-EEG, particularly under noisy or high-movement conditions.

These examples collectively underscore both the promise and the limitations of ear-EEG across diverse domains. While current findings demonstrate its feasibility, more comprehensive validation, improved signal processing, and hardware innovations are needed to close the performance gap with scalp-EEG. Further studies should also explore subject variability, device personalisation, and long-term wearability, which are pivotal for translating ear-EEG into dependable, real-world applications.

2.3 Ear-EEG recordings

The performance of ear-EEG has been evaluated through multiple studies, demonstrating that while its signal quality is generally lower than that of conventional scalp-EEG, it remains sufficient for reliable detection of neural responses. This trade-off in signal fidelity is considered acceptable given the significant advantages ear-EEG offers for unobtrusive, long-term monitoring.

To further evaluate the capabilities of ear-EEG, we analysed data from the Ear-EEG Sleep Monitoring 2019 (EESM19) dataset [76]. The recordings were collected using personalised dry IrO_x electrodes on 20 participants (7 males, 13 females) with an average age of 25.9 years (range: 23–36) [77]. A TMSi Mobita amplifier was used for signal acquisition. For the ASSR test, they were exposed to a 40 Hz amplitude-modulated at 1 kHz auditory stimulus [77]. A corresponding neural response at 40 Hz was expected, representing the ASSR. Fig. 2.2.5 shows the results across 20 subjects, comparing signal-to-noise ratio (SNR) measurements between scalp and ear-EEG. The SNR was defined as the power at 40 Hz relative to the average power within the 35–45 Hz band, excluding 40 Hz. Results demonstrate that ear-EEG consistently captured the 40 Hz ASSR, with performance comparable to that of scalp-EEG.

2.4 Current Challenges

Despite progress in ear-EEG technology, major limitations persist in anatomical fit, artifact robustness, and integration scalability. These limitations are not only barriers to widespread adoption but also present open research challenges. This section critically reviews existing literature on these topics, highlighting gaps that motivate the specific aims of this thesis. While various approaches have been explored to advance ear-EEG technology, several critical challenges remain that hinder its widespread adoption and clinical applicability. Three major issues in this field are the variability in ear anatomy, susceptibility to motion artifacts, and strict size constraints. These challenges are illustrated in Fig. 2.10.

2.4.1 Variance Auditory Meatus Curvature

To accurately capture EEG signals, it is essential to position multiple EEG channels in close proximity to the patient's auditory meatus. However, the anatomical variability of the human ear presents substantial challenges to using standardised ear-EEG electrodes, resulting in inconsistent performance. This challenge forms the central motivation of this thesis, which seeks to develop personalised ear-EEG electrodes to improve signal reliability and wearer comfort.

Various approaches have been explored in response to this challenge. A notable strategy involves utilising 3D scanning technology to meticulously capture the precise dimensions of

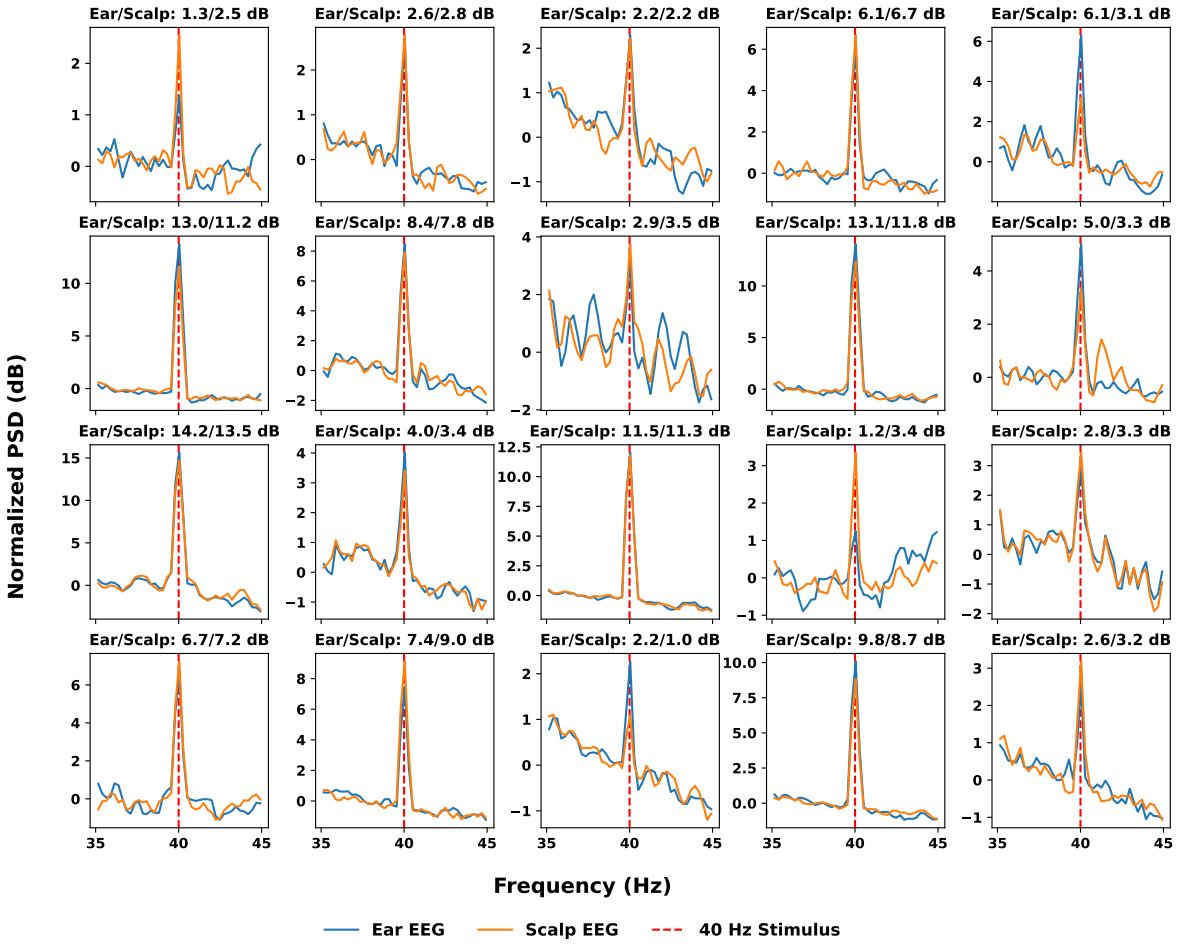

Figure 2.9: Comparison of ASSR test results between scalp-EEG and ear-EEG across 20 subjects from the EESM19 dataset, where the signal-to-noise ratio (SNR) is defined as the power at 40 Hz relative to the average power in the 35–45 Hz band, excluding 40 Hz [76].

an individual's auditory meatus. Subsequently, an electrode can be crafted with meticulous accuracy based on the acquired scanning data. This approach is reported by Kappel et al. [40], which has contributed to this area of research. However, a prevailing technique involves 3D printing personalised earpieces that incorporate pin electrodes placed at specific positions. With the continuous advancement of 3D printing technologies, electrodes can be seamlessly integrated into the earpiece alongside all required electrical components, resulting in a highly personalised and optimised solution.

As previously described in Wang et al. [38], this electrode utilises SMPs with integrated EAL and EEGDL layers. Its ability to thermally expand and spiral within the auditory meatus provides an effective solution for accommodating anatomical curvature variance. This innovative approach enables the electrode to seamlessly adapt to the unique curvature of the auditory meatus during the expansion process, resulting in a customised fit tailored to the individual's anatomical features. Kaveh et al. [3] also developed a user-generic ear-EEG wireless with an extendable plastic structure that effectively conforms its electrodes to the curvature of the ear.

The size of the ear canal can vary throughout different age groups. For instance, Japatti et al.

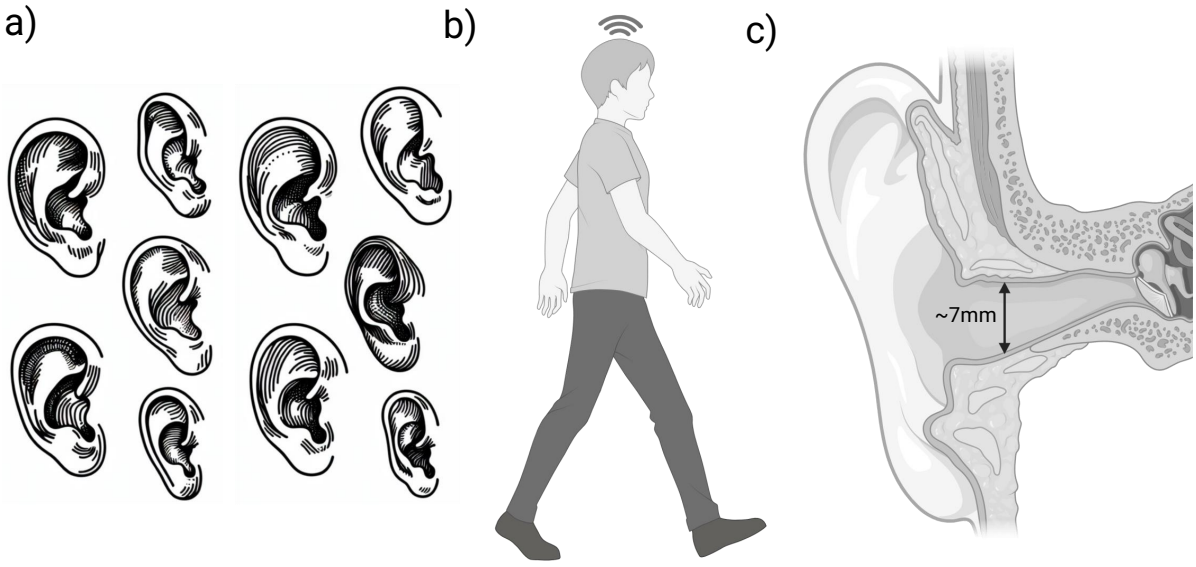

Figure 2.10: Three major challenges affecting hearable device performance and signal quality: (a) Variability in ear anatomy, differences in ear canal shape and size among users result in inconsistent performance. (b) Motion artifacts, as hearables are designed for daily wear, while movement during activities introduces noise, reducing signal quality. (c) Size constraints, the limited space within the ear canal, restrict the number and size of components that can be integrated into the device.

[78] reported that the right ear length, referring to the auricle, increases from 60.65 $\pm$ 4.711 mm in individuals aged 18 to 30 to 65.05 $\pm$ 3.572 mm in those aged 51 to 64 [78]. Although this refers to the outer ear, it illustrates how ear dimensions can change significantly with age. Having quoted the number from Japatti et al. [78], we appreciate that such precision to the third decimal place (1 μm resolution in measurement) is unlikely to have been achieved or even be necessary in design.

There are fourteen different ear shapes being classified [2]. There are also gender differences being found where men's first bend upper, lower, anterior, and posterior lengths for both ears are longer than those for women [79]. The separation of the human ear canal can be seen from the table 2.4.

Table 2.4: Percentage distribution of human ear dimensions, including length of the ear canal and area ranges, based on anthropometric data [2].

Length	**%**	**Area**	**%**
6 - 11	4.02%	210 - 361	9.05%
11 - 15	33.67%	361 - 511	36.68%
15 - 20	41.71%	511 - 662	36.18%
20 - 24	17.09%	662 - 812	15.08%
24 - 29	3.02%	812 - 963	2.51%

While personalisation through 3D scanning and shape-adaptive materials or structures has improved fitness for different individuals, these solutions often lead to increased system com-

plexity and manufacturing costs, as well as worse durability due to the need for deformation. Furthermore, the integration of multiple EEG channels into compact designs remains a significant challenge. This thesis addresses these limitations by proposing a 3D-printed ear-EEG electrode system that can be customised to individual anatomical features while maintaining stable electrode contact and minimising manufacturing burden.

Various strategies have been developed to account for anatomical and auditory differences. One approach involves using 3D-printing techniques to fabricate customised electrodes that provide a secure fit, a concept borrowed from long-standing practices in the hearing-aid industry [8]. Beyond individualised moulds, established solutions from audiology include biocompatible silicone interfaces and soft polymer materials that enhance comfort and minimise irritation during extended use. More recent prototypes have introduced innovations such as dry and flexible electrodes, conductive coatings, and micro-structured surfaces, all aimed at improving skin contact while reducing the need for extensive preparation [80]. Looking forward, potential advancements may include self-adaptive ear interfaces, refined impedance modelling to guide electrode design, and the adoption of standardised manufacturing pipelines from hearing aids to hearables, developments that could substantially enhance both signal quality and user acceptance.

2.4.2 Motion Artifacts

Motion artifacts represent an ongoing challenge in the field of ear-EEG measurements. These artifacts which are unwanted electrical signals induced by physical movements of the body or the measurement system, present a significant issue for the accurate acquisition of EEG signals [81]. While motion artifact cancellation is a crucial topic in mobile EEG research, it is outside the scope of this thesis. Some approaches that can be used for cancelling motion artifacts can be found in the following papers. For portable devices, users often need to wear them while engaging in daily activities such as walking. This makes motion artifacts an unavoidable challenge that must be addressed effectively. Strategies to mitigate motion artifacts include designing robust signal processing algorithms, employing adaptive filtering techniques, and integrating motion sensors like accelerometers to identify and compensate for movement-induced noise. These advancements are crucial to ensure the device's reliability and usability in real-world scenarios. Unlike scalp-EEG, ear-EEG is less affected by eye blinking but more susceptible to motion artifacts originating from jaw and head movements, primarily due to the extended wire connections involved [82]. The magnitude of these motion artifacts is a particular concern, often exceeding that of the EEG signal by at least an order of magnitude [81]. The consequences of these artifacts are far-reaching and include a reduced accuracy in automated signal sequence classification for clinical diagnostic purposes and disruptions in the smooth operation of BCI systems [81]. Given the need for daily monitoring and real-world applications of hearable devices, effectively managing and mitigating motion artifacts is crucial to ensure the reliability and clinical utility of ear-EEG measurements. Existing mitigation strategies, such as accelerometer-based noise filtering, have shown moderate

success [83], but they struggle to differentiate true neural signals from muscle activity. Novel approaches, such as adaptive filtering using independent component analysis (ICA) and deep learning-based artifact removal, have demonstrated promise [84], but their real-time applicability in wearable devices remains an open question due to computational constraints.

A study introduced an innovative ear-EEG electrode design that employs memory foam as its base material [33]. This choice of material effectively mitigates motion artifacts arising from both minor and substantial mechanical deformations of the ear canal walls [33]. This electrode design also incorporates using two microphones to capture acoustic signals traversing through dense head tissues and uses these signals to cancel the motion artifacts in the EEG signal [33].

2.4.3 Design Constraints and Miniaturisation Challenges

The task of seamlessly integrating the complete analog front end and the MCU into a single earpiece to facilitate the wireless transmission of digital signals to a designated device remains a substantial challenge in this field. This challenge is further accentuated by the necessity of minimising the distance between the electrode and the analog front end and the size of the auditory meatus [55]. One suggested approach entails the strategic distribution of electrical components around the external ear rather than direct insertion into the ear canal [3]. However, even with this approach, the visibility of these components remains noticeable, potentially causing social discomfort. In practical scenarios, this situation might require the use of additional accessories, such as a hat, to effectively conceal the components.

As previously mentioned, ASICs present a promising approach by enabling the integration of multiple functions into a compact form factor. However, producing them in small quantities can be prohibitively expensive. Although this is a viable solution for some applications, it is not the method adopted in this research. Instead, we focus on alternative strategies that leverage advancements in manufacturing and electronics to support ongoing miniaturisation. This trend plays a key role in enabling the integration of essential components within the limited space of the earpiece.

Despite progress through ASICs and distributed component designs, the trade-off between invisibility, comfort, and signal fidelity remains insufficiently explored [33, 51]. This work investigates these trade-offs using compact, ear-molded prototypes that incorporate embedded electrodes and shielding layers, aiming to optimise EEG signal quality without compromising wearability.

The content presented in chapters 3 to 7 is adapted from the publication:

- L. Yu, Z. Xu, L. H. Contreras, and O. Kavehei, "An Additively Manufactured 3D Printed Electronics System for Personalized ear-EEG," in *2024 International Conference on Electrical, Computer and Energy Technologies (ICECET)*, IEEE, 2024, pp. 1–6.

Statement of Contributions of Joint Authorship

- Leping Yu (Candidate): First author, formal analysis, investigation, methodology, software, visualization, validation, writing original draft, writing review and editing of the manuscript
- Zhangyu Xu: Methodology
- Luis Herbozo Contreras: Visualization
- Omid Kavehei (Principal Supervisor): conceptualization, aided in the analysis and reviewing and editing of the manuscript

In addition to the statements above, in cases where I am not the corresponding author of a published item, permission to include the published material has been granted by the corresponding author.

Leping Yu Date: Aug 08 2024

As supervisor for the candidature upon which this thesis is based, I can confirm that the authorship attribution statements above are correct to the best of my knowledge.

Dr. Omid Kavehei Date: Aug 08 2024

Chapter 3

Method

3.1 Ear-EEG Device Design and Fabrication

This research, as a proof of concept, demonstrates that it is possible to provide a customizable, 3D-printed ear-EEG electrode with integrated circuitry that can be easily modified for different anatomical shapes without increasing manufacturing complexity.

3.1.1 Overview of the Proposed Ear-EEG System

To address the challenges embedded in conventional EEG systems and the associated social awkwardness if and when wearable scalp-EEG systems are worn, a whole-system 3D-printed ear-EEG electrode has been developed purely through additive manufacturing that can be potentially designed and adjusted for different sizes, shapes, and forms of ear canals. This device is designed to sense EEG within the patient's ear, providing an experience similar to wearing ordinary earphones and be ultimately as durable and reusable. The AFE used in this configuration is the AFE4960, initially designed for ECG but adaptable for EEG applications. The nRF52833 MCU integration is implemented to manage the AFE and oversee data transmission. Data transmission is facilitated via the SPI protocol at a frequency of 1 MHz. These critical components are discreetly positioned on two boards interconnected through board connectors. Raw EEG data is sampled and filtered using a low-pass filter at 330 Hz before being transmitted to the MCU via a board-to-board connector. The MCU manages system operations and can wirelessly transmit the processed signal to external devices for further analysis, including different frequency domain analyses and montages.

The comprehensive description of the entire system is illustrated in Fig. 3.1. This figure depicts the overall system architecture, where the signal is gathered from the tripolar electrode, processed by AFE, transmitted by MCU, and displayed by a PC.

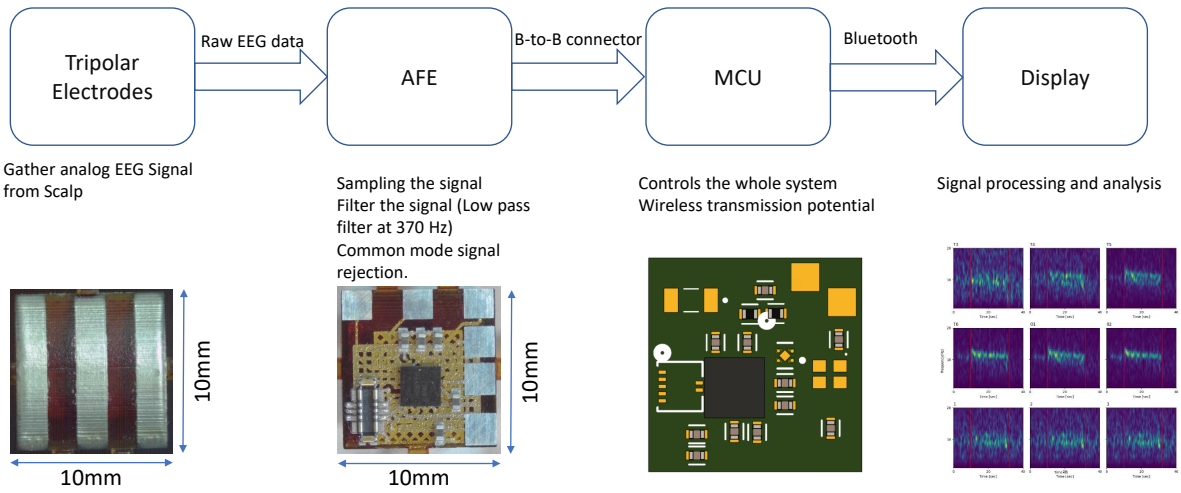

Figure 3.1: Block diagram of the proposed ear-EEG system illustrating the signal pathway from the electrode, through the analogue front end for amplification and filtering, and into the microcontroller for digitisation and further processing. The analogue and digital sections are interconnected via a board-to-board connector. B-to-B connector: Board-to-Board Connector, AFE: analogue front end, MCU: microcontroller.

3.1.2 3D-Printed Electrode and Silicone Housing

The entire device, including electrodes and the circuit board, is printed in a single operation using silver ink for the conductive paths and dielectric materials for insulation. Device fabrication was performed by Nano Dimension using their additive manufacturing system. The manufacturing process involves 3D modelling for conductive and dielectric components, ensuring precise fabrication by the 3D printer. Silver nanoparticle ink was used as the conductive material and cured by heat, whereas the dielectric material was solidified using UV curing. The integration of 3D printing technology enables the device to be manufactured in customised shapes to adapt to an individual patient's ear canal. This level of customisation ensures an accurate fit, enhancing the electrode-skin interface, which in turn improves signal quality and overall device performance. Additionally, customising the device to fit the unique shape of the ear canal ensures a more uniform distribution of pressure on the surrounding tissue, thereby significantly enhancing user comfort, especially during extended periods of wear. The electrode positions were determined based on the available surface area within the ear canal and concha. The major goal was to ensure consistent skin contact, mechanical durability, and comfort for the user. Placement was adjusted slightly between individuals to accommodate anatomical differences, but the overall positioning strategy remained consistent across subjects. While this study does not endorse specific brands, Nano-Dimension's conductive ink and dielectric formulations are noted for their biocompatibility and additional properties such as antibacterial and antifungal effects [85–88].

To ensure optimal fit within the ear canal of test subjects, a custom silicone rubber cover was created through moulding. The model consists of two pieces produced via 3D printing with Polylactide (PLA), seamlessly joined during the moulding process. Liquid silicone rubber was

carefully poured into the mould, and air bubbles were eliminated using a vibrator. The mould was then placed on a heat plate and left to cure for six hours. After curing, the silicone cover was carefully removed from the mould. This silicone rubber cover can be seen in Fig. 3.2.

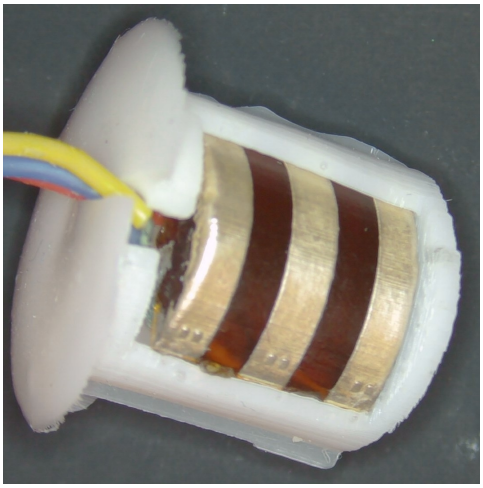

Figure 3.2: Silicone rubber cover created through moulding, with a wire used to connect the system to the host device for testing purposes. This cover provides flexibility and comfort for the wearer, ensuring a secure fit for the ear-EEG system.

3.1.3 Analog Front End and Microcontroller Integration

The AFE interfaces directly with the electrode. By placing the AFE directly in contact with the electrode on the earpiece, the distance between the front-end circuitry and the electrode-skin interface is minimised, thereby reducing susceptibility to ambient electromagnetic interference, particularly from power line sources (50/60 Hz). Power line noise is one of the most common and persistent forms of interference in biosignal recordings, as the human body and lead wires can act as antennas that pick up environmental electromagnetic fields. In addition to power lines, nearby electronic devices such as smartphones, displays, switching power supplies, and wireless communication modules can emit electromagnetic signals that further contaminate recordings. These interferences are particularly problematic in wearable systems, where shielding is limited and devices are used in uncontrolled environments. Integrating the front-end electronics close to the electrode minimises the length of exposed conductive paths, reduces the effective loop area, and improves common-mode rejection, significantly mitigating both power line and device-related noise. As noted by Seok et al. [81], robust hardware design, including local amplification, impedance matching, and careful component layout, is essential for preserving signal quality in electrophysiological recordings. Therefore, front-end placement plays a critical role in suppressing environmental noise and improving the signal-to-noise ratio in ear-EEG and other mobile biosensing systems.

The MCU is programmed to oversee the system operation, initialise the AFE, and transmit the acquired signals to a PC. The MCU manages the AFE and facilitates data transmission via the SPI protocol at a frequency of 1 MHz. The MCU board is connected to the board through

the board-to-board connection. Raw EEG data is sampled and filtered using a low-pass filter at 330 Hz, which performs rough filtering to remove high-frequency noise before being transmitted to the MCU. The MCU manages system operations and can wirelessly transmit the processed signal to external devices for further analysis, including different frequency domain analyses and montages. This setup ensures efficient and accurate data acquisition and transmission, making the device versatile and user-friendly for various neurophysiological monitoring applications. The designed circuit can be seen from Fig. 3.3.

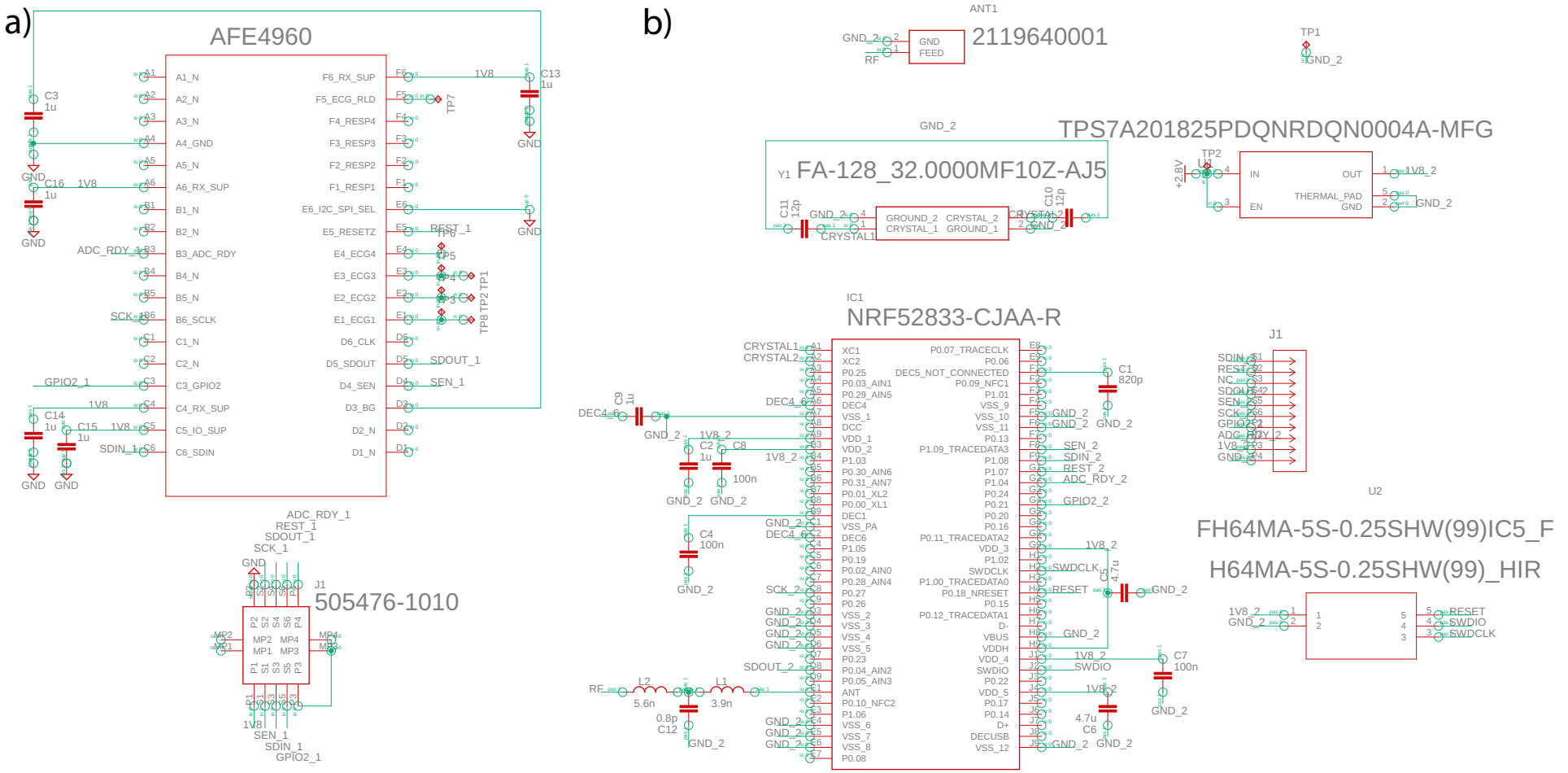

Figure 3.3: (a) Schematic diagram of the PCB for the ear-EEG side of the circuit, which includes the analog front end and a connector to the remaining part of the board. (b) Schematic diagram of the PCB for the module that collects data from the analog front end and transmits it via Bluetooth for further applications.

3.1.4 PCB Layout and Electronics Integration

The PCB was developed in Altium Designer with a four-layer stack-up, including a dedicated ground layer to improve signal integrity. Via-in-Pad routing was employed to optimise compactness and facilitate integration with the 3D-printed housing. The 3D model was designed and integrated using Fusion 360, enabling precise visualisation and alignment of electronic components within the device housing. To enhance manufacturability, the design minimises internal structures in the top electrode section, simplifying the 3D printing process. The electrode was designed as a half-cylinder to conform to the curvature of the ear canal. Using 3D printing in conjunction with CT scan data, the curvature can be customised to match the unique anatomy of any individual ear canal. 3 electrodes are designed separately to provide a 3-channel recording.

To bridge the electronic and mechanical designs, the PCB layout was exported from Altium using the PDF3D exporter and converted into an OBJ file for 3D modelling. The electrode connects to the system via three designated test pads, serving as the interface between the electrode and the rest of the circuit. The upper and lower parts of the device are joined at these pads, ensuring reliable electrical contact. For fabrication, the device is separated into two distinct print files, one containing conductive material and the other dielectric material, allowing dual-material 3D printing of the structure in a layer-by-layer process.

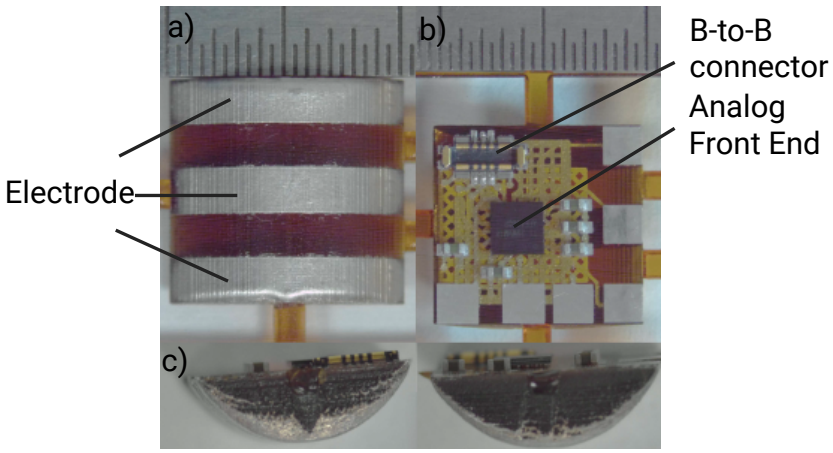

Figure 3.4: Photo of the circuit device for the analogue front end, the width of the component is 10 mm, the height is 3.7 mm. (a) Front view of the electrode. (b) Rear view showing the circuit board. (c) Side profile of the assembled electrode.

Fig. 3.4 illustrates the electrode and conductive components fabricated using silver ink. The entire device, including electrodes and the circuit board, is printed in a single operation with silver ink and dielectric materials. This manufacturing process involves 3D modelling for conductive and dielectric components, ensuring precise fabrication by the 3D printer.

3.1.5 Signal Acquisition and Processing

The captured EEG signals undergo various analytical procedures to evaluate the device's performance in different applications. Raw EEG data is sampled and filtered using a low-pass filter at 330 Hz before being transmitted to the MCU via a board-to-board connector. The electrode interfaces directly with the AFE. Furthermore, the design includes a board-to-board connector, facilitating seamless integration with a secondary board equipped with a microcontroller. This microcontroller manages data collection and transmission via Bluetooth, enhancing the device's versatility and usability.

The design is based on the manufacturing methods property, which is 3D printing that requires being produced layer by layer, while it is hard due to the current techniques to build complex details of the internal structure. This design enables on-demand manufacturing tailored to individual anatomies across different age groups and genders. Also, the rigid structure compared to the soft electrode needs to ensure a durable and reliable product suitable for everyday life.

3.2 Proposed Solution

To explore the potential for a more cost-effective approach, an alternative hearable device was developed using a standard instrumentation amplifier (INA) and commercially available electronic components. The goal of this design is to significantly reduce manufacturing costs while preserving sufficient signal quality for ear-EEG acquisition. The INA821 was selected due to its low input-referred noise and high common-mode rejection ratio (CMRR), both of which are essential for reliable biopotential measurements. The circuit schematic of this design is shown in Fig. 3.5.

Compared to the original design, which utilizes a dedicated AFE chip, this trades off integration and compactness in favour of lower component costs and increased flexibility in configuring gain and filtering parameters. The amplifier circuit was configured with a gain of approximately 2246.45, enabling the detection of low-amplitude EEG signals typically in the microvolt range. The LT6656 provides a stable 2.5 V reference bias to ensure consistent performance across temperature and power variations. The INA821 is operated in a single-stage amplification configuration, with resistor values carefully chosen to achieve the desired gain. Passive filtering is applied at both the input and output stages to attenuate high-frequency interference and prevent aliasing during analog-to-digital conversion. A physical prototype of the alternative hearable device is shown in Fig. 3.6. A custom connection board was fabricated by Synergy Electronics Pty Ltd. to interface the ear-EEG circuit board with external systems. After assembly, additional wiring was used to connect the circuit board to an external ADC, a reference electrode, and a power supply.

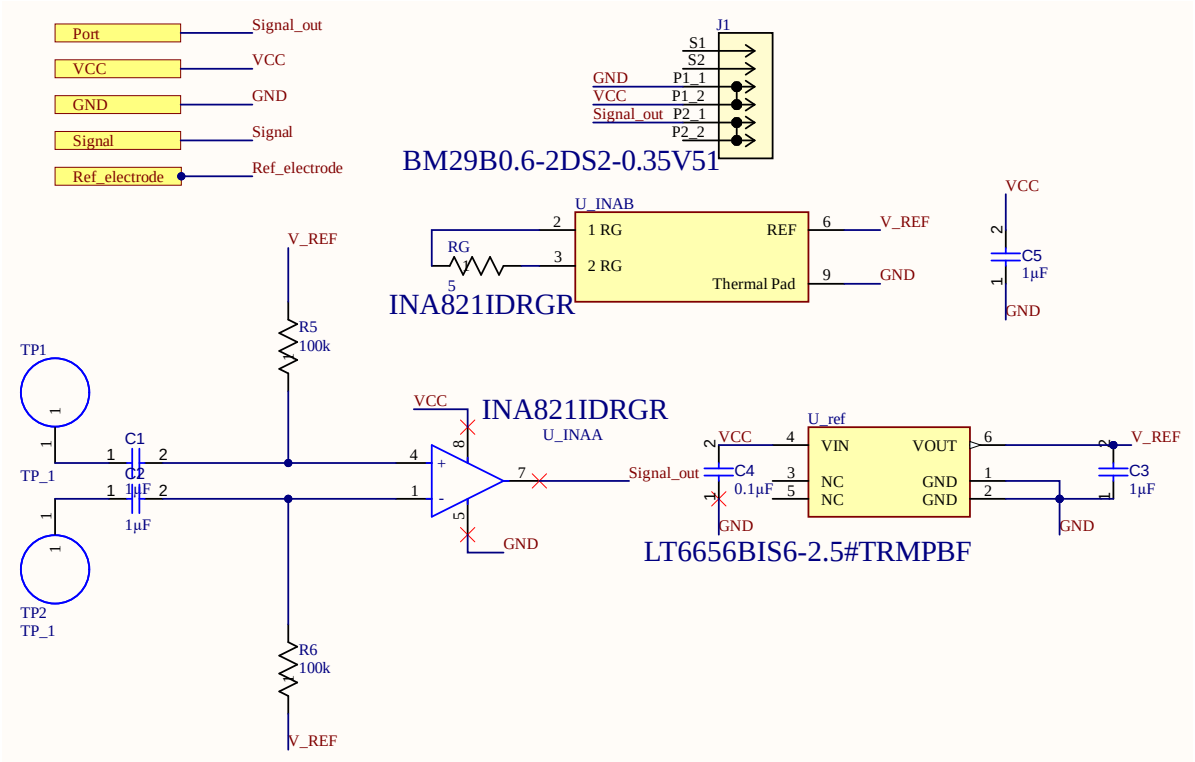

Figure 3.5: Circuit design for the proposed solution. The LT6656, a 2.5 V voltage regulator, is used to provide a stable reference voltage. The INA821 is used to reject common-mode noise and amplify the differential signal.

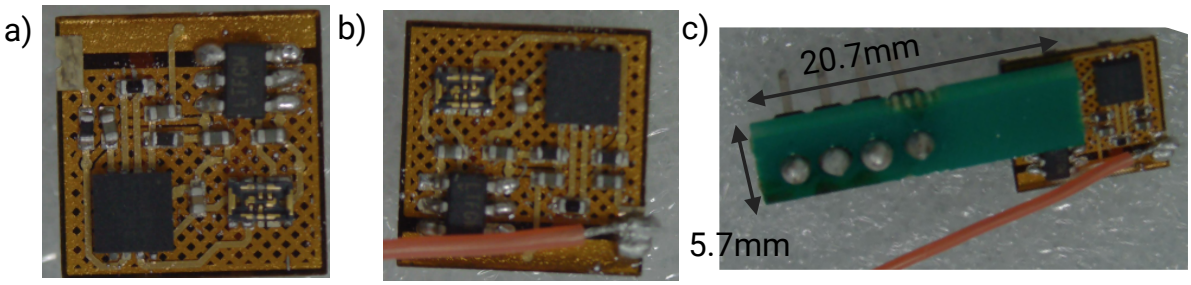

Figure 3.6: Prototype of the proposed hearable device: (a) the main circuit board, (b) the reference electrode connected to the board, and (c) the board-to-board connector used to link the AFE to the ADC.

3.3 Experiments

3.3.1 Participant and Materials

This study is exclusively centred around a healthy male subject for this proof of concept. The decision to use a single participant allows for a controlled environment where the efficacy and accuracy of the 3D-printed ear-EEG device can be rigorously tested without external variables influencing the results.

Figure 3.7: Photo of the scalp-EEG, the baseline for this study.

3.3.2 Data Acquisition

To verify the performance of the ear-EEG system, data are acquired simultaneously from both scalp-EEG and ear-EEG under the same conditions, allowing for a direct comparison of signal quality and performance.

The amplifier for the scalp-EEG used in this research is the NVX 52, a 52-channel commercial device manufactured by Medical Computer Systems Ltd. Recordings were conducted using Necro, the proprietary software provided by the developer of the scalp-EEG device. The conductive gel used in this study is Electro-gel, manufactured by Electro-Cap International, Inc. Both ear-EEG and scalp-EEG were sampled at a rate of 5000 Hz. The photograph of the scalp-EEG used in this study is shown in Fig. 3.7.

The participant was instructed to clean and dry his hair before recording. After the scalp-EEG was fitted onto the participant, electro-gel was applied to all scalp electrodes, and impedance was checked. If the impedance exceeded 20 kΩ, additional gel was applied until the impedance dropped below 20 kΩ. Scalp electrodes were positioned according to the 10-20 system [89]. The electrodes were coated with Electro-gel, and impedance was monitored. If the impedance exceeded 50 kΩ, more gel was applied to ensure optimal electrode-skin contact. This meticulous preparation protocol was implemented to standardise recording conditions and enhance the reliability of the collected EEG data. The screen and speaker of the computer which are being used to generate visual and audio stimuli were positioned 50 cm away from the subject. The ear-EEG and scalp-EEG ground electrodes were placed on the earlobe.

A series of tests was systematically conducted following standardised protocols to evaluate the performance of the ear-EEG electrode. During all tests, the participant was instructed to remain seated and motionless to minimise artifacts. Recordings were simultaneously acquired using both the ear-EEG device and a commercial scalp-EEG system. As scalp-EEG generally

offers higher signal quality due to its optimised electrode placement and larger inter-electrode distances, it served as the reference baseline. Despite these advantages of the scalp system, the ear-EEG device demonstrated sufficient signal quality for potential practical applications, offering the added benefits of portability and user comfort.

For the ASSR and Alpha Modulation tests, six electrodes were positioned on the scalp at T3, T4, T5, T6, O1, and O2 based on the 10-20 system. The 10-20 system is a standard system for electrode positioning with 21 electrodes which can be seen from Fig. 2.1 [13]. In the case of the Mismatch Negativity (MMN) and P300 tests, ten electrodes were utilised at T3, T4, T5, T6, O1, O2, FCz, Pz, CPz, and Fz based on the 10-20 system, all placed on the scalp. These standardised test configurations aim to assess and compare the performance of ear-EEG against commercial scalp-EEG across various neurophysiological measures.

A GUI was developed to control the stimulus and mark the data at specific time points to perform all tests. An impulse is introduced into one extra channel in the signal to mark the specific point for the stimulus that happened, so that accurate analysis can be conducted later.

3.3.3 Steady-State Tests

Steady-state refers to the brain's response to intermittent stimulation with short intervals between stimuli [90]. Steady-state in this context refers to the brain's sustained response to periodic sensory stimulation with short inter-stimulus intervals. For instance, ASSR uses auditory stimuli such as amplitude- or frequency-modulated tones (e.g., 40 Hz), while alpha modulation involves rhythmic visual or auditory cues designed to entrain alpha-band (8–12 Hz) oscillations. Research indicates that the brain's response stabilises approximately 12-20 seconds after stimulus onset, achieving a statistically steady state in EEG signals [91]. This stable state indicates that the brain's electrical activity settles into a predictable pattern, facilitating more effective study and analysis of brain responses [91]. Understanding the steady state in EEG signals is crucial for interpreting brain activity and investigating how the brain processes information under various experimental conditions [91].

Auditory Steady-State Response (ASSR)

The ASSR is a type of auditory evoked potential (AEP) that objectively measures hearing sensitivity in individuals with normal hearing and varying degrees of Sensorineural Hearing Loss (SNHL) [92]. First identified in 1981 at 40 Hz [93], the ASSR is generated by the superposition of transient responses [94]. This test is particularly relevant for ear-EEG monitoring due to the proximity of the electrodes to the temporal cortex, the source of the ASSR signal, making it well-suited for ear-EEG applications.

ASSR has proven valuable in verifying hearing loss in patients unable or unwilling to cooper-

ate with conventional behavioural or voluntary response audiometry, such as young children [95]. This non-invasive, objective method provides reliable results even in challenging clinical scenarios, making it a crucial tool in auditory assessments.

During an ASSR test, the participant is seated in a quiet room to minimise external distractions. The test involves presenting an auditory stimulus lasting 100 seconds, divided into five equal segments with distinct frequencies: 35, 37, 40, 43, and 45 Hz. These frequencies are selected for their relevance to the auditory system, with a carrier frequency of 1 kHz due to its sensitivity within the human auditory spectrum [3]. The 40 Hz frequency is considered to produce the largest amplitudes in the response signal [94]. Another study utilised a similar ASSR test with a 40 Hz sound amplitude modulated at 1 kHz for the same duration [3]. The test sound was generated in Python using amplitude modulation. The instantaneous amplitude of the modulated signal is given by Equation 3.1, where W_c is the amplitude of the carrier signal, W_m is the normalized amplitude of the modulating signal, and W_{me} is the resulting amplitude of the modulated signal. A 20-second gap is provided before the start of the test to allow the participant to sit still, and another 20-second gap follows the test to prevent motion artefacts in the signal.

$$W_m e = (1 + W_m) * W_c \tag{3.1}$$

Alpha Modulation

The assessment of alpha modulation is incorporated alongside the ASSR test. The EEG signal is divided into several frequency bands: delta (0.5 to 4 Hz), theta (4 to 7 Hz), alpha (8 to 12 Hz), sigma (12 to 16 Hz), and beta (13 to 30 Hz) [96]. Among these, the alpha band is particularly significant for its neurological features, often associated with the participant's attentional state [97]. This is a widely used experiment because alpha waves have a higher amplitude than other frequency bands, making them easier to detect [98].

In this examination, the participant is initially instructed to open their eyes and focus on a screen for a specified duration, and twenty seconds after the start of recording which is used to leave enough blank for the later signal processing and to help the participant to relax and stay still, an on-screen prompt signals the participant to close their eyes [3]. Following 20 seconds of eye closure, a distinct auditory cue, a beep, signals the participant to reopen their eyes. The ensuing phase requires the participant to remain motionless in a seated posture for 20 seconds. This entire procedure is repeated five times for each test set. The process is controlled by a computer, which plays sounds to indicate when to open and close the eyes. This test is performed in a quiet room to avoid any disturbance. The whole process is built into a GUI to control the whole process and mark the data points within the data.

These steady-state tests, encompassing ASSR and alpha modulation assessments, verify the ear-EEG device's performance and accuracy and highlight its potential for diverse applications

in neurophysiological monitoring and clinical diagnostics.

3.3.4 Event-Related Potential (ERP) Tests

ERPs refer to the small voltages generated within the brain in response to specific events or stimuli [99]. ERPs result from the summated activity of postsynaptic potentials, produced when a substantial number of similarly oriented cortical pyramidal neurons fire synchronously during information processing [100]. ERP tests are widely used for various purposes, including diagnosis and research. These signals originate from different brain regions, providing a comprehensive means to verify the electrode's ability to gather signals from diverse and distant sources [101].

The Mismatch Negativity (MMN) is an ERP component that reflects the brain's automatic detection of deviations in auditory stimuli from a regular pattern, without requiring conscious attention [102]. It represents pre-attentive auditory processing and is triggered when the deviant stimulus exceeds the brain's sensory discrimination threshold, which refers to the smallest detectable change in properties such as pitch, duration, or intensity. Although MMN is primarily studied in the auditory domain, it can also be elicited by changes in other sensory modalities, including somatosensory, olfactory, and visual inputs. Factors such as sound duration, rise time, inter-stimulus interval, and stimulus order can significantly influence the characteristics of the auditory MMN response [102].

The MMN test applied in this study follows the conventional auditory oddball paradigm, in which infrequent deviant tones (1000 Hz) are presented among frequent standard tones (800 Hz) [102]. Each tone lasts 124 ms, and the entire task takes approximately 15 minutes. To divert the participant's attention from the audio itself, they are asked to watch a movie during the test. A GUI computer controls the entire procedure, playing the video and sounds at specific times. The computer also logs the order of the generated tones for subsequent analysis. This paradigm is widely used in MMN research to elicit pre-attentive auditory responses. In this work, we implemented the paradigm using a custom Python-based GUI that synchronises tone presentation with a distractor video and logs stimulus order for subsequent analysis. The test signal is generated in Python using the `numpy` package for creating sound data and the `wave` package for exporting it as sound. The video used to draw the patient's attention during the test is sourced from YouTube and can be accessed through the following link: `https://www.youtube.com/watch?v=TtBOuPMZdoQ`.

The MMN test reveals a characteristic negative deflection approximately 200–220 ms after stimulus onset, consistent with the expected latency of the MMN component. To isolate this response, baseline correction using the -200 to 0 ms pre-stimulus interval and a deviant-minus-standard difference wave analysis were applied. MMN responses were identified using an automated detection algorithm based on both amplitude and latency constraints. A negative peak exceeding 20 μV within the 150–250 ms window was required for classification as an

MMN candidate. This conservative threshold, derived from MMN literature and pilot data, was chosen to reduce false positives due to the lower SNR in ear-EEG recordings. In addition, each candidate peak had to return clearly to baseline within 100 ms to ensure it reflected the expected MMN morphology. Trials meeting the threshold but lacking a sharp negative peak followed by a return to baseline were excluded. A subset of recordings was visually inspected to validate the automated detections.

The brain elicits the Active Oddball (P300) component in response to attended events that are unexpected or to unattended events that induce an orienting response, which refers to a rapid, automatic shift of attention toward a novel or salient stimulus in the environment [103]. The term "P" signifies a positive peak occurring at a specific time, while "300" refers to the typical response time in ms, around 300 ms post-stimulus [103]. This test is versatile and applicable in various domains, including detecting concealed knowledge [104] and BCI systems [105]. Consequently, the P300 test indicates EEG devices' performance and effectiveness, demonstrating their ability to capture and analyse significant neural responses accurately.

The P300 test designed for this study bears similarities to the MMN test. In the P300 experiment, the participant is exposed to the same auditory stimuli as in the MMN paradigm. However, the participant is instructed to count the occurrences of target tones silently. A GUI controls the entire procedure, with a button for the participant to indicate each target tone heard. The pressing result is also being recorded for further analysis purpose.

The Directional Hearing (N100) is an ERP elicited by discernible auditory stimuli without task demands [106]. This neural signal is primarily generated bilaterally in the supratemporal plane and the superior temporal gyrus [107], and can be observed across various functional paradigms, including auditory, visual, somatic, behavioural, and cognitive tasks [108]. In EEG recordings, the N100 manifests as a negative deflection occurring approximately 100 ms post-stimulus [108, 109], and is clinically used to detect hearing abnormalities in unresponsive patients or to evaluate optimal sedation levels in intensive care [110–112].

In this study, the N100 test was conducted to evaluate the capability of ear-EEG devices in capturing auditory evoked potentials. Responses were expected to occur approximately 100 ms post-stimulus, although exact timing varied across individuals [101]. Temporal and amplitude characteristics of the N100 component were assessed in comparison to conventional scalp-EEG recordings, allowing verification of the ear-EEG system's ability to detect neural responses while maintaining the advantages of improved comfort and wearability. Directional auditory stimuli were delivered via left, centre, and right channels to elicit N100 responses. The left channel consisted of four tones produced by a cello with an ascending pitch; the middle channel, three tones produced by a clarinet with an alternating pitch; and the right channel, five tones produced by an oboe with a descending pitch. The test signals were generated using Python with the `AudioSegment` package, enabling precise control of sound directionality and pitch, and allowing stimuli to be tailored to the experimental requirements. To enhance salience and participant engagement, the stimuli varied in spatial origin, pitch pattern, number of tones, and instrument type, though this introduces a design confound: differences in

timbre or pitch may also influence the N100 response, making it impossible to attribute ERP differences solely to spatial direction.

However, we acknowledge that this introduces a design confound, namely, a perfect correlation between direction and sound characteristics. This makes it impossible to definitively attribute ERP differences solely to spatial direction, since differences in timbre or pitch could also influence the N100 response.

Our current setup aimed to demonstrate the device's capability to detect reliable auditory ERPs, including N100, in response to lateralized stimuli. The primary goal was to verify signal acquisition, not to perform fine-grained analysis of spatial auditory processing. Future versions of this test will include counterbalanced or randomised stimuli, where direction and auditory features are fully decoupled. This will allow us to isolate the neural correlates of spatial hearing and better characterise the ear-EEG system's sensitivity to directional cues.

Overall, these ERP tests verify the performance and accuracy of the ear-EEG device, in the sense that they confirm the system can reliably capture expected ERP components such as N100 and P300.

3.3.5 Dipole Test

The proposed circuit design, developed as part of this thesis, addresses the specific challenges of ear-EEG signal acquisition and represents a key contribution of this work. To test the performance of the proposed circuit design, a custom dipole device was developed, as shown in Fig. 3.8. The dipole structure was 3D modelled using Fusion 360 and fabricated with a 3D printer with PLA. It consists of two wires, one connected to the stimulation signal and the other to ground. The exposed wire tips were coated with tin to reduce corrosion within saline. The saline solution used has a concentration of 0.9% sodium chloride by weight ratio, simulating physiological conditions. The dipole setup in saline was chosen to stimulate the electrical properties of the human body in a controlled environment. Saline solution approximates the conductivity of biological tissue, providing a physiologically relevant medium for signal transmission and pickup. The distance between the two dipole electrodes was fixed at 25 mm to ensure consistent field strength across tests. All tests were conducted at room temperature, and the depth and distance between the dipole and the electrode were kept constant to avoid variations in impedance.

The stimulation signal applied during testing was a 1mV sine wave at frequencies of 10 Hz and 20 Hz. Frequencies of 10 Hz and 20 Hz correspond to alpha and beta bands, which are commonly targeted in various EEG studies. Both the signal generation and response acquisition were performed using the Analog Discovery 2 device which is one commerically availability device that is manufactured by Digilent, a National Instruments company.

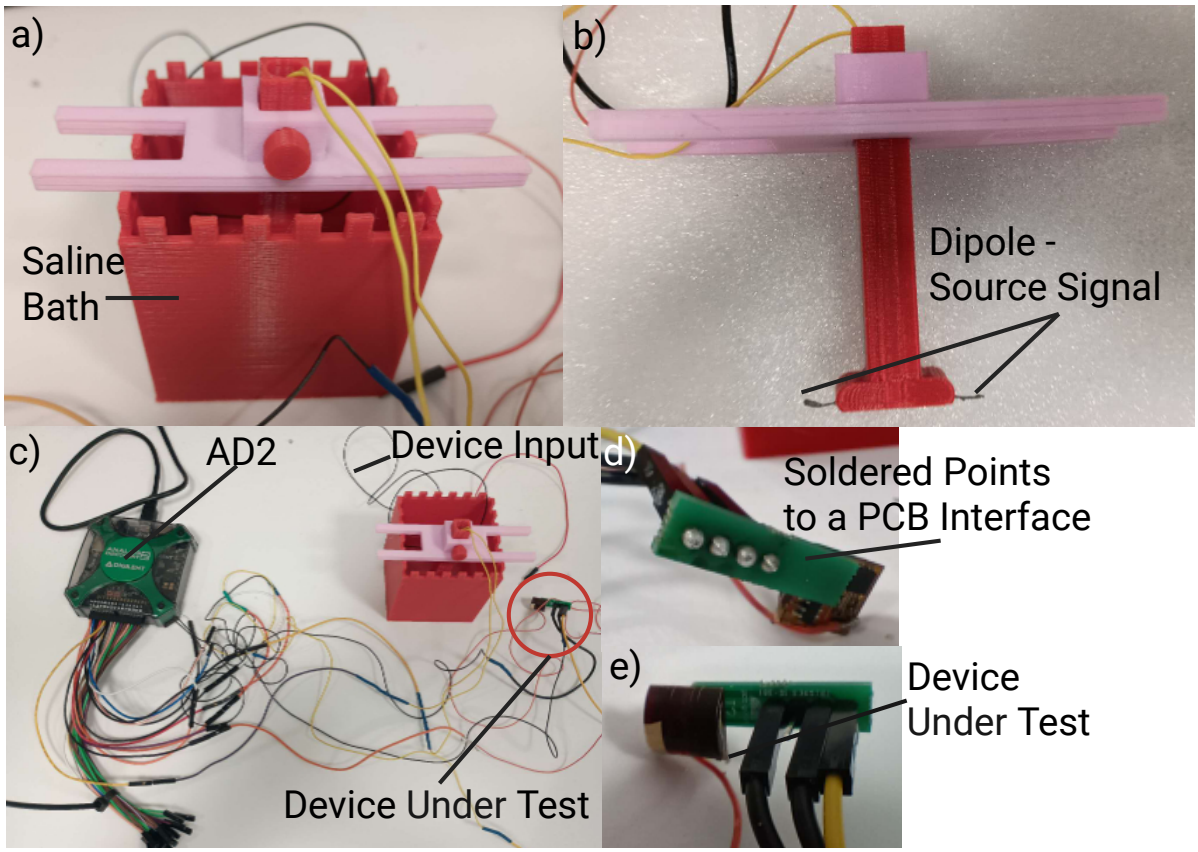

Figure 3.8: Dipole setup used for testing the proposed solution: (a) the complete assembled device including the 3D-printed dipole structure, and (b) the dipole itself, where one wire is connected to the stimulation signal and the other to ground. The exposed wire ends are immersed in 0.9% saline solution. (c) The complete test setup. The stimulation signal is output from the AD2 into the saline solution. The return signal is collected via an input wire submerged in the saline, passed through the electrode, processed by the AFE, and sampled by the AD2. (d) Rear view of the device under test. A connection board is used to route the output from the AFE to the AD2 for acquisition. (e) Front view of the device under test. The electrode surface was partially damaged after the experiment. AD2: Analog Discovery 2

3.4 Signal Processing

3.4.1 Filtering

In order to increase the SNR of the recorded signal before put it into analysis, filtering is going to be applied to remove the unwanted signal. The preprocessing pipeline for EEG signal analysis involves applying specific filtering procedures to enhance signal specificity. Raw EEG signals often contain noise from various sources, including power noise and other equipment-related interference induced by the power line and the operation of other devices. Also, it may include other biosignals like ECG or Electrooculography (EOG) which is generated by eye movements. Filtering is applied to keep only the interested frequency band to improve signal quality. The procedures include using a bandpass filter, which means only the band within the

corresponding range can be kept, complemented by a 50 Hz notch filter, which will reduce the signal to 50 Hz to eliminate extraneous frequency components.

For different tests, as the frequency of interest will be different, filters are applied variously across different tests. The bandpass filter is tailored explicitly for the ASSR test, refining the signal within the optimal frequency range for auditory stimuli (32 to 47 Hz). The gain roll-off in this method refers to the rate at which frequencies outside the target band (5–100 Hz) are attenuated, determined by the order of a digital Butterworth band-pass filter implemented in Python. A third-order design is used, resulting in a roll-off of 18 dB per octave, which provides a smooth yet effective suppression of unwanted frequency components. The Butterworth filter is chosen for its maximally flat frequency response in the passband, ensuring minimal signal distortion. This filtering approach is crucial for isolating relevant EEG activity while reducing artifacts and noise outside the physiological frequency range of interest. For the alpha modulation test, the bandpass filter is adjusted to a pass band of 5 Hz to 20 Hz, targeting the frequency spectrum associated with alpha oscillations and removing all the high-amplitude low-frequency signals. Similarly, for the MMN and P300 tests, the bandpass filter spans from 1 Hz to 30 Hz, encompassing the relevant frequency range for these responses [101]. In all tests, a 50 Hz notch filter is utilised to remove powerline noise, which is typically a significant noise in the signal while recording.

The filtering approach employs the Butterworth filter, a classic filter renowned for its smooth response. It can remove the unwanted frequencies without leading to too much distortion in the signal.

3.4.2 Montage and Segmentation in EEG

In the realm of EEG, the term "montage" encompasses the spatial arrangement of electrodes on the scalp and the amalgamation of their recorded signals [113]. Diverse montages in EEG serve specific purposes, emphasising particular facets of brain activity or aiding in identifying abnormalities. Common montage types include bipolar montages, which involve subtracting signals from adjacent electrodes, and referential montages, where one electrode is the reference for all others. It can help merge or cancel the features from different channels to further improve the SNR, therefore it is necessary to apply montages to enhance signal quality and enable more accurate interpretation of neural responses, particularly in low-amplitude recordings such as ear-EEG.

The strategic selection and extraction of relevant channels are pivotal in the subsequent EEG data analysis. In the context of scalp-EEG, the T4 channel, strategically positioned in proximity to the ear-EEG, is extracted for further analytical scrutiny. Concurrently, a montage procedure is implemented for ear-EEG channels, amalgamating information from all three channels to compute the mean value. This montage processing ensures a comprehensive representation of ear-EEG dynamics, thereby contributing to a holistic understanding of neural

activity within the auditory domain.

All ear-EEG channels are merged using the montage in this study. The T4 and T6 channels are merged for the scalp-EEG to enhance the SNR for any signal. The T4 and T6 channels were selected as they are closest to the temporal lobe and auricular area, making them physiologically relevant for comparison with ear-EEG signals. This proximity supports a more direct comparison between signals captured near the auditory cortex and those from the ear canal.

In this study, we applied averaging across all ear-EEG channels rather than differential processing. Given the compact spatial arrangement of ear electrodes and the expectation of globally evoked responses (e.g., in MMN and P300 paradigms), averaging helps preserve common signal components and improves SNR. Furthermore, it mitigates localised artefacts and avoids the signal cancellation that can occur with pairwise subtraction in closely spaced electrodes.

Different tests require tailored data segmentation strategies to isolate periods of interest and ensure meaningful analysis. For the ASSR test, segments are extracted specifically during the stimulus presentation period to isolate brain responses to auditory stimulation. In the alpha modulation test, the data is divided into a 40-second window, consisting of three distinct phases: 10 seconds before eye closure, 20 seconds with eyes closed, and 10 seconds after reopening. This segmentation allows for analysis of changes in alpha activity associated with eye state transitions. For tests involving transient stimuli, including MMN, P300, and N100, segmentation targets precise event-related responses. Each stimulus onset was segmented into a 1-second epoch, beginning 200 ms prior to the event and extending 800 ms afterwards [101]. This temporal window encompasses both pre-stimulus anticipatory activity and post-stimulus responses, thereby allowing a comprehensive evaluation of ERP components.

3.4.3 Frequency Domain Analysis

In order to demonstrate the change in the frequency response for both alpha modulation and ASSR better, STFT is applied. STFT is a signal processing technique that involves applying the Fourier transform to discrete segments of a signal, enabling the characterisation of the signal's frequency content as a function of time [114]. In the context of the ASSR and alpha wave tests, the EEG data undergo STFT processing after applying filtering procedures. This method facilitates the exploration of frequency variations over time, providing insights into the temporal dynamics of auditory steady-state responses and alpha wave modulation [115]. These two tests are expected to show a specific response at a particular period. Therefore, STFT is an appropriate way to verify the performance of the electrode as it can provide time and frequency resolution to indicate the corresponding response. Compared to the FFT, STFT can provide extra information about certain frequency changes corresponding to a specific time. Applying STFT allows for the clear visualisation of the start and end of the stimulus. Results from the alpha modulation and ASSR tests will be analysed using the STFT, with the number of points per segment (`nperseg`) set to 1.5 seconds' worth of samples (i.e., `nperseg`

= *sampling_rate* $\times$ 1.5), and the number of overlapping points (`noverlap`) set to 1.4 seconds' worth of samples (i.e., `noverlap` = *sampling_rate* $\times$ 1.4). These values were chosen to provide a balanced trade-off between time and frequency resolution. A longer segment improves frequency resolution, which is important for detecting narrow-band responses like the ASSR, while a higher overlap helps preserve temporal continuity and detail in the spectrogram. These parameters were selected empirically to ensure stable and interpretable time-frequency representations for both ASSR and alpha modulation tasks.

The equation for STFT is given by:

$$X_{STFT}[m,n] = \sum_{k=0}^{L-1} x[k]\, g[k-m]\, e^{-j2\pi nk/L} \tag{3.2}$$

where $x[k]$ denotes the discrete-time signal and $g[k-m]$ is the window function centred at time index m. In this study, a rectangular window is used, meaning that equal weight is applied to all samples within the window length L, and zero elsewhere [116].

The processing uses Python code and plotted into a figure for verification. The result of the verification is shown in a spectrogram showing the signal's strength in the specific time-specific frequency in different colours using the "viridis" colourmap setting.

The analysis of alpha power involves examining the evolution of average power within the 8–12 Hz frequency range, commonly referred to as alpha power, over time. [3]. This analytical methodology is employed to assess variations in the alpha wave throughout the experiment. Specifically, the average power during the eye-open and eye-closed periods is computed for further examination. This approach provides a more transparent and more quantifiable measure, and a clear difference can be seen in both periods of the corresponding response during specific periods.

The Relative mean alpha modulation (R_{AM}) is used to verify performance; it is calculated for both eye close and eye open periods separately, calculated using the following equation:

$$R_{AM} = \frac{P_{\mathrm{avg}}(\text{Alpha Band}_{\text{Eyes Closed}})}{P_{\mathrm{avg}}(\text{Alpha Band}_{\text{Eyes Open}})} \tag{3.3}$$

This method quantifies the response within the brain and helps indicate the measurement quality of the electrode.

In order to provide a quantitative analysis result for the ASSR, alpha power is being calculated. PSD is a fundamental signal processing and engineering metric, elucidating the power distribution within a signal concerning its frequency components [117]. This quantitative measure is instrumental in delineating the spectral characteristics of a signal, thereby offering a comprehensive understanding of the power distribution across different frequency bands. Compared

to the FFT, which is another method that can convert the signal from the time domain to the frequency domain, PSD gives a smoother and more stable representation.

In the current experimental framework, PSD analysis contributes to unravelling the spectral features of EEG signals, particularly in the context of alpha wave modulation. The results from ASSR, MMN, and P300 tests will be analysed using PSD. For the ASSR, specifically for the single-frequency test, the SNR will be calculated. SNR is computed by determining the ratio between the power at 40 Hz and the average power between 35 to 45 Hz, excluding 40 Hz itself deliberately excluded, as shown in Equation 3.4 [3]. This approach suits tests requiring frequency response analysis without extracting specific time-related information.

$$\text{SNR} = \frac{\text{P(40 Hz)}}{\text{P}_{\text{avg}}\text{(35 - 45 Hz)}} \tag{3.4}$$

For the ASSR test, segments are extracted specifically during the stimulus presentation period to isolate brain responses to auditory stimulation. In the alpha modulation test, the data is divided into a 40-second window, consisting of three distinct phases: 10 seconds before eye closure, 20 seconds with eyes closed, and 10 seconds after reopening. This segmentation allows for analysis of changes in alpha activity associated with eye state transitions. For tests involving transient stimuli, including MMN, P300, and N100, segmentation targets precise event-related responses. Time markers are used to extract windows spanning from 200 ms before to 800 ms after each stimulus onset, forming a 1-second epoch [101]. This window captures both anticipatory and evoked brain activity, enabling a detailed assessment of ERPs.

Chapter 4

Results

After processing the collected EEG data using the methods outlined in the previous chapters, the results from various tests, including ASSR, alpha modulation, and ERP tasks, are presented in this chapter. These results provide a comprehensive evaluation of the ear-EEG device's performance in capturing neural activity and are compared against traditional scalp-EEG recordings to validate signal quality and functional reliability.

4.1 Auditory Steady-State Response (ASSR)

The ASSR test was conducted to evaluate the ability of the ear-EEG device to capture auditory steady-state responses elicited by sound stimuli. Three types of comparisons were performed: (1) wet ear-EEG electrodes versus wet scalp-EEG electrodes, (2) dry ear-EEG electrodes versus wet scalp-EEG electrodes, and (3) single-stimulus ASSR performance evaluation.

4.1.1 Wet Electrode Results

The outcomes of the ASSR test conducted with wet ear-EEG electrodes are visually represented in Fig. 4.2 processed by STFT, delineating discernible frequencies in response to diverse stimuli. The changing of different frequencies at every 20 seconds can be seen, and a precise step-like shape can be seen in both results at corresponding frequency. Notably, scalp-EEG exhibits distinct frequency variations corresponding to different stimuli. The ASSR response for all frequencies can be seen for scalp-EEG, while for ear-EEG, it is clear for all frequencies above 40 Hz. The switch between different frequencies can be observed.

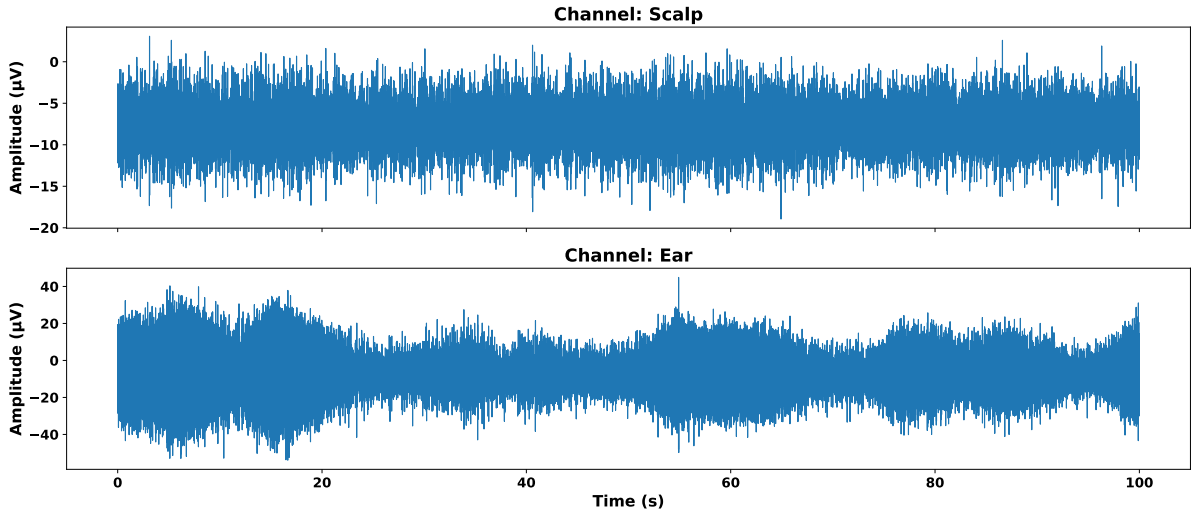

Figure 4.1: Raw ASSR signal for the scalp-EEG and wet ear-EEG electrode.

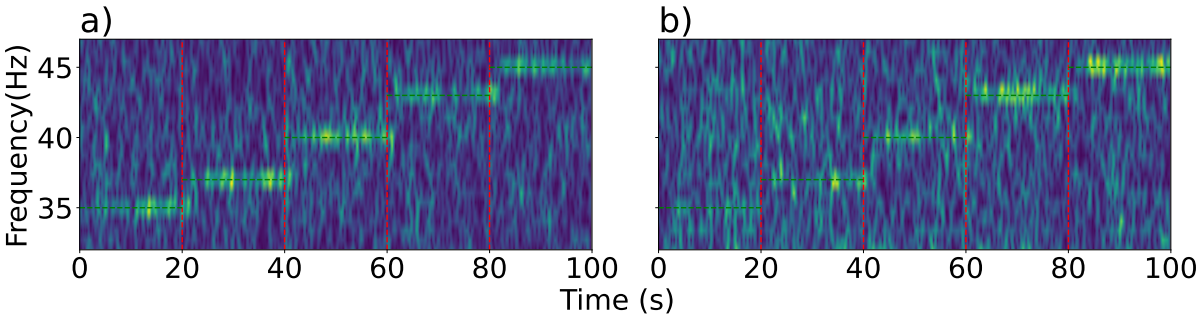

Figure 4.2: (a) Test result derived from scalp-EEG and (b) Test result derived from ear-EEG using wet electrodes. The red lines indicate the position of the frequency change. The green lines indicate the expected frequency.

4.1.2 Dry Electrode Comparison

To verify the performance of the electrode to be used as a dry electrode, the same test is performed for the electrode without conductive gel. Fig. 4.4 portrays the identical test executed utilising a dry ear-EEG electrode. The ear-EEG response closely mirrors that observed with the wet electrode, indicating minimal deviations in the ear-EEG electrode's performance. These findings imply that dry ear-EEG can capture similar responses while recording sound stimuli.

4.1.3 Single-Frequency Response (40 Hz)

A pure frequency test was conducted to evaluate the dry electrode's performance further to check the overall signal-noise ratio of the expected signal. Fig. 4.6 presents specific results for the 40 Hz stimulus over a 100-second time span, revealing comparable responses between dry ear-EEG and scalp-EEG. This test uses the electrode without applying the conductive gel, suggesting dry ear-EEG electrode performance equivalent to traditional scalp-EEG in

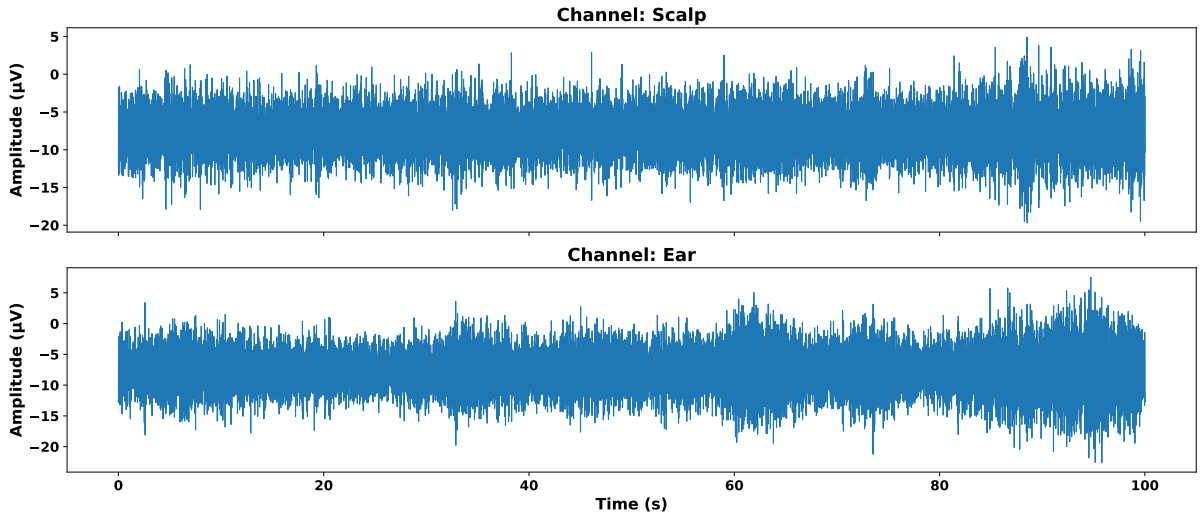

Figure 4.3: Raw Signal for ASSR comparison between wet EEG scalp-EEG and dry ear-EEG.

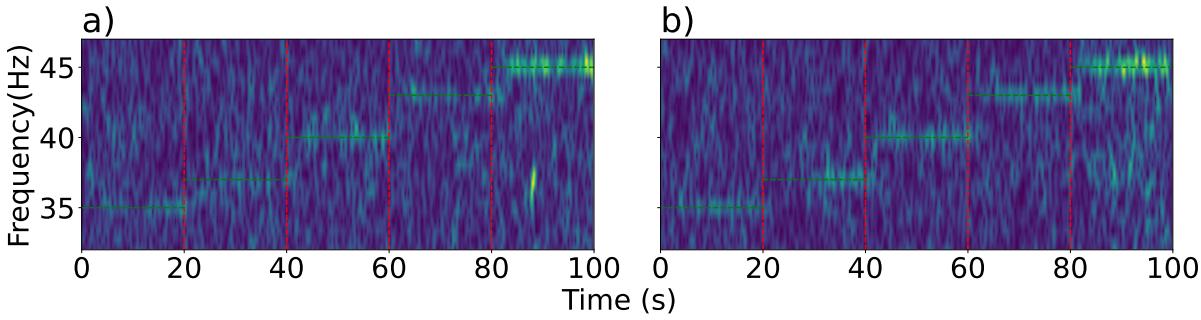

Figure 4.4: (a) Test result derived from scalp-EEG and (b) Test result derived from ear-EEG using dry electrodes. The red lines indicate the position of the frequency change. The green lines indicate the expected frequency.

response to sound stimuli. This observation supports the idea that ear-EEG offers comparable performance to scalp-EEG when recording signals associated with the temporal cortex. This aligns with findings that ear-EEG can reliably capture neural signals linked to auditory and motor tasks, showcasing its potential as a practical alternative for portable and user-friendly EEG applications. For example, ear-EEG's proximity to the temporal cortex enhances its capacity to detect auditory evoked potentials, making it effective for auditory tasks and brain-computer interface applications. The real-time data can be seen in Fig. 4.5.

4.1.4 Validation and Comparison of ASSR Detection in ear-EEG

Compared to the previous work provided by Kaveh et al. [3], the signal result from their ASSR test result is about 5.94 dB for ear-EEG, while for scalp-EEG, their result is 10.5 dB, while in our work, the SNR is highly similar compared to their work. Compared to the results presented by Mikkelsen et al. [76], as shown in Fig. 2.2.5, where the average SNR for scalp-EEG was 4.00 dB and 3.73 dB for ear-EEG, the performance achieved in this work demonstrates a comparable level of effectiveness to those reported in previous studies.

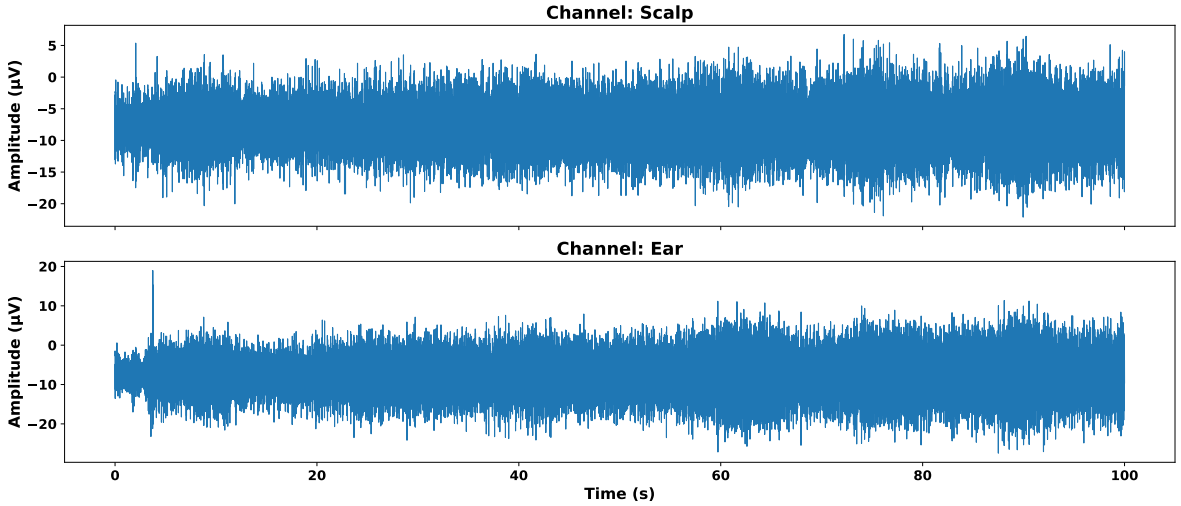

Figure 4.5: Real time data for the single stimulus ASSR test across 100 seconds.

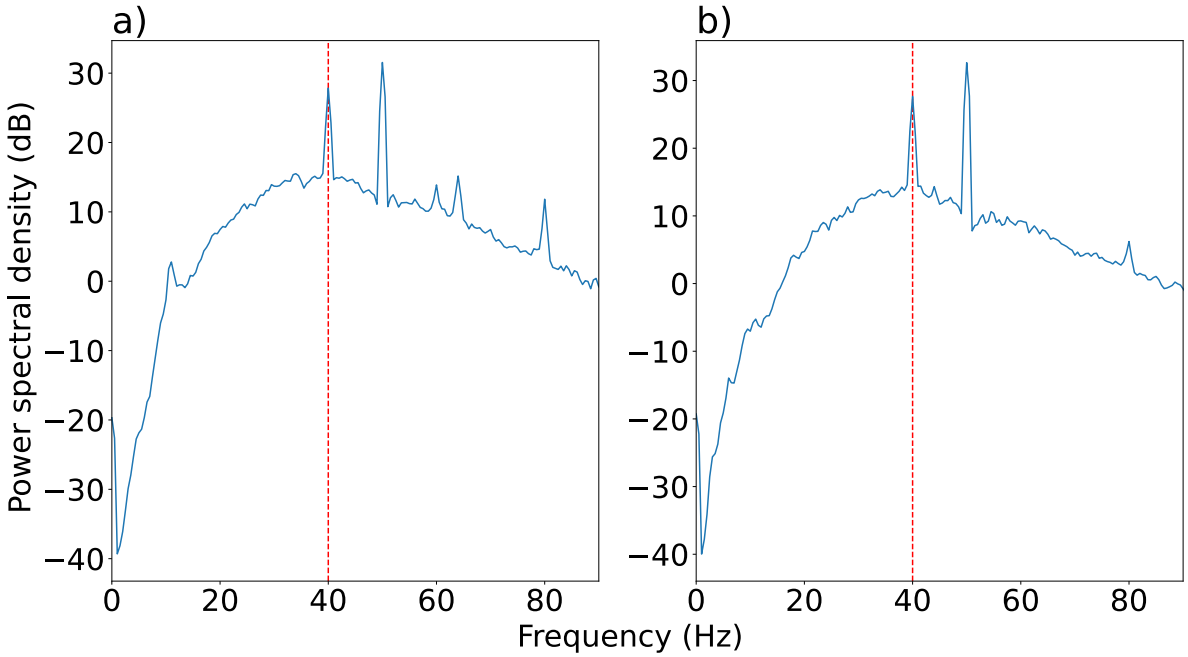

Figure 4.6: (a) Test result derived from scalp-EEG with an SNR of 11.36 dB, (b) Test result derived from ear-EEG with an SNR of 11.94 dB. The red lines indicate the 40 Hz. The signal at 50 Hz is the local powerline noise.

The test results indicate that the ear-EEG electrode performs comparably to scalp-EEG when exposed to steady-state sound stimuli with sufficient SNR. The testing results show that the ear-EEG can be a reliable auditory evaluation in daily life.

Figures 4.1, 4.3, and 4.5 display real-time ASSR signals. Although the overall amplitudes are comparable, the scalp-EEG traces remain relatively uniform over time, whereas the ear-EEG traces fluctuate more noticeably. This increased temporal variability suggests that additional noise or artifacts may be affecting the ear-EEG recordings.

4.2 Directional Hearing (N100)

Fig. 4.7 presents the time-domain waveforms from the first 12 trials, showing a prominent negative deflection characteristic of the N100 response, occurring approximately 200 ms after stimulus onset. The similarity between ear-EEG and scalp-EEG signals demonstrates that ear-EEG is capable of capturing reliable and robust auditory responses. Notably, the N100 peak reaches an average amplitude of around $-60\ \mu$V, underscoring its potential for applications in hearing research, BCI systems, and neurofeedback, particularly in mobile or home-based settings. However, it is also clear that ear-EEG signals show a higher level of background noise compared to scalp-EEG. This suggests that while ear-EEG shows promise, further refinement in electrode design or signal processing may be necessary to improve signal quality and reduce artifacts.

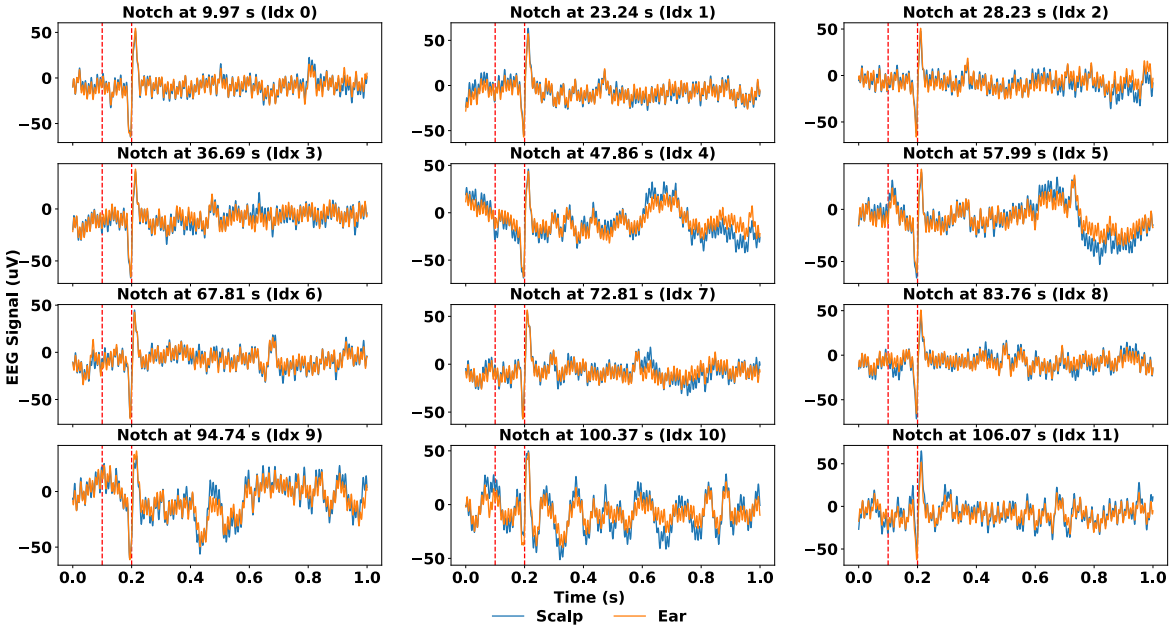

Figure 4.7: Time-domain waveforms from the first 12 trials showing a consistent negative deflection (N100) at approximately 200 ms, with an amplitude around $-60\ \mu$V. The ear-EEG and scalp-EEG signals exhibit highly similar patterns, indicating the reliability of ear-EEG in capturing auditory evoked potentials.

Fig. 4.8 displays the averaged response from 100 of the 150 recorded trials, further reinforcing the reliability and repeatability of the N100 signal when measured using ear-EEG.

These results contribute to the growing body of evidence supporting ear-EEG as a viable alternative to scalp-EEG for auditory evoked potential analysis. Its proximity to the auditory cortex, combined with its unobtrusive form factor, enables practical and reliable monitoring in both clinical and everyday environments.

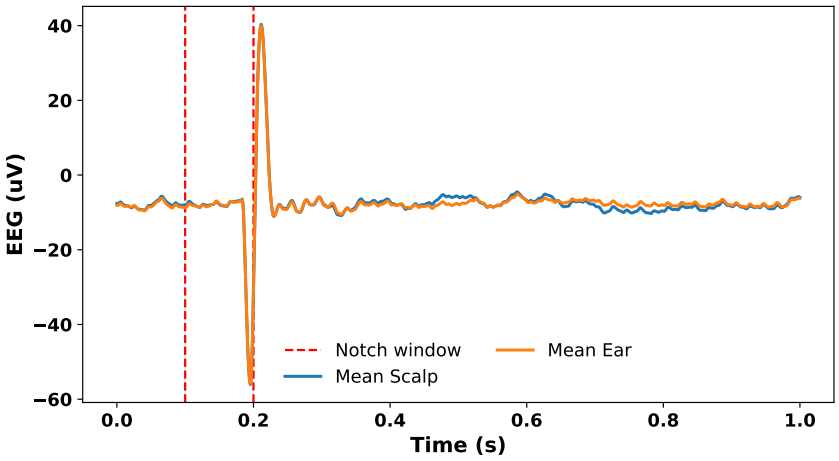

Figure 4.8: Average N100 response from 100 out of 150 trials, showing a clear and consistent negative peak around 200 ms.

4.3 Passive Oddball (MMN)

Fig. 4.9 shows the MMN response, with a characteristic negative deflection observed approximately 200–220 ms after stimulus onset. While some ear-EEG recordings demonstrate amplitudes comparable to scalp-EEG, most ear-EEG responses are attenuated, consistent with the reduced signal strength typical of ear-EEG.

While some ear-EEG recordings demonstrated MMN amplitudes comparable to those seen in scalp-EEG, most responses were attenuated, consistent with the reduced signal strength characteristic of ear-EEG. Nonetheless, the waveform morphology, a distinct negative peak followed by a return to baseline, remained similar across modalities. In several cases, MMN was only detectable in scalp-EEG, underscoring the limitations of ear-EEG in capturing weaker or more subtle components. To characterise the overall trend, the average waveform across all detected MMN events was computed as shown in Fig. 4.10, revealing a consistent notch near 200 ms. These findings suggest that although ear-EEG shows promise for non-invasive auditory monitoring, particularly in mobile or long-term settings, further work is needed to enhance signal quality and reduce artifacts for more reliable detection across individuals and sessions.

4.4 Active Oddball (P300)

In the P300 test, a positive deflection is expected within the 300–400 ms time window for both scalp-EEG and ear-EEG, consistent with findings reported by Meiser and Bleichner [101]. This expected response is evident in the real-time waveform shown in Fig. 4.11, where a distinct peak appears at approximately 350 ms for both modalities. Although the amplitude of the P300 response recorded from ear-EEG is lower than that from scalp-EEG, it is still significantly elevated above baseline (scalp-EEG), indicating a detectable neural response. Com-

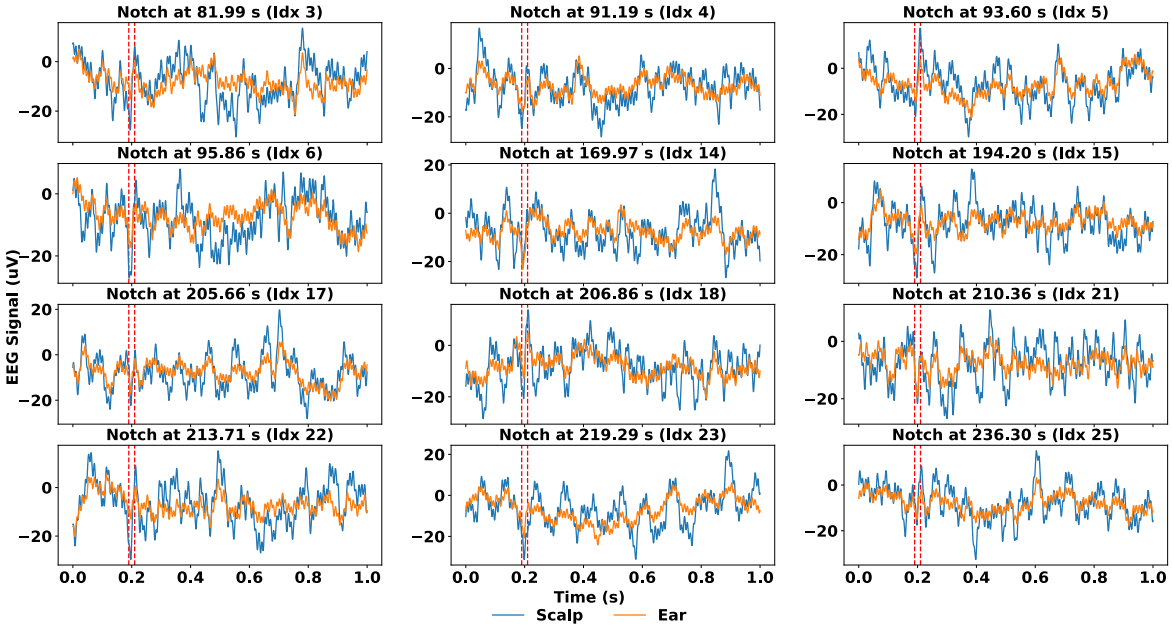

Figure 4.9: Time-domain waveform of the MMN test. A negative deflection is observed approximately 200 ms after stimulus onset, corresponding to the expected MMN response.

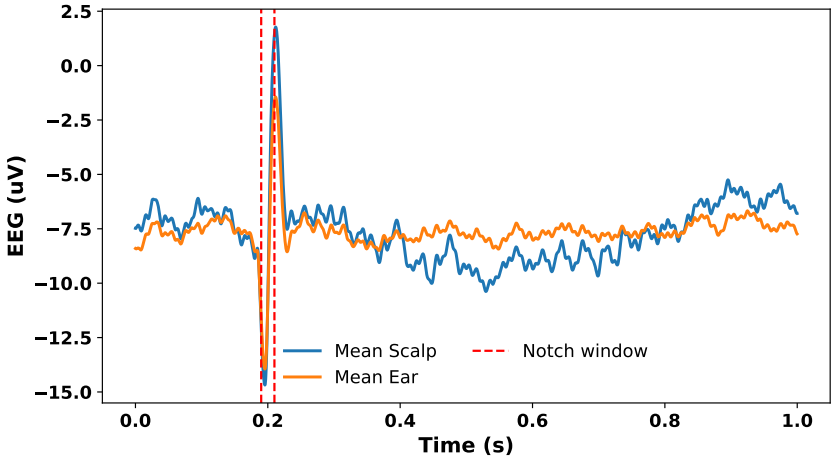

Figure 4.10: Averaged MMN waveform across all trials. A clear negative peak around 200 ms post-stimulus confirms the typical MMN pattern.

pared to scalp-EEG, the P300 waveform in ear-EEG exhibits a less pronounced but similarly timed trend. This resemblance in waveform morphology suggests that ear-EEG can effectively capture the P300 component, albeit with a reduced signal-to-noise ratio. Overall, the results highlight the potential of ear-EEG for detecting event-related potentials such as P300, despite inherent limitations in signal amplitude.

Fig. 4.12 illustrates the average EEG response aligned to detected spikes. While a positive peak is evident around 300–400 ms across all channels, the signal does not exhibit a clearly dominant amplitude compared to adjacent time periods, suggesting a relatively weak or variable P300 component.

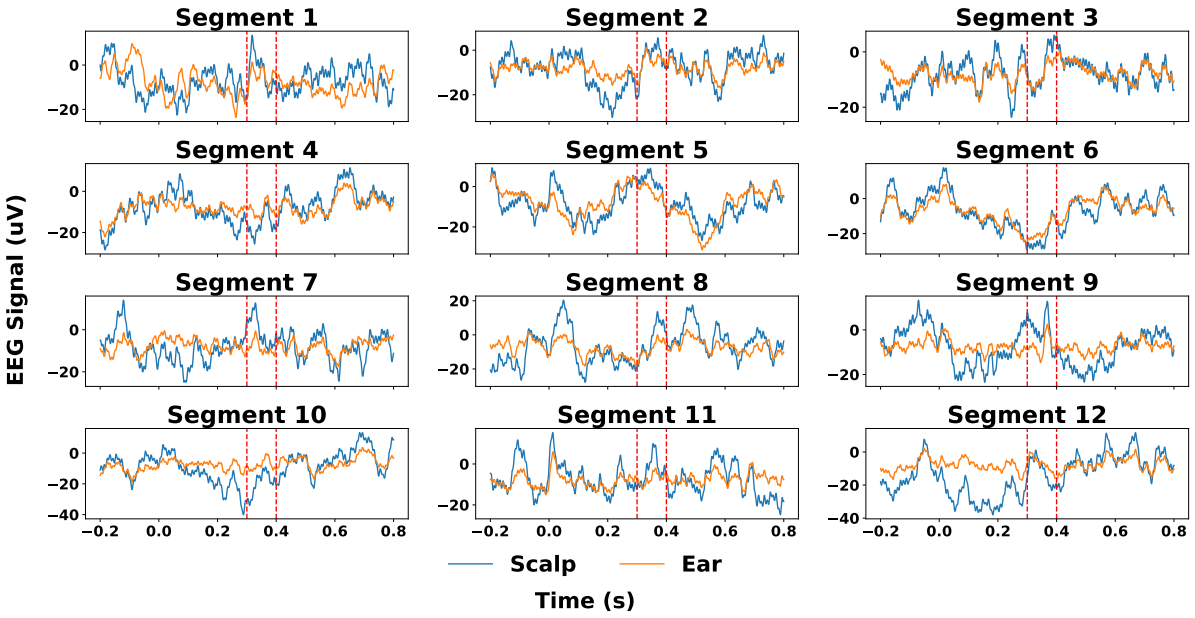

Figure 4.11: P300 test results in the time domain. A positive peak is expected to occur between 300 and 400 milliseconds after the stimulus onset, indicating the presence of a P300 component.

In the P300 test, a positive deflection is expected within the 300-400 ms time window for both scalp-EEG and ear-EEG, consistent with findings reported by Meiser and Bleichner [101]. This expected response is evident in the real-time waveform shown in Fig. 4.11, where a distinct peak appears at approximately 350 ms for both modalities. Although the amplitude of the P300 response recorded from ear-EEG is generally lower than that from scalp-EEG, some ear-EEG recordings demonstrate comparable peak amplitudes. Nonetheless, most ear-EEG signals tend to have reduced amplitude relative to scalp-EEG, reflecting the inherent challenges of signal acquisition at the ear site. Despite these amplitude differences, the overall waveform morphology and timing are similar, indicating that ear-EEG can effectively capture the P300 component. However, the lower signal-to-noise ratio in ear-EEG may affect the detection of smaller or less robust event-related potentials. Since P300 has maximal amplitude over parietal areas, and ear-EEG lacks access to these sites, the reduced amplitude in ear-EEG is consistent with the expected topography of this ERP component. These results underscore the potential of ear-EEG for practical, non-invasive brain monitoring, while highlighting the need for continued optimisation in device design and signal processing to improve reliability and signal quality.

Despite the similar morphology and timing observed between scalp and ear-EEG signals, the P300 test yielded the weakest results compared to other paradigms such as N100 and ASSR. This is likely due to the topographical nature of the P300 component, which typically exhibits maximum amplitude over parietal regions that ear-EEG electrodes cannot adequately access. As such, the reduced amplitude and lower signal-to-noise ratio in ear-EEG recordings are consistent with known limitations of the modality. These findings underscore both the promise and the current limitations of ear-EEG for detecting higher-order cognitive responses, highlighting the need for further optimisation in electrode placement, signal processing, and

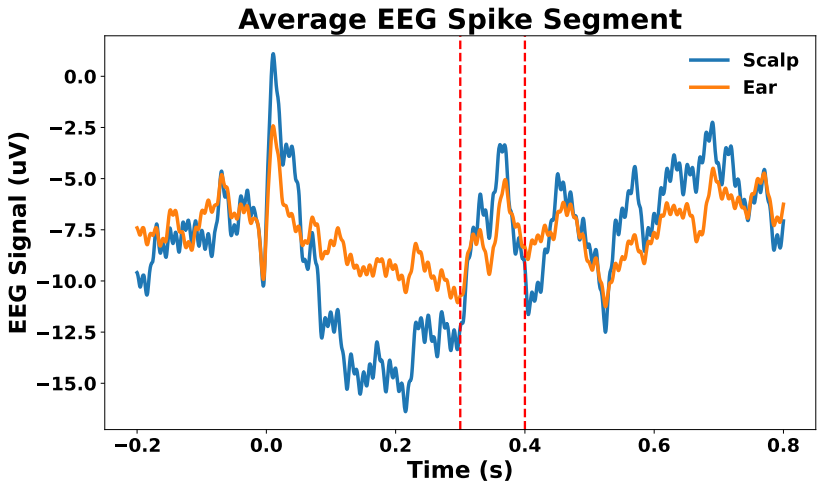

Figure 4.12: Average waveform across all detected spike segments. A positive deflection is observable in the 300–400 ms window across all channels, consistent with a P300 response, although the amplitude is not substantially larger than surrounding activity.

experimental design.

4.5 Alpha Modulation

As a regular EEG test that is related to human attention, alpha modulation is also performed. In the investigation of Alpha Modulation, an expected response within the frequency range of 8 to 12 Hz during periods of closed eyes is the alpha band for EEG signal [3, 118]. Fig. 4.13 shows the real-time raw EEG data from the alpha modulation test. It can be observed that the overall amplitude range is larger in the scalp-EEG compared to the ear-EEG.

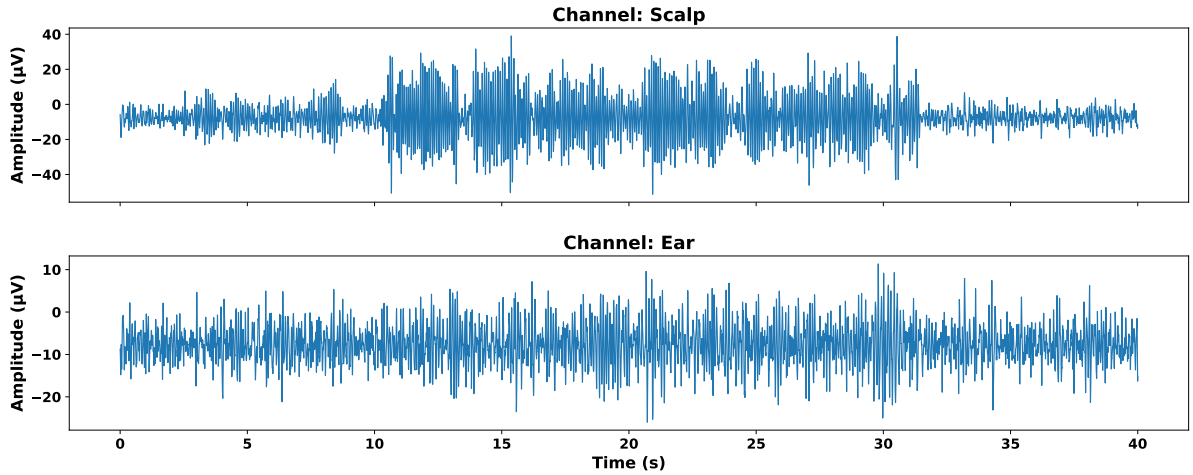

Figure 4.13: Raw EEG signals recorded during the alpha modulation test. Both channels show an increase in amplitude after the 10-second mark, corresponding to the eye-closure period. However, the scalp-EEG exhibits a more pronounced increase, indicating greater sensitivity to alpha modulation compared to the ear-EEG channel.

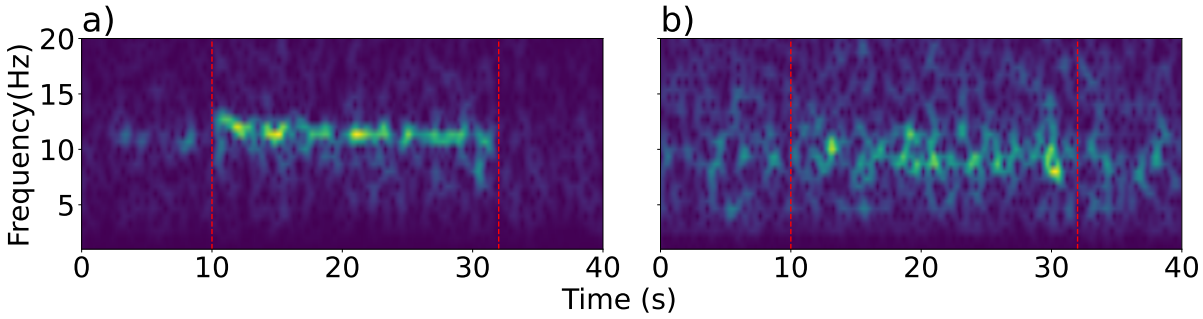

Figure 4.14: (a) Test result derived from scalp-EEG and (b) Test result derived from ear-EEG. Analysis of Alpha Modulation using STFT, with red delineation marking intervals corresponding to closed-eye conditions.

As depicted in Fig. 4.14, tangible patterns emerge within the scalp-EEG, indicating distinct

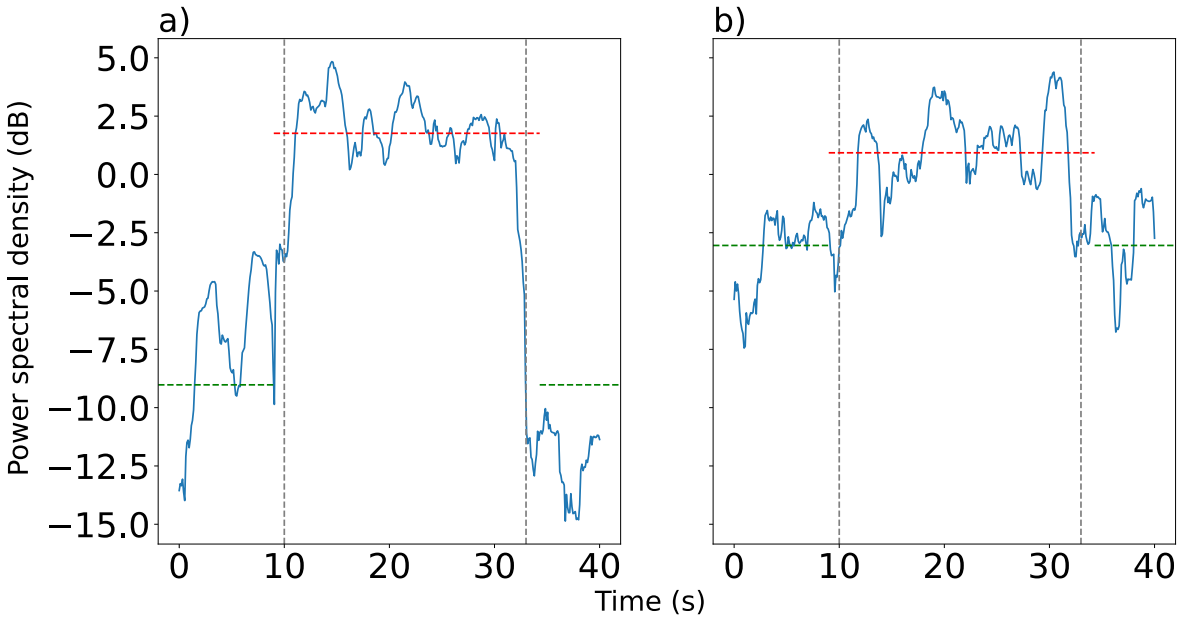

Figure 4.15: (a) Test result derived from scalp-EEG, the average power difference between eye closed and eye open is 10.71 dB, and (b) Test result derived from ear-EEG, the average power difference between eye closed and eye open is 3.45 dB. Grey delineation indicates epochs of closed-eye conditions. The green horizontal line represents the average power during eye-open periods, while the red horizontal line signifies the average power during eye-closed periods.

responses during intervals of closed eyes versus open-eye periods. A meticulous examination of the data, emphasising power spectrum density within the 8-12 Hz frequency range, further underscores these observations. The STFT analysis reveals that the alpha band activity is more pronounced during the eyes-closed condition, with an apparent increase in amplitude in the expected frequency range. This finding aligns with established knowledge about alpha rhythm modulation associated with ocular states.

The signal is also analysed with PSD to verify the SNR of the signal response. Fig. 4.15 provides additional insights through analysis of PSD. It distinctly portrays a notable increase

in power density during the eyes-closed periods, providing substantial evidence supporting the proposition that neural dynamics exhibit distinct characteristics contingent upon the state of ocular activity. The PSD analysis demonstrates a marked difference in power between the eyes-closed and eyes-open conditions. Specifically, the power differential of 10.71 dB in scalp-EEG underscores a robust and precise modulation of alpha activity, a well-documented phenomenon in EEG studies. In contrast, the ear-EEG shows a power differential of 3.45 dB, indicating a less pronounced but still detectable modulation. Here, the power values are expressed in decibels (dB) relative to the average power during the eyes-open periods, which serves as the reference level for the dB calculation.

Further scrutiny of the results reveals that while both ear-EEG and scalp-EEG channels exhibit the anticipated alpha modulation response, there are notable differences in the magnitude and clarity of this response. The scalp-EEG achieves an R_{AM} (Relative Alpha Modulation) value of 5.79 and a power differential of 10.71 dB, indicating a robust and precise modulation of alpha activity, in line with established literature. In contrast, the ear-EEG shows a lower R_{AM} of 2.3 and a power differential of 3.45 dB. Although this difference in power may not meet conventional thresholds for strong physiological significance, it nonetheless reflects a consistent alpha modulation pattern aligned with the subject's ocular state.

The reduced alpha modulation observed in ear-EEG is likely attributable to factors such as limited spatial resolution, suboptimal electrode placement, or attenuated signal amplitude due to the ear canal's anatomical constraints. Despite these limitations, the detection of a directionally consistent alpha response suggests that ear-EEG retains sufficient sensitivity to capture relevant neural dynamics. This supports its potential utility in scenarios where comfort, discretion, and long-term wearability are prioritised, even if some trade-offs in signal strength are expected.

4.6 Proposed Solution Test

The recorded signals in response to 10 Hz and 20 Hz sinusoidal stimulation are shown in Figures 4.16 and 4.17. Clear peaks are observed at the respective stimulation frequencies, indicating successful detection by the proposed setup. The corresponding SNR values are 44.44 dB for 10 Hz and 39.07 dB for 20 Hz.

For both test conditions, a clear peak is observed in the PSD at the respective stimulation frequencies, indicating successful detection of the input signal. Specifically, the 10 Hz signal exhibits a dominant peak centred at 10 Hz with minimal spectral leakage, with an SNR of 44.04 dB, while the 20 Hz response similarly shows a strong, isolated peak at 20 Hz with an SNR of 39.07 dB. These results demonstrate that the proposed setup preserves frequency specificity and is capable of capturing low-amplitude periodic signals with minimal distortion. In the time domain, the raw voltage traces reflect clean sinusoidal patterns without obvious noise or baseline drift.

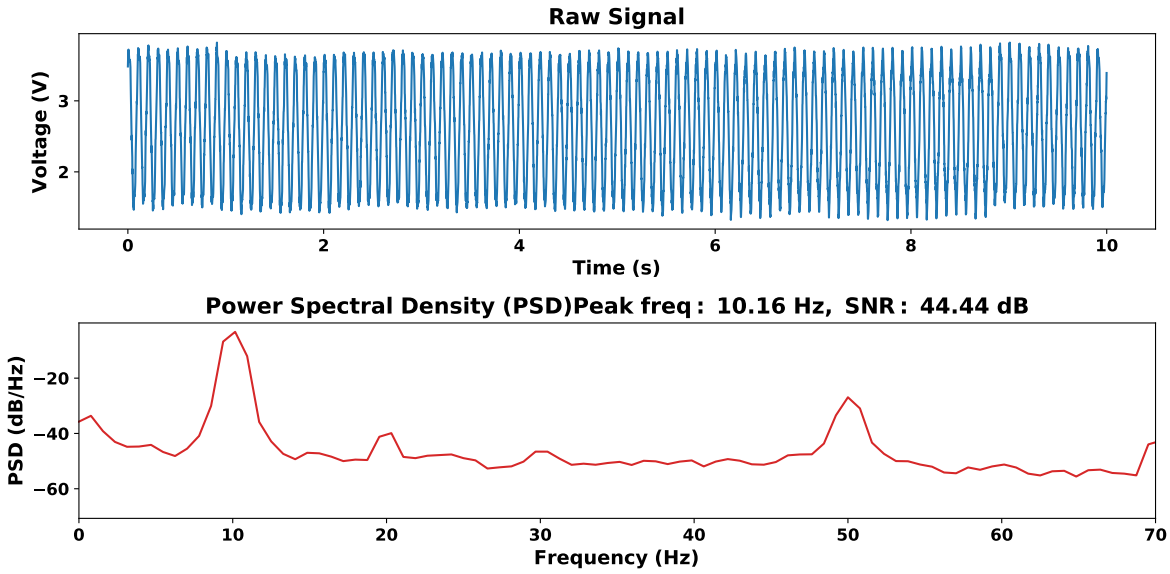

Figure 4.16: PSD and raw signal in response to a 10 Hz sinusoidal stimulation. A clear peak is observed at 10 Hz, indicating successful detection. The SNR is calculated as the ratio between the peak power and the mean power excluding the ± 0.5 Hz band around 10 Hz, is 44.44 dB.

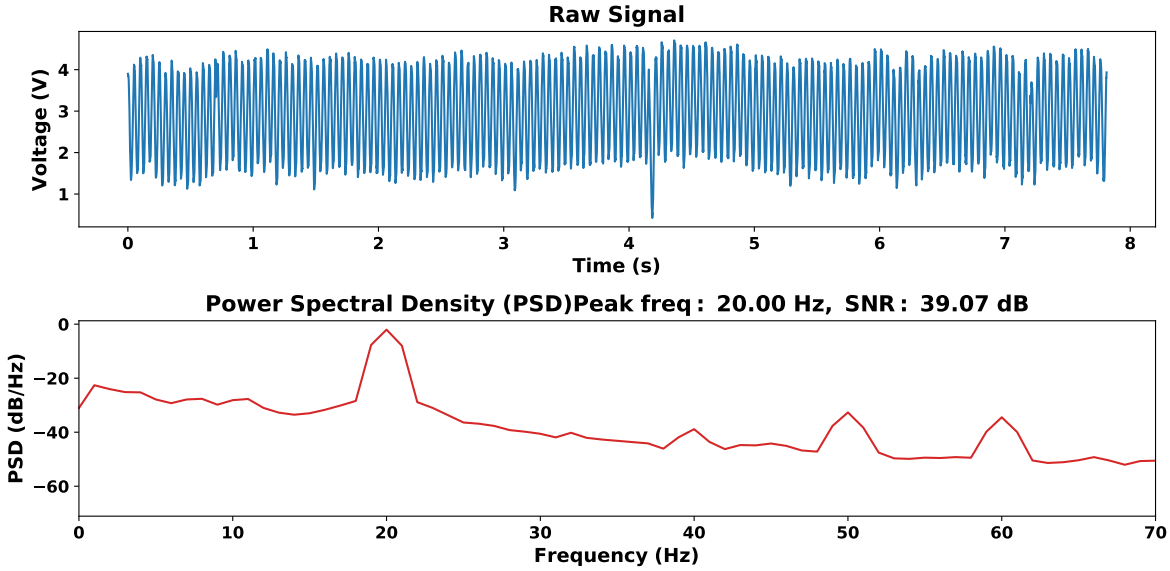

Figure 4.17: PSD and raw signal in response to a 20 Hz sinusoidal stimulation. A clear peak is observed at 20 Hz, indicating successful detection. The SNR is calculated as the ratio between the peak power and the mean power excluding the ± 0.5 Hz band around 20 Hz, is 39.07 dB.

Overall, the proposed solution proves to be a viable method for acquiring periodic stimulation signals from saline, with both spectral and temporal results confirming fidelity to the input waveform.

Chapter 5

Conclusion and Future Development

This paper introduced a 3D-printed ear-EEG device designed for personalised monitoring, with the potential for wireless signal transmission for further analysis. Leveraging CT or camera scanning technology to obtain a 3D model of the patient's ear enables the creation of a fully customised device through 3D printing. This approach tailors the device to the individual's unique ear anatomy, enhancing both fit and comfort, which is particularly beneficial for extended daily wear. Various tests, including ASSR, Alpha Modulation, and P300, were conducted to assess its performance in capturing EEG signals from both steady-state and transient stimuli. The results confirmed the device's capability to capture signals from diverse brain activities accurately. This research, as a proof of concept, shows that for an ear-EEG device that is produced from 3D printing, which means it has the potential to be made into the shape of any ear canal with the corresponding circuit board on it that can produce a reasonable recording result for further applications.

The overall contribution of this thesis can be summarised as the exploration of 3D printing as a novel method for manufacturing ear-EEG devices, integrating both the electrode and the analogue front end into a single print. Additionally, the thesis investigates various test protocols suitable for verifying the performance and reliability of ear-EEG systems.

The ear-EEG device effectively records responses to various transient stimuli and demonstrates commendable performance in capturing EEG signals induced by steady-state sound stimuli. These findings suggest that ear-EEG can provide results comparable to traditional scalp-EEG across various EEG stimuli, especially sound-related stimuli, showcasing its potential for versatile applications in neurophysiological monitoring. The results indicate that ear-EEG is suitable for long-term daily monitoring and can provide reliable data for various studies.

Furthermore, the device's compact and non-intrusive design enhances user comfort, making it ideal for continuous wear. This aspect is crucial for prolonged monitoring applications, such as sleep studies and continuous health monitoring. The customisation offered by 3D printing ensures that the device can be tailored to different ear shapes and sizes, addressing

the common issue of poor fit and discomfort associated with standard EEG devices.

The potential for wireless data transmission further elevates the utility of the ear-EEG device. By incorporating wireless technology, the device can transmit real-time data to external systems for immediate analysis. Notably, this feature is beneficial in clinical settings where timely data interpretation is essential for patient care. Moreover, the wireless capability enables seamless integration with mobile and wearable technologies, paving the way for innovative telemedicine and remote health monitoring applications.

5.1 Future Directions

The future of hearables holds significant potential for advancements in both signal quality and overall performance. Emerging technologies and innovative design approaches can enhance their accuracy, reliability, and usability. With these advancements, hearables will not only improve in capturing high-quality physiological signals but also expand into new applications, further integrating into healthcare, wellness, and daily life.

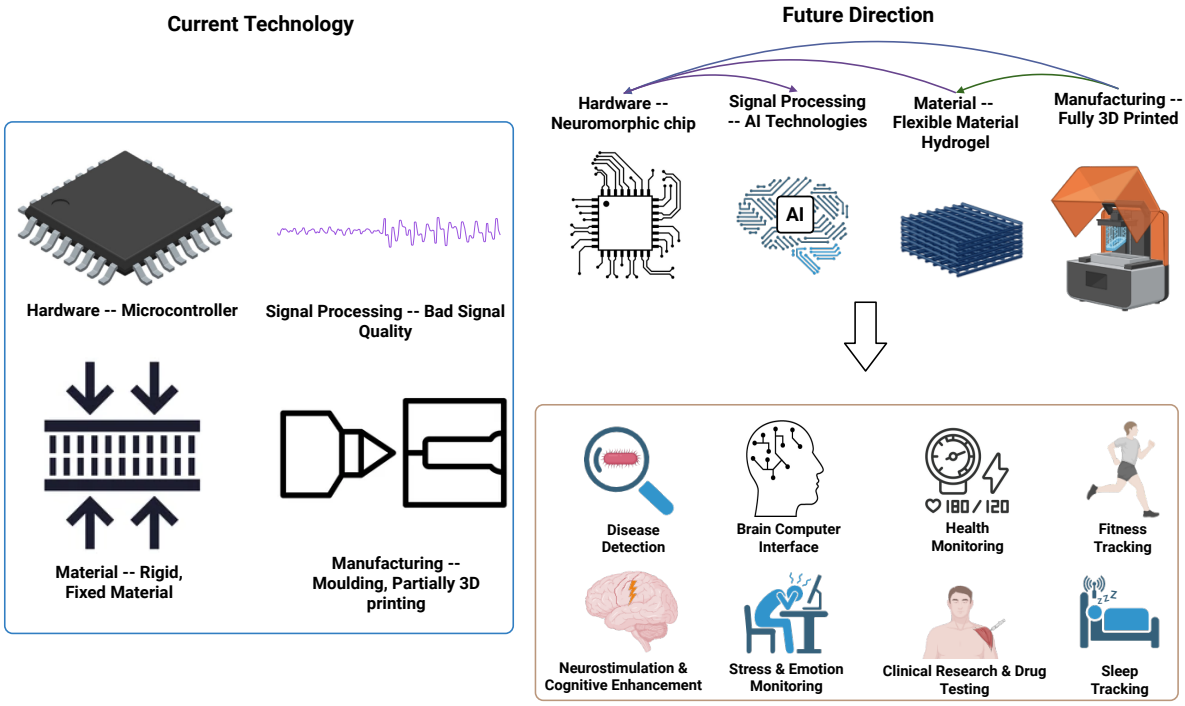

Figure 5.1: By utilising new technologies such as improved hardware devices, advanced signal processing techniques, novel materials, and cutting-edge manufacturing methods, a wide range of applications has become possible.

5.1.1 Multi-Sensor Hearables

The integration of multiple sensors into hearable devices enables the collection of diverse biological signals, enhances data fusion capabilities, and improves signal quality through noise cancellation across different sensors. By utilising machine learning and advanced signal processing, multi-sensor hearables can extract more meaningful insights from physiological data, supporting both consumer wellness and clinical applications.

Żyliński et al. [119] introduced a hearable device capable of monitoring ECG, PPG, and heart sounds, providing comprehensive and multimodal heart rate monitoring. Similarly, Montanari et al. [120] developed a hearable that integrates kinetic, acoustic, optical, and thermal sensors with machine learning for advanced data analysis. These innovations show the potential of hearables as multi-functional platforms for real-time health monitoring.

In future developments, integrating an omnidirectional (360-degree) camera into the hearable system could significantly enhance seizure monitoring by capturing the video of the patient's full-body movements and environmental influence during or before the seizure. Many seizures would show distinct motor patterns, such as sudden falls, convulsions, or automatisms, which would be hard to determine from the EEG signals themselves, particularly when using spatially constrained systems like ear EEG. With the integration of omnidirectional video with EEG data, clinicians would gain a more comprehensive view of how seizure onset and progression occur, aiding in the classification of seizure types and the localisation of involved cortical regions. Moreover, this approach enables remote and real-world monitoring, supporting continuous assessment outside hospital settings. Similar approaches using video-EEG systems have demonstrated clinical utility in epilepsy diagnostics and treatment planning [121].

Such advancements demonstrate the potential of multi-sensor systems to transform hearables into powerful tools for continuous health tracking, with applications spanning general wellness to clinical diagnostics.

5.1.2 Advanced Signal Processing Techniques

As mentioned before, one of the key challenges in hearables is enhancing the SNR from different noise sources, such as motion artifacts, to ensure high-quality physiological data acquisition. Techniques such as filtering to remove noise and artifacts, segmentation to isolate relevant events, and feature extraction to identify critical signal patterns are commonly employed. These approaches are particularly useful in capturing bioelectrical signals like EEG, ECG, and PPG, as well as acoustic and temperature signals. Due to the compact nature of hearables, designing efficient AFE circuits remains a challenge. To address this, IC AFE designs have been explored to optimise signal acquisition while minimising size and power consumption [56].

To overcome size and power constraints, several low-cost and efficient solutions have been developed. For instance, Teversham et al. [57] designed a low-cost physiological monitoring system using an ESP32 microcontroller, integrating AFE components such as a bandpass filter, differential amplifier, and notch filter. This approach enables real-time signal decoding at a fraction of the cost of traditional medical devices, demonstrating the feasibility of low-cost, wearable physiological monitoring. Utilising external computational resources for additional signal processing offers another practical solution for enhancing portability and efficiency. Hölle and Bleichner [58] introduced a system where a commercial amplifier and general-purpose hearable sensors were paired with a smartphone for real-time sound and biometric signal analysis. By offloading computation to a smartphone, the hearable device itself can remain compact and energy-efficient while still benefiting from advanced signal processing capabilities. Power efficiency is a critical factor for long-term hearable use. Lee et al. [45] developed a low-power communication system utilising body channel transmission, reducing power consumption and enabling continuous monitoring over extended periods. This type of innovation is essential for daily health monitoring applications such as heart rate tracking, respiratory monitoring, and stress detection. Dedicated chips designed for hearables focus on optimising high input impedance and low noise to effectively capture bioelectrical and acoustic signals in real-world environments. For example, Zheng [54] introduced a Time-Division Multiplexing (TDM)-based AFE with a capacitively coupled chopper design, achieving superior noise performance. Similarly, Jin et al. [60] developed a low-power AFE ASIC tailored for wearable applications, ensuring minimal power consumption while maintaining signal integrity.

The integration of AI further enhances hearable capabilities by improving signal interpretation and automation. Mai et al. [61] implemented a 1D-Convolutional Neural Network (1D-CNN) model on an embedded system, using FFT and PSD for real-time emotion classification. AI-powered processing can also help remove signal artifacts and improve accuracy in biometric authentication and health monitoring applications. For instance, Jayas et al. [62] developed an algorithm to detect motion and muscle artifacts in physiological signals, improving data quality for more reliable analysis. AI integration also enables hearables to provide autonomous health insights. Some devices can analyse physiological signals in real time and deliver results directly to users without requiring professional intervention. Neuromorphic chips, for example, allow on-device AI processing with extremely low power consumption, making them well-suited for continuous monitoring applications [65]. Similarly, FPGAs have been explored for energy-efficient AI inference. Al-Ashmouny et al. [66] demonstrated the use of FPGA-based processing for sleep apnoea detection using physiological signals, showcasing the potential for real-time health assessments in wearable applications.

These advancements in AFE design, power efficiency, and AI-driven processing are transforming hearables into powerful, multi-functional health monitoring tools. Hearables are becoming more useful in a wider range of applications, from monitoring heart health and sleep to improving cognitive function and biometric security. This is because they are overcoming problems with cost, size, and signal processing.

5.1.3 Deployment of AI Models

Advances in artificial intelligence and edge computing hardware have significantly increased the feasibility of deploying AI models on wearable devices. These advancements offer substantial benefits, such as delivering actionable insights to users, enabling early detection of health issues, and assisting healthcare professionals by prioritising critical data. Additionally, on-device model training supports the creation of personalised models tailored to individual users' unique physiological characteristics. However, due to the inherent constraints of hearables, including limited computational resources and restricted input data channels, these models must be designed to operate efficiently under such conditions.

In the domain of EEG signals, Herbozo Contreras et al. [122] proposed an ultra-low-power seizure detection model specifically optimised for integration into wearable devices, making it a promising candidate for next-generation hearables. Similarly, Zhu et al. [123] developed a lightweight edge model for sleep staging using single-channel EEG data, making it well-suited for hearable applications. Huang et al. [124] further contributed by developing a dedicated chip for deploying AI models on edge devices.

For ECG signals, Huang et al. [125] designed a model for ECG classification tailored to resource-constrained edge devices. Huang et al. [126] introduced a preprocessing-free model for detecting heart abnormalities, optimised for devices with limited resources. Furthermore, Huang et al. [127] presented a framework enabling the training of large models directly on edge devices, facilitating resource-efficient solutions. Moreover, Meza-Rodriguez et al. [128] successfully deployed a heart abnormality classification model and deployed it on an MCU, demonstrating the feasibility of integrating advanced AI capabilities into edge hardware.

These examples underscore the transformative potential of integrating AI into wearables. By enabling real-time data analysis, personalised health solutions, and enhanced user accessibility, AI-driven wearables are poised to revolutionise health monitoring and medical diagnostics, making them invaluable tools in clinical and consumer settings.

5.1.4 Advanced Material Technologies

Advancements in material technologies have enabled the development of electrodes and components that enhance adaptability and comfort, allowing for a more personalised fit within the ear canal. These innovations improve both the functionality and wearability of in-ear biosignal monitoring systems, addressing challenges such as signal quality, durability, and long-term usability.

Ahn et al. [129] introduced a technology utilising 3D printing with silver ink to create stretchable electrodes that can be directly applied to the skin for biosignal monitoring. Kumar et al. [130] made a flexible supercapacitor that can power wearable devices. Xu et al. [131] made

a stretchable battery that can be charged wirelessly, which makes fully flexible wearable systems even more possible. Hydrogel-based electrodes also have their own distinct benefits, especially when it comes to making semi-dry electrodes. Ge et al. [36] developed an EEG electrode incorporating hydrogels to achieve both low impedance and high longevity. However, the effectiveness of generalised ear-EEG electrodes may vary significantly due to the use of elastic materials. Since these electrodes rely on the tension of plastic components, variations in material elasticity can impact electrode-skin contact, potentially leading to inconsistencies in impedance and signal quality.

These advancements collectively pave the way for the development of fully flexible, high-performance in-ear biosignal monitoring systems. By improving comfort, durability, and energy efficiency, these materials enhance the practicality of hearables for long-term health monitoring and medical applications.

5.1.5 Advanced Manufacturing Technology

Recent advancements in manufacturing technology have significantly improved the efficiency and feasibility of producing complex, highly specialized hearable devices. Techniques such as 3D printing have revolutionised the production process, enabling precise customisation to accommodate individual anatomical and functional requirements [132].

For instance, 3D printing allows for the fabrication of personalised ear canal components, enhancing both comfort and signal quality by ensuring an optimal fit [3]. Additionally, advanced material technologies, such as biocompatible polymers and conductive inks, facilitate the seamless integration of sensors and electronic components directly into the device structure. This integration reduces assembly complexity, improves signal fidelity, and enhances device durability.

Furthermore, miniaturisation techniques have enabled the development of compact, low-profile hearables capable of housing multifunctional sensors, wireless communication modules, and energy-efficient processing units. These innovations help address challenges related to anatomical variability, device miniaturisation, and long-term wearability, paving the way for the next generation of customised, high-performance hearable devices.

5.1.6 Brain Computer Interface (BCI) and Clinical Monitoring

As portable devices for detecting EEG signals, hearables have the potential to significantly advance BCI technology by providing a discreet, wearable alternative to traditional EEG systems. BCIs enable direct communication between the brain and external devices, with applications ranging from neuroprosthetic control and cognitive monitoring to assistive communication for individuals with disabilities. Currently, common BCI setups often require either

invasive electrodes, such as electrocorticography (ECoG) implants, or non-invasive scalp-EEG systems, which rely on wet electrodes and multi-channel headsets that are not suitable for most of the possible users. While scalp-EEG provides higher spatial resolution than ear-EEG, its bulky setup, gel-based electrodes, and susceptibility to movement artifacts limit its practical use outside of laboratory settings.

With the development of high-quality ear-EEG recording, hearables have the potential to overcome several limitations of traditional EEG systems. They offer a more user-friendly and non-invasive interface for brain–computer interface (BCI) applications, enable continuous brain monitoring in real-world environments, and enhance social acceptability by resembling everyday earbuds rather than conspicuous medical devices. However, several specific challenges must still be addressed to enable the effective use of ear-EEG for BCI applications. First, low spatial resolution remains a significant limitation, as the limited number of electrode positions in ear-EEG restricts the amount of brain activity that can be captured with high signal quality [28]. This can lead to missed or low-SNR neural signals, reducing BCI performance. Future improvements may involve the development of multi-electrode arrays or advanced signal reconstruction techniques to enhance spatial resolution. Second, processing constraints arise due to the need for low-latency, real-time signal processing, which is challenging given the limited computational resources, thermal dissipation, and power budgets in compact hearable devices [133]. Solutions may include lightweight edge-computing frameworks, neuromorphic processors, or dedicated BCI accelerators to improve efficiency. Third, wireless data transmission poses difficulties, as real-time BCIs demand fast and reliable communication. While BLE is energy-efficient, it offers limited bandwidth, and emerging methods such as BCC may provide alternatives with reduced interference and improved reliability [134, 135]. Finally, power constraints are a critical concern; the small form factor of hearables limits battery capacity, requiring all signal processing and computational models to be highly power-efficient to support prolonged use.

Advancements in technology are poised to significantly enhance the effectiveness of wearable and hearable devices in clinical monitoring. Emerging innovations in sensor design, artificial intelligence, and wireless communication can transform current applications in clinical research, drug testing, and sleep tracking. These devices, already capable of providing continuous, non-invasive physiological data, will become even more powerful with improved accuracy, miniaturisation, and user comfort. For example, in sleep monitoring, next-generation hearables could offer more precise and personalised assessments outside of clinical environments. This can provide the researchers and clinicians with extra data for them to understand sleep and related disease without much influence of the subject's sleeping quality which may influence the recording results [136]. AI-driven analysis can further enable real-time interpretation of complex biosignals, supporting adaptive treatment plans and early detection of health issues. As noted by Dimitrov [137], the long-term potential of wearables lies in their ability to integrate into daily life. Nakamura et al. [138] has already demonstrated how ear-EEG combined with machine learning can achieve promising results, paving the way for even more intelligent and adaptive health monitoring systems in the future.

Ethics Statement

This study was approved by the Human Research Ethics Committee of the University of Sydney (Project ID: 2024/HE000105, Recording scalp-EEG and ear-EEG from human subjects for testing and verifying the ear-EEG device). All participants provided written informed consent prior to participation. The research was conducted in accordance with the ethical standards of the committee and the principles outlined in the Declaration of Helsinki.
The confirmation letter for ethics approval can be accessed via link.

Data Availability

The data gathered from this test can be accessed via this link.

Code Availability

The code used for this thesis can be accessed via this link.

References

[1] Nisreen Said Amer and Samir Brahim Belhaouari. EEG signal processing for medical diagnosis, healthcare, and monitoring: A comprehensive review. *IEEE Access*, 11: 143116–143142, 2023.

[2] JC Martinez, Goh Zhi Hwee, Luis Yap, Kenneth Wei De Chua, Savitha Kamath, Conrad Kang Rui Chung, Wendy Yu Bing Teo, Charmaine Kai Ling Tan, Stylianos Dritsas, and Robert E Simpson. Lexicon for classifying ear-canal shapes. *Scientific Reports*, 13(1): 11866, 2023.

[3] Ryan Kaveh, Justin Doong, Andy Zhou, Carolyn Schwendeman, Karthik Gopalan, Fred L Burghardt, Ana C Arias, Michel M Maharbiz, and Rikky Muller. Wireless user-generic ear EEG. *IEEE Transactions on Biomedical Circuits and Systems*, 14(4): 727–737, 2020.

[4] Tobias Banaschewski and Daniel Brandeis. Annotation: what electrical brain activity tells us about brain function that other techniques cannot tell us–a child psychiatric perspective. *Journal of Child Psychology and Psychiatry*, 48(5):415–435, 2007.

[5] Michal Teplan et al. Fundamentals of EEG measurement. *Measurement Science Review*, 2(2):1–11, 2002.

[6] Ying Gu, Evy Cleeren, Jonathan Dan, Kasper Claes, Wim Van Paesschen, Sabine Van Huffel, and Borbála Hunyadi. Comparison between scalp EEG and behind-the-ear EEG for development of a wearable seizure detection system for patients with focal epilepsy. *Sensors*, 18(1):29, 2018.

[7] Netiwit Kaongoen, Jaehoon Choi, Jin Woo Choi, Haram Kwon, Chaeeun Hwang, Guebin Hwang, Byung Hyung Kim, and Sungho Jo. The future of wearable EEG: A review of ear-EEG technology and its applications. *Journal of Neural Engineering*, 2023.

[8] David Looney, Cheolsoo Park, Preben Kidmose, Mike Lind Rank, Michael Ungstrup, Karin Rosenkranz, and Danilo P Mandic. An in-the-ear platform for recording electroencephalogram. In *2011 Annual International Conference of the IEEE Engineering in Medicine and Biology Society*, pages 6882–6885, 2011.

[9] Timo Kirschstein and Rüdiger Köhling. What is the source of the EEG? *Clinical EEG and Neuroscience*, 40(3):146–149, 2009.

[10] Kyle E Mathewson, Tyler JL Harrison, and Sayeed AD Kizuk. High and dry? comparing active dry EEG electrodes to active and passive wet electrodes. *Psychophysiology*, 54(1):74–82, 2017.

[11] Hao Zhang, Qing-Qi Zhou, He Chen, Xiao-Qing Hu, Wei-Guang Li, Yang Bai, Jun-Xia Han, Yao Wang, Zhen-Hu Liang, Dan Chen, et al. The applied principles of EEG analysis methods in neuroscience and clinical neurology. *Military Medical Research*, 10(1):67, 2023.

[12] Bing Zou, Yubo Zheng, Mu Shen, Yingying Luo, Lei Li, and Lin Zhang. Beats: An open-source, high-precision, multi-channel EEG acquisition tool system. *IEEE Transactions on Biomedical Circuits and Systems*, 16(6):1287–1298, 2022.

[13] Valer Jurcak, Daisuke Tsuzuki, and Ippeita Dan. 10/20, 10/10, and 10/5 systems revisited: their validity as relative head-surface-based positioning systems. *Neuroimage*, 34 (4):1600–1611, 2007.

[14] Richard W Homan. The 10-20 electrode system and cerebral location. *American Journal of EEG Technology*, 28(4):269–279, 1988.

[15] Fayez Alshamsi and Trent Lewis. Discrimination of neuropsychiatric disease using EEG and neurophysiological biomarker toolbox (NBT) with machine learning. *IOSR Journal of Computer Engineering*, 22(5):32, 2020.

[16] Yoko Hoshi. Functional near-infrared spectroscopy: potential and limitations in neuroimaging studies. *International Review of Neurobiology*, 66:237–266, 2005.

[17] Udaya Seneviratne and Wendyl Jude D'Souza. ambulatory EEG. *Handbook of clinical neurology*, 160:161–170, 2019.

[18] Dianne Dash, Lizbeth Hernandez-Ronquillo, Farzad Moien-Afshari, and Jose F Tellez-Zenteno. Ambulatory EEG: a cost-effective alternative to inpatient video-EEG in adult patients. *Epileptic Disorders*, 14:290–297, 2012.

[19] Frank Gilliam, Ruben Kuzniecky, and Edward Faught. Ambulatory EEG monitoring. *Journal of Clinical Neurophysiology*, 16(2):111–115, 1999.

[20] John S Ebersole. Ambulatory cassette EEG. *Journal of Clinical Neurophysiology*, 2 (4):397, 1985.

[21] Ulrike Baum, Frauke Kühn, Marcel Lichters, Anne-Katrin Baum, Renate Deike, Hermann Hinrichs, and Thomas Neumann. Neurological outpatients prefer EEG home-monitoring over inpatient monitoring—an analysis based on the utaut model. *International Journal of Environmental Research and Public Health*, 19(20):13202, 2022.

[22] Andreas Schulze-Bonhage, Francisco Sales, Kathrin Wagner, Rute Teotonio, Astrid Carius, Annette Schelle, and Matthias Ihle. Views of patients with epilepsy on seizure prediction devices. *Epilepsy & behavior*, 18(4):388–396, 2010.

[23] Jaiver Macea, Miguel Bhagubai, Victoria Broux, Maarten De Vos, and Wim Van Paesschen. In-hospital and home-based long-term monitoring of focal epilepsy with a wearable electroencephalographic device: Diagnostic yield and user experience. *Epilepsia*, 64(4):937–950, 2023.

[24] Nick Hunn. Hearables – the new wearables, 2014. URL https://wt-obk.wearable-technologies.com/2014/04/hearables-the-new-wearables/. Accessed: 2025-03-13.

[25] McGregor Joyner, Sheng-Hsiou Hsu, Stephanie Martin, Jennifer Dwyer, Denise Fay Chen, Reza Sameni, Samuel H Waters, Konstantin Borodin, Gari D Clifford, Allan I Levey, et al. Using a standalone ear-EEG device for focal-onset seizure detection. *Bioelectronic Medicine*, 10(1):4, 2024.

[26] Michela Masè, Alessandro Micarelli, and Giacomo Strapazzon. Hearables: new perspectives and pitfalls of in-ear devices for physiological monitoring. a scoping review. *Frontiers in Physiology*, 11:568886, 2020.

[27] Gang Li, Boon-Leng Lee, and Wan-Young Chung. Smartwatch-based wearable EEG system for driver drowsiness detection. *IEEE Sensors Journal*, 15(12):7169–7180, 2015.

[28] David Looney, Preben Kidmose, and Danilo P Mandic. Ear-EEG: user-centered and wearable BCI. *Brain-Computer Interface Research: A State-of-the-Art Summary-2*, pages 41–50, 2014.

[29] Kaare B Mikkelsen et al. EEG recorded from the ear: Characterizing the Ear-EEG method. *Frontiers in Neuroscience*, 9, 2015.

[30] Preben Kidmose, David Looney, Lars Jochumsen, and Danilo P Mandic. Ear-EEG from generic earpieces: A feasibility study. In *35th Annual International Conference of the IEEE Engineering in Medicine and Biology Society (EMBC)*, pages 543–546, 2013.

[31] Gennady Sintotskiy and Hermann Hinrichs. In-ear-EEG–a portable platform for home monitoring. *Journal of Medical Engineering & Technology*, 44(1):26–37, 2020.

[32] Leping Yu, Zhangyu Xu, Luis Herbozo Contreras, and Omid Kavehei. An additively manufactured 3D printed electronics system for personalized ear-EEG. In *2024 International Conference on Electrical, Computer and Energy Technologies (ICECET*, pages 1–6, 2024.

[33] Valentin Goverdovsky, Wilhelm Von Rosenberg, Takashi Nakamura, David Looney, David J Sharp, Christos Papavassiliou, Mary J Morrell, and Danilo P Mandic. Hearables: Multimodal physiological in-ear sensing. *Scientific Reports*, 7(1):6948, 2017.

[34] José Juez, David Henao, Fredy Segura, Rodrigo Gómez, Michel Le Van Quyen, and Mario Valderrama. Development of a wearable system with in-ear EEG electrodes for the monitoring of brain activities: An application to epilepsy. In *2nd IEEE International Congress of Biomedical Engineering and Bioengineering (CI-IB&BI)*, pages 1–4, 2021.

[35] Hongyu Liang, Yongxuan Wang, Honghui Li, Yuying Wang, Peter Xiaoping Liu, and Rong Liu. Development and characterization of a dry ear-EEG sensor with a generic flexible earpiece. *IEEE Transactions on Instrumentation and Measurement*, 72:1–12, 2023.

[36] Xueyang Ge, Yongxin Guo, Chenbo Gong, Runyi Han, Jingrui Feng, Jingwei Ji, Zhengcan Sun, Jing Gao, Fei Bian, and Zhaopeng Xu. High-conductivity, low-impedance, and high-biological-adaptability ionic conductive hydrogels for Ear-EEG acquisition. *ACS Applied Polymer Materials*, 5(10):8151–8158, 2023.

[37] Minjae Kim, Seungjae Yoo, and Chul Kim. Miniaturization for wearable EEG systems: recording hardware and data processing. *Biomedical Engineering Letters*, 12(3):239–250, 2022.

[38] Zhouheng Wang, Nanlin Shi, Yingchao Zhang, Ning Zheng, Haicheng Li, Yang Jiao, Jiahui Cheng, Yutong Wang, Xiaoqing Zhang, Ying Chen, et al. Conformal in-ear bioelectronics for visual and auditory brain-computer interfaces. *Nature Communications*, 14(1):4213, 2023.

[39] Martin G Bleichner, Bojana Mirkovic, and Stefan Debener. Identifying auditory attention with ear-EEG: ceegrid versus high-density cap-EEG comparison. *Journal of Neural Engineering*, 13(6):066004, 2016.

[40] Simon L Kappel, Mike L Rank, Hans Olaf Toft, Mikael Andersen, and Preben Kidmose. Dry-contact electrode ear-EEG. *IEEE Transactions on Biomedical Engineering*, 66(1): 150–158, 2018.

[41] Dong-Hwa Jeong and Jaeseung Jeong. In-ear EEG based attention state classification using echo state network. *Brain Sciences*, 10(6):321, 2020.

[42] Max Eickenscheidt, Patrick Schäfer, Yara Baslan, Claudia Schwarz, and Thomas Stieglitz. Highly porous platinum electrodes for dry ear-EEG measurements. *Sensors*, 20(11):3176, 2020.

[43] Christian Bech Christensen, Renskje K Hietkamp, James M Harte, Thomas Lunner, and Preben Kidmose. Toward EEG-assisted hearing aids: Objective threshold estimation based on ear-EEG in subjects with sensorineural hearing loss. *Trends in Hearing*, 22: 2331216518816203, 2018.

[44] Kaare B Mikkelsen, David Bové Villadsen, Marit Otto, and Preben Kidmose. Automatic sleep staging using ear-EEG. *Biomedical Engineering Online*, 16(1):1–15, 2017.

[45] Jaehyuk Lee, Kyoung-Rog Lee, Unsoo Ha, Ji-Hoon Kim, Kwonjoon Lee, Surin Gweon, Jaeeun Jang, and Hoi-Jun Yoo. A 0.8-v 82.9-μw in-ear BCI controller ic with 8.8 PEF EEG instrumentation amplifier and wireless BAN transceiver. *IEEE Journal of Solid-State Circuits*, 54(4):1185–1195, 2019.

[46] Simon L Kappel and Preben Kidmose. High-density ear-EEG. In *39th Annual International Conference of the IEEE Engineering in Medicine and Biology Society (EMBC)*, pages 2394–2397, 2017.

[47] Yuchen Xu, Ernesto De la Paz, Akshay Paul, Kuldeep Mahato, Juliane R Sempionatto, Nicholas Tostado, Min Lee, Gopabandhu Hota, Muyang Lin, Abhinav Uppal, et al. In-ear integrated sensor array for the continuous monitoring of brain activity and of lactate in sweat. *Nature Biomedical Engineering*, 7(10):1307–1320, 2023.

[48] Yousef Rezaei Tabar, Kaare B Mikkelsen, Mike Lind Rank, Martin Christian Hemmsen, Marit Otto, and Preben Kidmose. Ear-EEG for sleep assessment: a comparison with actigraphy and PSG. *Sleep and Breathing*, 25:1693–1705, 2021.

[49] Wayne J Staab, Walter Sjursen, David Preves, and Tom Squeglia. A one-size disposable hearing aid is introduced. *The Hearing Journal*, 53(4):36–38, 2000.

[50] Jade Naicker. Medical illustration in anatomy. In *Graphic Medicine, Humanizing Healthcare and Novel Approaches in Anatomical Education*, pages 63–83. Springer, 2023.

[51] David Looney, Preben Kidmose, Cheolsoo Park, Michael Ungstrup, Mike Lind Rank, Karin Rosenkranz, and Danilo P Mandic. The in-the-ear recording concept: User-centered and wearable brain monitoring. *IEEE Pulse*, 3(6):32–42, 2012.

[52] Martin G Bleichner, Micha Lundbeck, Matthias Selisky, Falk Minow, Manuela Jäger, Reiner Emkes, Stefan Debener, and Maarten De Vos. Exploring miniaturized EEG electrodes for brain-computer interfaces. an EEG you do not see? *Physiological Reports*, 3 (4):e12362, 2015.

[53] Julie Uchitel, Ernesto E Vidal-Rosas, Robert J Cooper, and Hubin Zhao. Wearable, integrated EEG–fnirs technologies: A review. *Sensors*, 21(18):6106, 2021.

[54] Huiyong Zheng. A tdm-based analog front-end for ear-EEG recording with 83-g ω input impedance, 384-mv dc tolerance and 0.47-μ vrms input-referred noise. *arXiv preprint arXiv:2402.17538*, 2024.

[55] Mona Mozaffari, Robert Nash, and Abigail S Tucker. Anatomy and development of the mammalian external auditory canal: implications for understanding canal disease and deformity. *Frontiers in Cell and Developmental Biology*, 8:617354, 2021.

[56] Jiawei Xu, Srinjoy Mitra, Chris Van Hoof, Refet Firat Yazicioglu, and Kofi AA Makinwa. Active electrodes for wearable EEG acquisition: Review and electronics design methodology. *IEEE Reviews in Biomedical Engineering*, 10:187–198, 2017.

[57] James Teversham, Steven S Wong, Bryan Hsieh, Adrien Rapeaux, Francesca Troiani, Oscar Savolainen, Zheng Zhang, Michal Maslik, and Timothy G Constandinou. Development of an ultra low-cost SSVEP-based BCI device for real-time on-device decoding. In *2022 44th Annual International Conference of the IEEE Engineering in Medicine & Biology Society (EMBC)*, pages 208–213, 2022.

[58] Daniel Hölle and Martin G Bleichner. Smartphone-based ear-electroencephalography to study sound processing in everyday life. *European Journal of Neuroscience*, 58(7): 3671–3685, 2023.

[59] Virag Varga, Gergely Vakulya, Alanson Sample, and Thomas R Gross. Enabling interactive infrastructure with body channel communication. *Proceedings of the ACM on Interactive, Mobile, Wearable and Ubiquitous Technologies*, 1(4):1–29, 2018.

[60] Han Jin, Weimin Hu, Yajie Zhao, Yizhou Jiang, Yongjie Ye, Shouyan Wang, and Yajie Qin. A 1.5 mm 2 4-channel EEG/BIOZ acquisition asic with 15.2-bit 3-step ADC based on a signal-dependent low-power strategy. *IEEE Transactions on Biomedical Circuits and Systems*, 2023.

[61] Ngoc-Dau Mai, Ha-Trung Nguyen, and Wan-Young Chung. Real-time on-chip machine-learning-based wearable behind-the-ear electroencephalogram device for emotion recognition. *IEEE Access*, 11:47258–47271, 2023.

[62] Tanuja Jayas, A Adarsh, Kartik Muralidharan, Jayavardhana Gubbi, Arpan Pal, et al. Computer aided detection of dominant artifacts in ear-EEG signal. In *2023 IEEE International Conference on Systems, Man, and Cybernetics (SMC)*, pages 4423–4428, 2023.

[63] Gustavo Torres Gaona, David Blanquez Caurel, Adrian Valls Carbo, Xavier Raurich Fabregas, Jesus Valls Garcia-Muñoz, Lluis Munso Ponti, Josep Lluis Arcos, Adrian Trejo, and Angel Aledo-Serrano. A prospective controlled study for EEG records comparison between Scalp-EEG and Ear-EEG wearable device, for subsequent analysis by an artificial intelligence-based system: SERAS-EEG study. *medRxiv*, pages 2023–10, 2023.

[64] Ying Sun, Xiaolin Liu, Rui Na, Shuai Wang, Dezhi Zheng, and Shangchun Fan. Cross-domain feature distillation framework for enhancing classification in Ear-EEG brain-computer interfaces. In *Adjunct Proceedings of the 2023 ACM International Joint Conference on Pervasive and Ubiquitous Computing & the 2023 ACM International Symposium on Wearable Computing*, pages 706–711, 2023.

[65] Mohammadali Sharifshazileh, Karla Burelo, Johannes Sarnthein, and Giacomo Indiveri. An electronic neuromorphic system for real-time detection of high frequency oscillations (hfo) in intracranial EEG. *Nature Communications*, 12(1):3095, 2021.

[66] Khaled M Al-Ashmouny, Hisham M Hamed, and Ahmed A Morsy. FPGA-based sleep apnea screening device for home monitoring. In *2006 International Conference of the IEEE Engineering in Medicine and Biology Society*, pages 5948–5951, 2006.

[67] Aishi Zhou, Li Zhang, Xiaoyang Yuan, and Changsheng Li. A signal prediction-based method for motor imagery EEG classification. *Biomedical Signal Processing and Control*, 86:105139, 2023.

[68] Josemir W Sander. The epidemiology of epilepsy revisited. *Current Opinion in Neurology*, 16(2):165–170, 2003.

[69] Peter Camfield and Carol Camfield. Incidence, prevalence and aetiology of seizures and epilepsy in children. *Epileptic Disorders*, 17(2):117–123, 2015.

[70] A Ulate-Campos, F Coughlin, M Gaínza-Lein, I Sánchez Fernández, PL Pearl, and T Loddenkemper. Automated seizure detection systems and their effectiveness for each type of seizure. *Seizure*, 40:88–101, 2016.

[71] Madison Milne-Ives, Rosiered Brownson-Smith, Ananya Ananthakrishnan, Yihan Wang, Cen Cong, Gavin P Winston, and Edward Meinert. The use of ai in epilepsy and its applications for people with intellectual disabilities: commentary. *Acta Epileptologica*, 7(1):13, 2025.

[72] Yousef R Tabar, Kaare B Mikkelsen, Nelly Shenton, Simon L Kappel, Astrid R Bertelsen, Reza Nikbakht, Hans O Toft, Chris H Henriksen, Martin C Hemmsen, Mike L Rank, et al. At-home sleep monitoring using generic ear-EEG. *Frontiers in Neuroscience*, 17:987578, 2023.

[73] Kenneth Borup, Preben Kidmose, Huy Phan, and Kaare Mikkelsen. Automatic sleep scoring using patient-specific ensemble models and knowledge distillation for ear-EEG data. *Biomedical Signal Processing and Control*, 81:104496, 2023.

[74] Metin C Yarici, Pierluigi Amadori, Harry Davies, Takashi Nakamura, Nico Lingg, Yiannis Demiris, and Danilo P Mandic. Hearables: Ear EEG based driver fatigue detection. *arXiv preprint: 2301.06406*, 2023.

[75] Carmen van Klaren, Anneloes Maij, Laurie Marsman, and Alwin van Drongelen. The evaluation of cEEGrids for fatigue detection in aviation. *Sleep Advances*, 5(1):zpae009, 2024.

[76] Kaare B. Mikkelsen, Preben Kidmose, and Yousef Rezaei Tabar. Ear-EEG sleep monitoring 2019 (EESM19)-OpenNeuro, 2019. OpenNeuro dataset.

[77] Kaare Bjarke Mikkelsen, Yousef Rezai Tabar, Laura Rævsbæk Birch, Simon Lind Kappel, Christian Bech Christensen, Lars Dalskov Mosgaard, Marit Otto, Martin Christian Hemmsen, Mike Lind Rank, and Preben Kidmose. Ear-EEG sleep monitoring data sets. *Scientific Data*, 12(1):301, 2025.

[78] Sharanbasappa R Japatti, Priyanka J Engineer, B Manjunatha Reddy, Akash U Tiwari, Chidambar Y Siddegowda, and Reshma B Hammannavar. Anthropometric assessment of the normal adult human ear. *Annals of Maxillofacial Surgery*, 8(1):42–50, 2018.

[79] Jen-Fang Yu, Kun-Che Lee, Ren-Hung Wang, Yen-Sheng Chen, Chun-Chieh Fan, Ying-Chin Peng, Tsung-Hsien Tu, Ching-I Chen, and Kuei-Yi Lin. Anthropometry of external auditory canal by non-contactable measurement. *Applied Ergonomics*, 50: 50–55, 2015.

[80] P Burgar. Design of flexible dry cnt/pdms electrodes for in-ear eeg. Master's thesis, Delft University of Technology, 2022.

[81] Dongyeol Seok, Sanghyun Lee, Minjae Kim, Jaeouk Cho, and Chul Kim. Motion artifact removal techniques for wearable EEG and PPG sensor systems. *Frontiers in Electronics*, 2:685513, 2021.

[82] Simon L Kappel, David Looney, Danilo P Mandic, and Preben Kidmose. Physiological artifacts in scalp EEG and ear-EEG. *Biomedical Engineering Online*, 16(1):1–16, 2017.

[83] Edoardo Occhipinti, Harry J Davies, Ghena Hammour, and Danilo P Mandic. Hearables: Artefact removal in ear-EEG for continuous 24/7 monitoring. In *2022 International Joint Conference on Neural Networks (IJCNN)*, pages 1–6, 2022.

[84] Souvik Phadikar, Nidul Sinha, and Rajdeep Ghosh. Automatic EEG eyeblink artefact identification and removal technique using independent component analysis in combination with support vector machines and denoising autoencoder. *IET Signal Processing*, 14(6):396–405, 2020.

[85] Lara Natta, Francesco Guido, Luciana Algieri, Vincenzo M Mastronardi, Francesco Rizzi, Elisa Scarpa, Antonio Qualtieri, Maria T Todaro, Vincenzo Sallustio, and Massimo De Vittorio. Conformable AlN piezoelectric sensors as a non-invasive approach for swallowing disorder assessment. *ACS Sensors*, 6(5):1761–1769, 2021.

[86] Gaia de Marzo, Vincenzo M Mastronardi, Luciana Algieri, Federica Vergari, Filippo Pisano, Luca Fachechi, Sergio Marras, Lara Natta, Barbara Spagnolo, Virgilio Brunetti, et al. Sustainable, flexible, and biocompatible enhanced piezoelectric chitosan thin film for compliant piezosensors for human health. *Advanced Electronic Materials*, 9(9): 2200069, 2023.

[87] M Mariello, TWA Blad, VM Mastronardi, F Madaro, F Guido, U Staufer, N Tolou, and M De Vittorio. Flexible piezoelectric AlN transducers buckled through package-induced preloading for mechanical energy harvesting. *Nano Energy*, 85:105986, 2021.

[88] Alan BG Lansdown et al. A pharmacological and toxicological profile of silver as an antimicrobial agent in medical devices. *Advances in Pharmacological and Pharmaceutical Sciences*, 2010, 2010.

[89] American Electroencephalographic Society. Guideline thirteen: Guidelines for standard electrode position nomenclature. *Journal of Clinical Neurophysiology*, 11(1): 111–113, 1994.

[90] Benjamin Solf, Stefan Schramm, Maren-Christina Blum, and Sascha Klee. The influence of the stimulus design on the harmonic components of the steady-state visual evoked potential. *Frontiers in human Neuroscience*, 14:343, 2020.

[91] David Regan. Some characteristics of average steady-state and transient responses evoked by modulated light. *Electroencephalography and Clinical Neurophysiology*, 20(3):238–248, 1966.

[92] Peggy Korczak, Jennifer Smart, Rafael Delgado, Theresa M Strobel, and Christina Bradford. Auditory steady-state responses. *Journal of the American Academy of Audiology*, 23(03):146–170, 2012.

[93] Gian Battista Azzena, Guido Conti, Rosamaria Santarelli, Fabrizio Ottaviani, Gaetano Paludetti, and Maurizio Maurizi. Generation of human auditory steadystate responses (SSRs). i: Stimulus rate effects. *Hearing research*, 83(1-2):1–8, 1995.

[94] Jorge Bohórquez and Özcan Özdamar. Generation of the 40-hz auditory steady-state response (ASSR) explained using convolution. *Clinical Neurophysiology*, 119(11):2598–2607, 2008.

[95] Monik Alamanda and Marc H Hohman. Auditory steady-state response. In *StatPearls [Internet]*. StatPearls Publishing, Treasure Island (FL), 2023. URL https://www.ncbi.nlm.nih.gov/books/NBK597346/.

[96] Chetan S Nayak and Arayamparambil C Anilkumar. EEG normal waveforms. statpearls. *Treasure Island, FL: StatPearls Publishing. http://www. ncbi. nlm. nih. gov*, 2020.

[97] Wolfgang Klimesch. Alpha-band oscillations, attention, and controlled access to stored information. *Trends in Cognitive Sciences*, 16(12):606–617, 2012.

[98] Jos J. Eggermont. Chapter 3 - the alpha and delta rhythms and their interaction with other brain rhythms. In Jos J. Eggermont, editor, *Brain Oscillations, Synchrony, and Plasticity*, pages 43–58. Academic Press, 2021. ISBN 978-0-12-819818-6. doi: https://doi.org/10.1016/B978-0-12-819818-6.00005-4. URL https://www.sciencedirect.com/science/article/pii/B9780128198186000054.

[99] Shravani Sur and Vinod Kumar Sinha. Event-related potential: An overview. *Industrial Psychiatry Journal*, 18(1):70–73, 2009.

[100] Nancy Nicholson Peterson, Charles E Schroeder, and Joseph C Arezzo. Neural generators of early cortical somatosensory evoked potentials in the awake monkey. *Electroencephalography and Clinical Neurophysiology/Evoked Potentials Section*, 96(3): 248–260, 1995.

[101] Arnd Meiser and Martin G Bleichner. Ear-EEG compares well to cap-EEG in recording auditory ERPs: A quantification of signal loss. *Journal of Neural Engineering*, 19(2): 026042, 2022.

[102] Risto Näätänen, Petri Paavilainen, Teemu Rinne, and Kimmo Alho. The mismatch negativity (mmn) in basic research of central auditory processing: a review. *Clinical Neurophysiology*, 118(12):2544–2590, 2007.

[103] Walter S Pritchard. Psychophysiology of P300. *Psychological bulletin*, 89(3):506, 1981.

[104] Lawrence A Farwell and Sharon S Smith. Using brain mermer testing to detect knowledge despite efforts to conceal. *Journal of Forensic Sciences*, 46(1):135–143, 2001.

[105] Francesco Piccione, Flavio Giorgi, P Tonin, Konstantinos Priftis, Silvio Giove, S Silvoni, G Palmas, and F Beverina. P300-based brain computer interface: reliability and performance in healthy and paralysed participants. *Clinical Neurophysiology*, 117(3): 531–537, 2006.

[106] Timm Rosburg, Nash N Boutros, and Judith M Ford. Reduced auditory evoked potential component N100 in schizophrenia—a critical review. *Psychiatry Research*, 161(3): 259–274, 2008.

[107] Risto Näätänen and Terence Picton. The n1 wave of the human electric and magnetic response to sound: a review and an analysis of the component structure. *Psychophysiology*, 24(4):375–425, 1987.

[108] Xiaoming Du, Fow-Sen Choa, Ann Summerfelt, Laura M Rowland, Joshua Chiappelli, Peter Kochunov, and L Elliot Hong. N100 as a generic cortical electrophysiological marker based on decomposition of tms-evoked potentials across five anatomic locations. *Experimental Brain Research*, 235:69–81, 2017.

[109] Michiel van Elk, Roy Salomon, Oliver Kannape, and Olaf Blanke. Suppression of the N1 auditory evoked potential for sounds generated by the upper and lower limbs. *Biological Psychology*, 102:108–117, 2014.

[110] Martyn Hyde. The N1 response and its applications. *Audiology and Neurotology*, 2(5): 281–307, 1997.

[111] Catherine Fischer, Jacques Luauté, Patrice Adeleine, and Dominique Morlet. Predictive value of sensory and cognitive evoked potentials for awakening from coma. *Neurology*, 63(4):669–673, 2004.

[112] Heidi Yppärilä, Silvia Nunes, Ilkka Korhonen, Juhani Partanen, and Esko Ruokonen. The effect of interruption to propofol sedation on auditory event-related potentials and electroencephalogram in intensive care patients. *Critical Care*, 8:1–8, 2004.

[113] Jayant N Acharya and Vinita J Acharya. Overview of EEG montages and principles of localization. *Journal of Clinical Neurophysiology*, 36(5):325–329, 2019.

[114] Nasser Kehtarnavaz. Chapter 7: Frequency Domain Processing. In Nasser Kehtarnavaz, editor, *Digital Signal Processing System Design (Second Edition)*, pages 175–196. Academic Press, Burlington, second edition edition, 2008. ISBN 978-0-12-374490-6.

[115] M Kemal Kıymık, İnan Güler, Alper Dizibüyük, and Mehmet Akın. Comparison of STFT and wavelet transform methods in determining epileptic seizure activity in EEG signals for real-time application. *Computers in Biology and Medicine*, 35(7):603–616, 2005.

[116] Jont B Allen and Lawrence R Rabiner. A unified approach to short-time fourier analysis and synthesis. *Proceedings of the IEEE*, 65(11):1558–1564, 2005.

[117] Richard N Youngworth, Benjamin B Gallagher, and Brian L Stamper. An overview of power spectral density (PSD) calculations. *Optical Manufacturing and Testing VI*, 5869:206–216, 2005.

[118] Mona Sazgar, Michael G Young, Mona Sazgar, and Michael G Young. Overview of EEG, electrode placement, and montages. *Absolute Epilepsy and EEG Rotation Review: Essentials for Trainees*, pages 117–125, 2019.

[119] Marek Żyliński, Amir Nassibi, Edoardo Occhipinti, Adil Malik, Matteo Bermond, Harry J Davies, and Danilo P Mandic. Hearables: In-ear multimodal data fusion for robust heart rate estimation. *BioMedInformatics*, 4(2):911–920, 2024.

[120] Alessandro Montanari, Ashok Thangarajan, Khaldoon Al-Naimi, Andrea Ferlini, Yang Liu, Ananta Narayanan Balaji, and Fahim Kawsar. OmniBuds: A sensory earable platform for advanced bio-sensing and on-device machine learning. *arXiv preprint arXiv:2410.04775*, 2024.

[121] Lan S Chen, Wendy G Mitchell, Elizabeth J Horton, and O Carter Snead III. Clinical utility of video-EEG monitoring. *Pediatric Neurology*, 12(3):220–224, 1995.

[122] Luis Fernando Herbozo Contreras, Zhaojing Huang, Leping Yu, Armin Nikpour, and Omid Kavehei. Biological plausible algorithm for seizure detection: Toward AI-enabled electroceuticals at the edge. *APL Machine Learning*, 2(2), 2024.

[123] Liqiang Zhu, Changming Wang, Zhihui He, and Yuan Zhang. A lightweight automatic sleep staging method for children using single-channel EEG based on edge artificial intelligence. *World Wide Web*, 25(5):1883–1903, 2022.

[124] Yu-De Huang, Kai-Yen Wang, Yun-Lung Ho, Chang-Yuan He, and Wai-Chi Fang. An edge AI system-on-chip design with customized convolutional-neural-network architecture for real-time EEG-based affective computing system. In *2019 IEEE Biomedical Circuits and Systems Conference (BioCAS)*, pages 1–4, 2019.

[125] Zhaojing Huang, Luis Fernando Herbozo Contreras, Wing Hang Leung, Leping Yu, Nhan Duy Truong, Armin Nikpour, and Omid Kavehei. Efficient edge-AI models for robust ECG abnormality detection on resource-constrained hardware. *Journal of Cardiovascular Translational Research*, pages 1–14, 2024.

[126] Zhaojing Huang, Luis Fernando Herbozo Contreras, Leping Yu, Nhan Duy Truong, Armin Nikpour, and Omid Kavehei. S4D-ECG: A shallow state-of-the-art model for cardiac abnormality classification. *Cardiovascular Engineering and Technology*, pages 1–12, 2024.

[127] Zhaojing Huang, Leping Yu, Luis Fernando Herbozo Contreras, Kamran Eshraghian, Nhan Duy Truong, Armin Nikpour, and Omid Kavehei. Advancing privacy-aware machine learning on sensitive data via edge-based continual μ-training for personalized large models. *medRxiv*, pages 2024–05, 2024.

[128] Moises Meza-Rodriguez, Lewis De La Cruz, and José Alonso Cáceres-DelAguila. Development of an electrocardiographic signal classifier for bundle branch blocks, applying tiny machine learning. In *2023 IEEE XXX International Conference on Electronics, Electrical Engineering and Computing (INTERCON)*, pages 1–6, 2023.

[129] Bok Y Ahn, Eric B Duoss, Michael J Motala, Xiaoying Guo, Sang-Il Park, Yujie Xiong, Jongseung Yoon, Ralph G Nuzzo, John A Rogers, and Jennifer A Lewis. Omnidirectional printing of flexible, stretchable, and spanning silver microelectrodes. *Science*, 323(5921):1590–1593, 2009.

[130] Prajwal Kumar, Eduardo Di Mauro, Shiming Zhang, Alessandro Pezzella, Francesca Soavi, Clara Santato, and Fabio Cicoira. Melanin-based flexible supercapacitors. *Journal of Materials Chemistry C*, 4(40):9516–9525, 2016.

[131] Sheng Xu, Yihui Zhang, Jiung Cho, Juhwan Lee, Xian Huang, Lin Jia, Jonathan A Fan, Yewang Su, Jessica Su, Huigang Zhang, et al. Stretchable batteries with self-similar serpentine interconnects and integrated wireless recharging systems. *Nature Communications*, 4(1):1543, 2013.

[132] Jeevan Persad and Sean Rocke. A survey of 3D printing technologies as applied to printed electronics. *IEEE Access*, 10:27289–27319, 2022.

[133] Ali Haider and Bijay Guragain. Challenges and future trends of EEG as a frontier of clinical applications. In *2023 IEEE International Conference on Electro Information Technology (eIT)*, pages 484–498, 2023.

[134] S Preetha and M Sasikala. Design of asynchronous low-complexity SSVEP-based brain control interface speller. *Computers in Biology and Medicine*, 190:110062, 2025.

[135] Stefan Debener, Cornelia Kranczioch, and Maarten De Vos. Electroencephalography: Current trends and future directions. *Neuroeconomics*, pages 359–373, 2016.

[136] Lei Wang, Paul Y Kim, David E McCarty, Clifton Frilot II, Andrew L Chesson Jr, Simona Carrubba, and Andrew A Marino. EEG recurrence markers and sleep quality. *Journal of the Neurological Sciences*, 331(1-2):26–30, 2013.

[137] Dimiter V Dimitrov. Medical internet of things and big data in healthcare. *Healthcare Informatics Research*, 22(3):156–163, 2016.

[138] Takashi Nakamura, Valentin Goverdovsky, Mary J Morrell, and Danilo P Mandic. Automatic sleep monitoring using ear-EEG. *IEEE journal of Translational Engineering in Health and Medicine*, 5:1–8, 2017.